

Investigating the role of CBX2 in ER-positive breast cancer

Ella Jane Waters

201501212

MSc by Research

Supervisor: Dr Mark Wade

Second Supervisor: Dr Cheryl Walter

Date: 24/09/2019

Faculty of Health Science



Acknowledgements

I would like to thank Dr Mark Wade for facilitating this project, being a great supervisor and for his continued guidance and support throughout.

I would also like to thank Dr Cheryl Walter for the additional and valuable assistance, and for her kind words and support.

Additionally, I would like to thank Chloe Warren for her continued encouragement and help in the laboratory.

I would also like to thank Mrs Kath Bulmer, Dr Pedro Beltran-Alvarez and Dr Barbara Guinn for their knowledge and experience.

I finally want to thank my family and friends for their patience and support throughout this year.

Abstract

Breast cancer is the most common form of cancer in women, with oestrogen receptor (ER) positive breast cancers being the most common subtype. Although there are targeted endocrine therapies for this receptor, resistance mechanisms mean that they are not always effective. Post-translational modifications of histone proteins are important for regulating gene expression. It is known that the pattern of modifications is different in cancerous tissue compared to normal tissue. Epigenetic reader proteins recognise histone post-translational modifications and help remodel the adjacent chromatin landscape, resulting in gene expression or repression. This means epigenetic reader proteins are possible novel therapeutic targets. CBX2 is an example of an epigenetic reader protein which is overexpressed in ER-positive breast cancer. The aim of this study was to analyse the role of CBX2 in ER-positive breast cancer. This was assessed by knocking down *CBX2* gene and protein expression, using siRNAs in MCF-7 and T47D cell lines and analysing changes to cellular phenotype and gene expression regulation. It was determined that CBX2 in the breast cancer cell lines was a nuclear activated phosphorylated form of the protein, and that knockdown of CBX2 has little effect on H2AK119ub and H3K27me3, but causes decrease of H3K27ac. Phenotypic experiments analysed the effect of CBX2 on cell growth, using MTS and apoptosis assays, and showed that CBX2 knockdown reduced cell number and increased cell death. RNA-Sequencing analysis identified that CBX2 has a role in regulating genes within the cell cycle and ER-signalling pathway. The effect on ER-target genes was validated by quantitative-PCR. Additional investigation of the RNA-Seq data will further validate the role of CBX2 in ER-positive breast cancer. Continued research is important for developing therapies for the future treatment of this cancer.

Key words: ER-positive breast cancer, post-translational modifications, epigenetics, CBX2

Abbreviations List

AF – Activating function

AKT – Protein kinase B

AP – Activator protein

APS – Ammonium persulphate

AT – Adenine-thymine

BET – Bromodomain and extra-terminal domain

BSA – Albumin standard

CBP – CREB binding protein

CBX – Chromobox

CDK - Cyclin-dependent kinase

ChIP – Chromatin immunoprecipitation

Chromodomain - Chromatin organiser modifier domain

CIP – Calf intestinal alkaline phosphatase

CK2 – Casein kinase II

CCND1 – Cyclin D1

DBD – DNA binding domain

ddH₂O – Double distilled water

DNA – Deoxyribonucleic acid

DTT - Dithiothreitol

DZNeP - 3-deazaneplanocin

E1 – Ubiquitin activating enzyme

E2 – Ubiquitin conjugating enzyme

E3 – Ubiquitin ligase

EGFR - Epidermal growth factor receptors

EP300 – Histone acetyltransferase p300

ER – Oestrogen receptor

ERE – Oestrogen response element

FBS – Foetal bovine serum

FOXA1 - Forkhead box protein A1

HATs – Histone acetyltransferases

HDACs – Histone deacetylases

HER2 - Human epidermal growth factor receptor 2

HKMTs – Histone lysine methyltransferases

HPH – Human polyhomeotic homolog

IB - Immunoblot

LBD – Ligand binding domain

MAPK - Mitogen-activated protein kinases

mTOR - Mammalian target of rapamycin

NaCl – Sodium chloride

NFκB - Nuclear factor Kappa B

PBS – Phosphate buffer saline

PcG – Polycomb group complex

PCGF – Polycomb group factor

PI – Protease inhibitor

PI3K – Phosphoinositide 3-kinase

PMSF – Phenylmethane sulphonyl fluoride

PR – Progesterone receptor

PRC – Polycomb repressor complex

PTM – Post-translational modification

PVDF - Polyvinylidene difluoride

QC – Quality control

RB – Retinoblastoma

RIN – RNA integrity number

RING – E3-ligase protein

SAM - S-adenosylmethionine

SAP – Shrimp alkaline phosphatase

SDS – Sodium dodecyl sulphate

SDS-PAGE – Sodium dodecyl sulphate polyacrylamide gel electrophoresis

SERD – Selective oestrogen receptor degraders

SERM – Selective oestrogen receptor modulator

siRNA - Small interfering ribonucleic acids

siSCR – Scrambled small interfering ribonucleic acids

SRR – Serine rich region

TBS-T - Tris-buffered saline and tween

TEMED - Tetramethylethylenediamine

TNBC – Triple negative breast cancer

TSG – Tumour suppressor gene

WR – Working reagent

YAP – Yes-associated protein

Contents

Acknowledgements.....	i
Abstract.....	ii
Abbreviations List.....	iii
List of Figures.....	ix
List of Tables.....	xi
Chapter 1: Introduction.....	1
1.1 Cancer.....	1
1.2 Breast Cancer.....	1
1.2.1 HER2-positive and TNBC.....	3
1.3 ER- Positive Breast Cancer.....	3
1.3.1 Resistance to treatments.....	6
1.4 Post-translational Modifications.....	7
1.5 PTM in Cancer.....	10
1.6 Epigenetic reader proteins as therapeutic targets.....	13
1.7 CBX2 epigenetic reader protein.....	14
1.7.1 CBX2 and cancer.....	16
1.7.2 CBX2 in breast cancer.....	16
Chapter 2: Hypothesis.....	18
2.1 Hypothesis: CBX2 plays a role in ER-positive breast cancer.....	18
2.2 Objectives:.....	18
2.3 Ethical Considerations.....	18
Chapter 3: Materials and Methods.....	19
3.1 Cell Culture.....	19
3.1.1 Cell trypsinisation.....	19
3.1.2 siRNA transfections.....	19
3.1.3 Oestrogen-stimulated experiments.....	20
3.2 Western blot.....	20
3.2.1 Protein lysis.....	20
3.2.2 Gel electrophoresis.....	21
3.2.3 Gel transfer.....	22
3.2.4 Antibody incubation and visualisation.....	22
3.3 RNA extraction.....	23

3.4	RT qPCR	24
3.4.1	Reverse transcription	24
3.4.2	qPCR	25
3.5	Immunoprecipitation	26
3.6	Shrimp Alkaline Phosphatase.....	27
3.7	Calf Intestinal Alkaline Phosphatase Treatment	28
3.7.1	BCA Assay.....	28
3.7.2	CIP	29
3.8	Nuclear and Cytoplasmic Extraction	29
3.9	MTS Assay	30
3.10	Phase Contrast Microscopy	30
3.11	Apoptosis Assay	30
3.12	RNA Sequencing.....	31
3.13	Statistical analysis	32
Chapter 4: Results		33
4.1	Knockdown of CBX2 confirmed by RT-qPCR	33
4.2	Knockdown of CBX2 confirmed by Western blot.....	35
4.3	CBX2 at 72kDa is a phosphorylated form of the protein	36
4.4	CBX2 is localised in the nucleus	37
4.5	CBX2 isolated by immunoprecipitation	38
4.6	Effect of CBX2 knockdown on histone modifications	40
4.7	CBX2 knockdown reduces cell growth.....	44
4.8	CBX2 causes cell apoptosis	46
4.9	RNA-Sequencing.....	47
4.9.1	RNA-Seq samples passed QC	47
4.9.2	Cluster heat map.....	48
4.9.3	More genes are upregulated	49
4.9.4	Top 20 enriched pathways.....	50
4.9.5	CBX2 in the cell cycle.....	51
4.9.6	Gene Set Enrichment Analysis	52
4.10	pS2 and CCND1 expression decreases with CBX2 knockdown	55
Chapter 5: Discussion		58
5.1	CBX2 is phosphorylated in ER-positive breast cancer cells.....	58
5.2	CBX2 impacts certain histone modifications	60
5.3	CBX2 knockdown inhibits cell growth.....	62
5.4	Gene expression analysis	64

5.5	Conclusions and Future Perspectives	66
Chapter 6:	References.....	68
Appendices.....		I

List of Figures

Figure 1.1. The 20 most common cancers in the UK.	2
Figure 1.2. The structure of the ER α	4
Figure 1.3. The mechanism of oestrogen receptor signalling.....	5
Figure 1.4. The nucleosomal histone core.	8
Figure 1.5. Aberrant activity of epigenetic writers, readers and erasers.	11
Figure 1.6. Components of the PRC1 and PRC2 complex.	15
Figure 1.7. mRNA expression of CBX2.	17
Figure 4.1. Relative <i>CBX2</i> mRNA expression.	34
Figure 4.2. Western blot showing CBX2 knockdown.	35
Figure 4.3. Western blot showing CBX2 phosphorylation in MCF-7 cells.....	37
Figure 4.4. Western blot showing CBX2 located in the nucleus.	38
Figure 4.5. Immunoprecipitation Western blot.	39
Figure 4.6. Western blot probed for H2AK119ub.	41
Figure 4.7. Western blot probed for H3K27me3.	42
Figure 4.8. Western blot showing the effect of CBX2 knockdown on H3K27ac.....	43
Figure 4.9. MTS assay graph showing effect of CBX2 knockdown on cell proliferation.	44
Figure 4.10. Microscopy images of MCF-7 and T47D cells.	45
Figure 4.11. Western blots showing CBX2 knockdown effect on cell apoptosis.	46
Figure 4.12. A Pearson correlation coefficient.	48
Figure 4.13. Cluster heat map showing gene expression.	49
Figure 4.14. A volcano plot showing 4280 genes being significantly up regulated and 2776 genes significantly down regulated.	50
Figure 4.15. The top 20 pathways that CBX2 is significantly involved in.....	51
Figure 4.16. The genes involved in the cell cycle, within G1, S, G2 and M phases.....	52
Figure 4.17. Genes significantly upregulated (red) or down regulated (blue) at the G2 to M checkpoint.....	53
Figure 4.18. Genes significantly upregulated in red and significantly downregulated in blue within MYC target genes.....	53
Figure 4.19. E2F target genes significantly upregulated (red) or downregulated (blue).....	54
Figure 4.20. Genes significantly upregulated (red) or downregulated (blue) in the late oestrogen response.	55
Figure 4.21. Relative <i>pS2</i> mRNA expression in siCBX2-3 and 4 transfected MCF-7 (A) and T47D (B) cells.....	56

Figure 4.22. Relative *CCND1* mRNA expression in siCBX2-3 and 4 transfected MCF-7 (A) and T47D (B) cells. 57

List of Tables

Table 3.1. The siRNAs used for transfecting, along with the company, catalogue numbers and the sequences.	20
Table 3.2. The composition of Buffer A and B. pH with hydrochloric acid as required.....	21
Table 3.3. The composition of running and stacking gels.....	21
Table 3.4. The composition of running buffer, transfer buffer and 10×TBS. All made up to 1L with ddH ₂ O.....	22
Table 3.5. Antibodies used for Western blots, including the type, company and catalogue numbers.	23
Table 3.6. Primers used in qPCR with the catalogue numbers and companies.....	26
Table 3.7. qPCR run, repeated for 40 cycles, including the temperature and time at each stage.	26
Table 3.8. Preparation of diluted BSA standards.....	28
Table 4.1. QC for each sample with the RIN number.	47

Chapter 1: Introduction

1.1 Cancer

Cancer consists of a group of diseases, caused by the uncontrollable growth of cells, forming a malignant tumour mass. This can be due to certain genes not functioning correctly due to random genetic mutations, hereditary factors or external mutagens such as radiation (Wu et al., 2018). Oncogenes are proto-oncogenes activated by mutation, such as the *myc* gene, which instigate uncontrolled cell proliferation and encode for proteins which induce cancer. Tumour suppressor genes (TSG), such as *p53* and retinoblastoma gene (*RB*), prevent cells from becoming cancerous by initiating apoptosis or halting the cell cycle. Loss of function mutations of TSG can also result in unregulated cell growth (Lee and Muller, 2010). The combination of activated oncogenes and loss of TSG by mutations can result in genome instability and drive cancer progression (Aguilera and García-Muse, 2013). There are over 100 distinct types of cancer and many more subtypes (Hanahan and Weinberg, 2000), which are characterised into sarcoma, carcinoma, leukaemia or lymphoma groups, with some of these being more prevalent than others.

1.2 Breast Cancer

15% of newly diagnosed cancers are tumours originating in the breast (Figure 1.1). Breast cancer is the leading cause of cancer in women, with 1 in 8 women in the UK affected (Cancer Research UK, 2015). It is caused by uncontrollable growth of breast cells, with the vast majority being due to a sporadic mutation, rather than hereditary factors (Kenemans et al., 2004). Breast cancer is not one single disease but is characterised into subtypes with different therapeutic requirements (Dai et al., 2015). Intra-tumour heterogeneity can exist due to stem cell plasticity, meaning multiple subtypes can also occur within one tumour (Yeo and Guan, 2017).

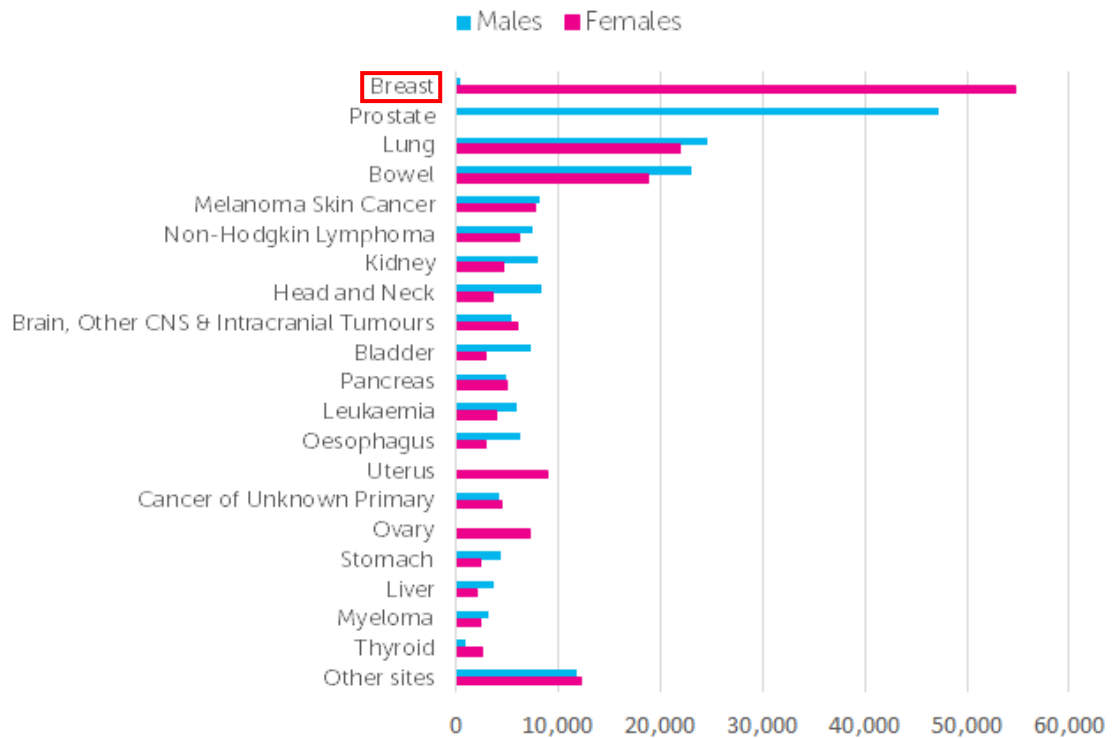


Figure 1.1. The 20 most common cancers in the UK, with breast cancer highlighted. Adapted from (Cancer Research UK, 2015).

A patient's diagnosis is currently classified based on hormone receptor status, these being oestrogen receptor (ER) or progesterone receptor (PR) positive, human epidermal growth factor receptor 2 (HER2) receptor positive, or triple negative breast cancer (TNBC), with each of these being grouped into different molecular subtypes (Yersal and Barutca, 2014). Molecular subtypes are defined based on their gene expression profiles, and are broadly characterised as either luminal A, luminal B, HER2-enriched, basal and normal-like breast cancers (Perou et al., 2000). Luminal A generally consists of ER and PR positive, but HER2 negative breast cancers, whereas luminal B includes ER and PR positive, and HER2 positive breast cancers. HER2-enriched cancers are HER2 positive, but ER and PR negative, and basal-like breast cancer mainly encompasses TNBC (Hon et al., 2016). Hormone receptor positive cancers have targeted therapies, but resistance to these therapies can develop. Some subtypes, such as TNBC, have no targeted therapies. There is therefore a major unmet clinical need for new therapeutics for all breast cancer subtypes.

1.2.1 HER2-positive and TNBC

The HER2-positive breast cancer subtype make up approximately 20% of breast cancer diagnosis (Ahmed et al., 2015). These cancer cells overexpress HER2, which is a tyrosine kinase receptor protein within the epidermal growth factor receptor family, therefore is a major biomarker of this breast cancer sub-type (Singla et al., 2017). Therapeutics include the monoclonal antibodies Trastuzumab and Pertuzumab, and the small molecule inhibitor Lapatinib, all often combined with chemotherapy (Martin and López-Tarruella, 2016). They work by extracellular binding to the HER2 receptor binding domains on the tumour cells, and then mediate cell proliferation and apoptosis.

TNBC is the rarest classification, accounting for about 15% of breast cancers (Yao et al., 2017). These cancer cells do not express oestrogen or progesterone receptors, and lack HER2 overexpression and gene amplification, hence the term 'triple negative'. Due to the lack of these receptors, there are no targeted therapies towards these compared to the other types of breast cancer, therefore traditional chemotherapy is given (Wahba and El-Hadaad, 2015). The heterogeneity of these TNBC cells mean that chemotherapy varies in effectiveness from patient to patient. However, some of the subtypes of TNBC do express an androgen receptor which has a role in tumour development, meaning this is a possible therapeutic target (Gucalp and Traina, 2016). More effective therapeutic targets need to be developed, which will result in a better prognosis and outcome for patients with this disease.

1.3 ER- Positive Breast Cancer

The most common type of breast cancers are ER-positive, accounting for approximately 80% of all newly diagnosed breast cancers (Bulut and Altundag, 2015). These cells grow in response to oestrogen, and 65% of the patients have cells that also grow in response to progesterone. ER-positive breast cancers are also heterogeneous in terms of gene expression, hence are a numerous and diverse group (Cancer Genome Atlas Network, 2012).

There are two types of ER; ER α and ER β . ER α is upregulated in the majority of breast cancers, whereas ER β is often decreased in tumour cells (Roger et al., 2001). ER α is coded for by the *ESR1* gene. It has a deoxyribonucleic acid (DNA) binding domain, containing zinc finger motifs, N-terminal activating function (AF1) domain, a ligand

binding domain (AF2), a hinge region and the C-terminal (Figure 1.2) (Lipovka and Konhilas, 2016). There are three different types of oestrogen; oestrone, 17 β -oestradiol and oestriol. Oestradiol is the most common form found in women (Thomas and Potter, 2013). The ligand binding domain of the ER is where oestradiol binds, and the DNA-binding domain binds to oestrogen response elements (ERE) in the promoter and enhancer regions of ER target genes. The AF domains regulate the transcriptional activity of ER via binding of nuclear receptor coactivator proteins (Nilsson et al., 2001). When not bound to the ligand, the ER exist as monomers that are bound to heat shock proteins.

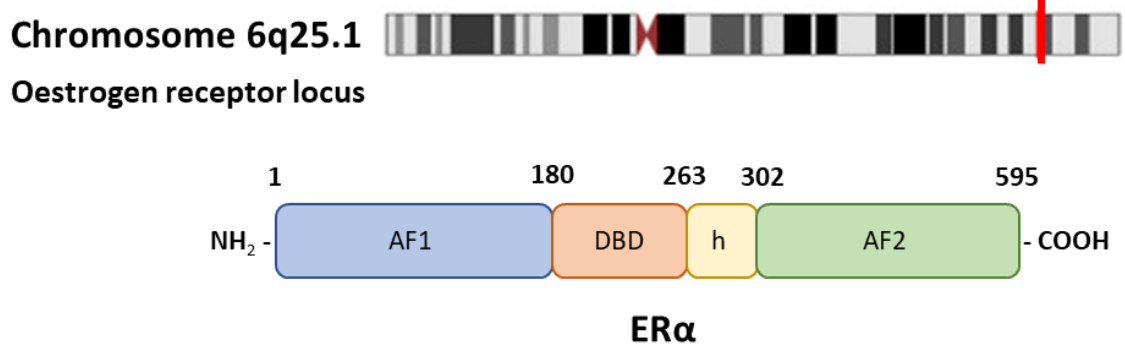


Figure 1.2. The structure of the ER α . This contains both activating function domains (AF), the DNA binding domain (DBD), the ligand binding domain (LBD) and a hinge region (h). Adapted from (Hilton et al., 2018).

Oestrogen is produced in the ovaries, and diffuses from the bloodstream to tumour cells and binds to ER α . It dissociates the heat shock proteins, causing the ligand-binding domain to form a hydrophobic surface and the oestrogen-ER α complex to dimerise and translocation to the nucleus (Figure 1.3). The activated ER α homodimer can then bind to cis-regulatory elements, such as EREs (5'- AGGTCAnnnTGACCT -3'), facilitated by pioneer factor proteins such as Forkhead box protein A1 (FOXA1) (Tecalco-Cruz et al., 2017). ERE binding promotes binding of RNA polymerase II, thereby activating gene expression of target genes which ultimately promote proliferation of ER-positive breast cancer cells (Björnström and Sjöberg, 2005). Co-activator proteins that bind and work with the ER to activate transcription by chromatin remodelling include CREB binding protein (CBP) and histone acetyltransferase p300 (EP300).

ER activity can also be non-genomic in function, by binding indirectly to DNA by tethering to other transcription factors, for example, activator protein 1 (AP-1) and nuclear factor Kappa B (NFκB). ER interacting with cell membrane-associated growth factor receptors, such as HER2 and epidermal growth factor receptors (EGFR), activate downstream signal transduction pathways, including PI3K/AKT, mitogen-activated protein kinases (MAPK) and stress responses within the cytoplasm (Osborne et al., 2001). This activates secondary messengers such as calcium ions and nitric oxide, and causes crosstalk between signal transduction pathways and activated co-regulatory genes.

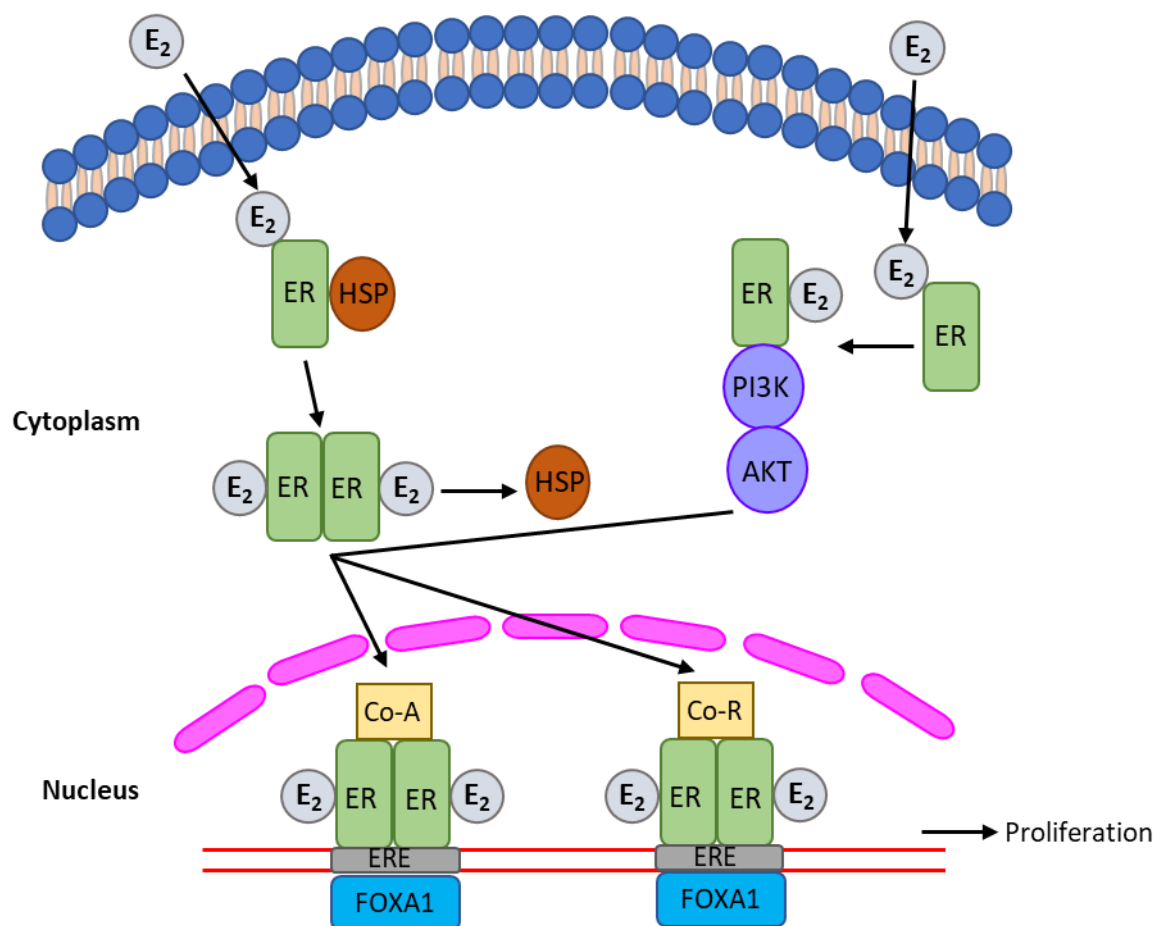


Figure 1.3. The mechanism of oestrogen receptor signalling, from the cytoplasm to the nucleus. ER can bind directly to the ERE on DNA but can also bind indirectly via other pathways, such as PI3K/AKT. Figure Author's own.

As the ER is required for ER-positive breast cancer growth, it is the primary target for therapeutic intervention. Therapeutics include endocrine therapy, that either inhibit the ER directly to prevent the cells from growing, or prevent the ovaries from producing

oestrogen. Types of endocrine therapy include SERMS (selective estrogen receptor modulators) and SERDS (selective estrogen receptor degraders). Tamoxifen is the most commonly used form of SERM endocrine therapy. It inhibits ER-signalling by binding to the ER and preventing oestrogen binding, impeding the expression of essential genes, and stopping the proliferation of cancer cells (Chang, 2012). Tamoxifen is usually administered for 5 years, reducing recurrence in patients and mortality rates for the following 10-15 years (Song et al., 2017). An example of SERD therapy is Fulvestrant. This binds to the ER, preventing oestrogen from binding. If the Fulvestrant-ER complex enters the nucleus, it is transcriptionally inactive because the drug disables AF1 and AF2 (Osborne et al., 2004). This complex is unstable, meaning degradation of the ER protein is accelerated. Other targeted treatments inhibit mammalian target of rapamycin (mTOR), or cyclin-dependent kinases CDK4 and CDK6. There are also inhibitors of phosphoinositide 3-kinase (PI3K) and protein kinase B (AKT) (Turner et al., 2017).

1.3.1 Resistance to treatments

20% of ER-positive breast cancer patients experience distant recurrence and cancer related death (Colleoni et al., 2016). Resistance is the biggest issue with the conventionally used treatments and occurs via multiple mechanisms, such as hypersensitivity to low levels of oestrogen after treatment and ER α independent proliferation of tumour cells due to mutations, epigenetic changes and alternative activation of the receptor (Williams and Lin, 2013).

ESR1 can have recurrent mutations in the ligand binding domain, such as in Y537 and D538 residues (Toy et al., 2013). Missense mutations in these can result in independent ER activation, reducing sensitivity to the therapies targeting the ER. Another cause of resistance can be due to *ESR1* genomic aberrations, including *ESR1* gene rearrangements with an adjacent *CCDC170* gene. This fusion encodes amino-terminally truncated *CCDC170* proteins that increase cell motility, reduce endocrine sensitivity and enhance tumour formation with ERE-independent transcriptional activity (Veeraraghavan et al., 2014). Epigenetic alterations can also alter ER activity, such as DNA methylation repressing ER expression leading to loss of the ER, and reduced or increased activity of histone acetyltransferases (HATs) or histone deacetylases (HDACs) respectively, resulting in alternative gene expression and then reduced ER expression (Abdel-Hafiz, 2017).

As ER crosstalks with other signalling pathways, alternative proliferation and survival signals with ER regulated activity can also occur. Increased HER signalling via PI3K and MAPK pathways can post-translationally modify ER by phosphorylation, thereby making the receptor active in the absence of oestrogen, resulting in the tumour being resistant to therapies targeting the ER-oestrogen interaction (Pietras and Marquez-Garban, 2007). Furthermore, the activity of the ER coregulators can be changed. For example, increased FOXA1 levels can cause tamoxifen-bound ER-DNA binding to be reprogrammed onto different EREs, causing different genes to be regulated than if Tamoxifen was not present, leading to continued cell growth (Nardone et al., 2015).

As there are so many possible mechanisms for resistance to occur due to the complexity of ER-signalling, the precise resistance mechanisms for each individual ER-positive cancer case are unclear and endocrine therapy resistance remains a major clinical obstacle. It is therefore important to identify alternative potential therapeutic targets in ER-positive breast cancer which could be utilised as second-line therapies or in combination with traditional endocrine therapy to treat this disease.

1.4 Post-translational Modifications

Recently, dysregulated epigenetic regulation has been shown to have an important role in breast cancer development, suggesting that targeting the epi-genome may be a novel therapeutic strategy (Karsli-Ceppioglu et al., 2014). Epigenetic regulatory proteins cause chemical modifications to DNA and associated histone proteins which regulate gene expression, rather than explicitly altering the genetic code. DNA is tightly organised around a nucleosomal histone core, containing two of each histone: H2A, H2B, H3 and H4 (Figure 1.4). 145-147 base pairs of DNA is wrapped around this core and a linker histone, H1, is bound to the outside for stability (Lawrence et al., 2016). The nucleosome has basic histone amino N-terminal tails protruding out, which can directly contact adjacent nucleosomes (Tropberger and Schneider, 2013). These tails can undergo post-translational modifications (PTM) by chromatin-modifying enzymes which affects the direct interactions between the nucleosomes, and so the structure of the chromatin and therefore the accessibility for transcriptional or replication machinery. The histone code hypothesis is that PTMs function to recruit chromatin modulation proteins to local chromatin, and it is these chromatin-associated proteins on histone tails that determine the functional outcome of PTMs, whether this be by transcriptional activation or

repression (Jenuwein, 2001). The term euchromatin describes open regions of the genome containing active genes that undergoes cyclical changes during the cell cycle. Heterochromatin has compact regions with inactive genes and is refractive to cell-cycle cyclical changes (Huisinga et al., 2006). Chromatin modulation proteins determine the function of PTM by repositioning nucleosomes and activating downstream signalling, blocking the access of remodelling complexes, or influencing the recruitment of chromatin modifiers and transcription factors (Badeaux and Shi, 2013).

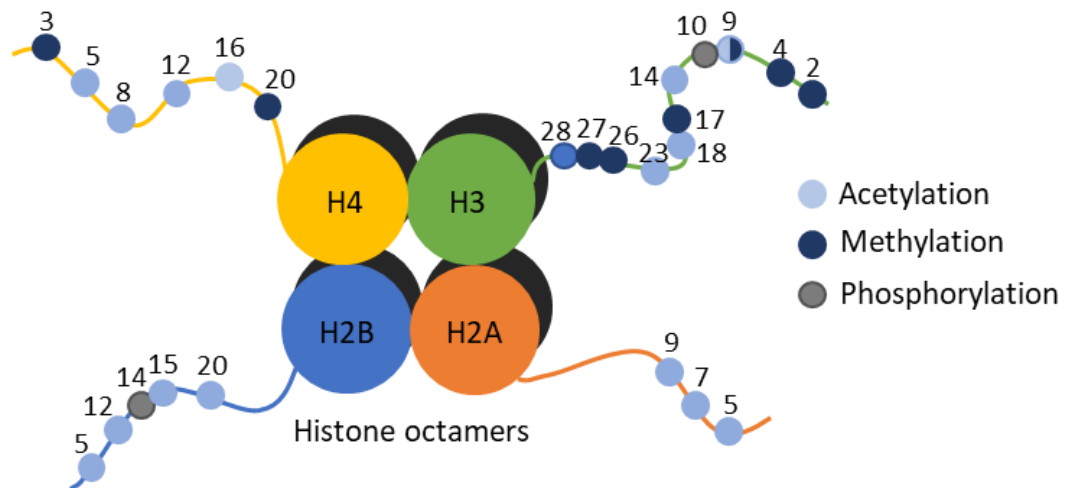


Figure 1.4. The nucleosomal histone core, containing H2A, H2B, H3 and H4. These have histone tails protruding. The numbers on the histone tails represent which lysine amino acid can be modified by which chemical group. Adapted from (Kishimoto et al., 2006).

Histones can be post-translationally modified in many ways, including acetylation, methylation, phosphorylation, ubiquitination and sumolation of specific amino acid residues. They are modified by epigenetic regulatory proteins, including epigenetic writer and eraser proteins. Epigenetic readers recognise specific PTM marks on histones, or a combination of marks and variants (Gillette and Hill, 2015). Histone writers are the enzymes which add PTMs to histones, and erasers remove these.

Histone acetylation is regulated by HATs and HDACs (Legube and Trouche, 2003). HATS post-translationally add an acetyl moiety to the ϵ -amino group of a lysine residue, and HDACs reverse this (Yang and Seto, 2007). Type-A HATs control enzyme recruitment, activity and substrate specificity. They have three main groups of enzymes: GNAT, MYST and CBP/p300 families, along with Rtt109 and Gcn5/PCAF (Marmorstein and Zhou, 2014). Each enzyme modifies multiple sites within the N-terminal tails, neutralising the

positive charge of the histones and thereby disrupting electrostatic interactions between histones and negatively charged DNA. This leads to less compact chromatin, so the transcriptional machinery can access DNA (Bannister and Kouzarides, 2011). Sites of acetylation are also present on the globular core, having a direct structural effect on nucleosome and chromatin dynamics. Type-B HATs acetylate free histones only; not the histones in chromatin (Sternier and Berger, 2000). HDACs oppose the HATs, so they reverse lysine acetylation and restore the positive charge (Ruijter et al., 2003). As this stabilises chromatin, HDACs are considered transcriptional repressors. There are four classes of HDACs; HDAC I, II, III, and IV. A single enzyme or complex can deacetylate multiple sites within histones, meaning they have a low substrate specificity.

Histones can also be modified by phosphorylation on serines, threonines and tyrosines in N-terminal tails, and this modification has a rapid turnover. Phosphorylation is carried out by kinases, which transfer a phosphate group from ATP to the hydroxyl group of target amino acid side chains. They add a negative charge to the histone, influencing chromatin structure by disrupting DNA-histone interactions and are often associated with transcriptional regulation of proliferative genes (Brehove et al., 2015). An example of this is H3S28 phosphorylation displacing polycomb repressor complexes, thereby inducing demethylation and acetylation of H3K27me₃, causing transcriptional activation (Rossetto et al., 2012). Phosphatases oppose the action of kinases by removing the phosphate groups from amino acids.

Histones are also modified by methylation, on the side chains of lysine and arginine amino acids. Methylation doesn't alter the charge of the histone protein, just the hydrophobic and steric properties, so it doesn't directly alter chromatin structure (Upadhyay and Cheng, 2011). Instead, methylation act as signals to other chromatin remodelling proteins. Methylation is most common on lysine residues on H3 and H4. Lysines are mono, di or tri-methylated by specific histone lysine methyltransferases (HKMT), mostly on N-terminal tails. These catalyse the transfer of a methyl group from S-adenosylmethionine (SAM) to ε-lysines amino group. The majority of these have a SET domain, which harbours the enzymatic activity. The exceptions that do not have this domain instead methylate within the globular histone core, as with DOT1 (Feng et al., 2002). Certain lysines are associated with transcriptional activation, such as H3K4me, and others with transcriptional repression, for example H3K9me. Arginines are

methylated by type I and type II arginine methyltransferases. These form an 11-protein family. Arginine and lysine methyltransferases have specific active sites to distinguish themselves from other SAM-dependent enzymes. Histone demethylases reverse the arginine and lysine methylation.

Another modification is histone ubiquitination, which is the addition of ubiquitin to a lysine residue on a substrate. It requires the ubiquitin activating enzyme (E1), ubiquitin-conjugating enzyme (E2) and ubiquitin ligase (E3). This can result in marking proteins for degradation, changing the histone mass and therefore nucleosomal dynamics, or affect protein interactions (Meas and Mao, 2015). The functions are determined by whether the histones are monoubiquitinated to regulate repair, such as on H2A and H2B (Weake and Workman, 2008), or polyubiquitinated to target proteins for degradation (Sadowski and Sarcevic, 2010). The modifications can be removed by the thiol protease deubiquitinating enzymes.

Crosstalk can occur between histone modifications. One modification may depend on another, or the binding of a protein to a modification may be disrupted by an adjacent modification. Moreover, an enzymes' catalytic activity could be affected due to a substrate modification. Synergy between modifications may be required to recruit specific factors, as well as cooperation between histone modifications and DNA methylation (Kouzarides, 2007).

1.5 PTM in Cancer

Histone PTM's can be misregulated in various cancers. The outcome of this could be either altering gene expression programmes including aberrant regulation of oncogenes or TSG, or by histone modifications affecting genome integrity or chromosome segregation (Khan, 2015). The study of histone modifications in cancer may therefore result in possible cancer biomarkers and allow the epigenetic regulatory proteins that read, write and erase PTMs to possibly be targeted therapeutically (Figure 1.5).

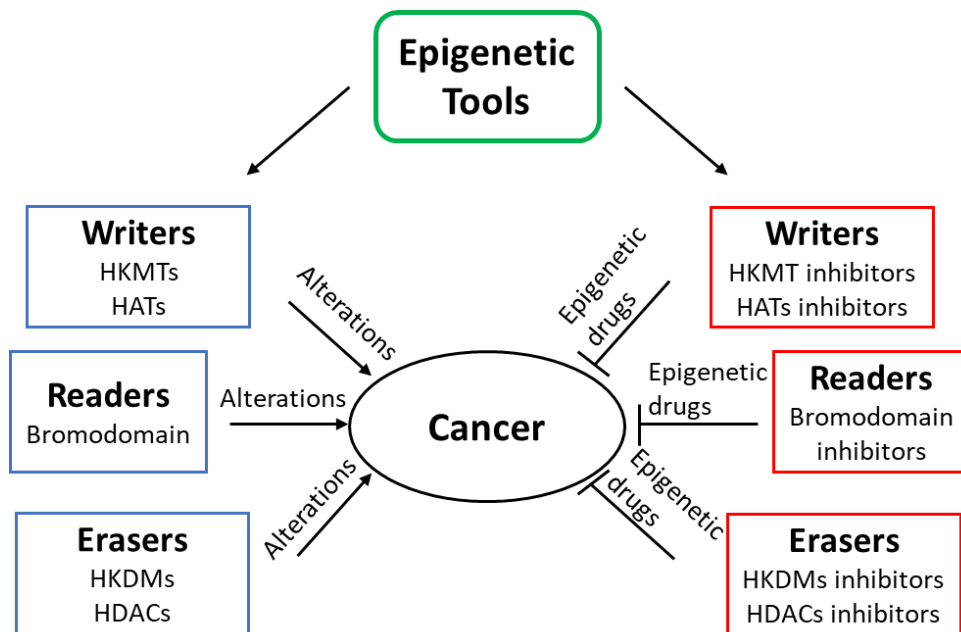


Figure 1.5. Aberrant activity of epigenetic writers, readers and erasers cause gene expression changes that can lead to cancer. Epigenetic drugs can inhibit these, potentially stopping the cancer growth. Adapted from (Biswas and Rao, 2018).

Studies have indicated that a single histone modification could predict a differential prognosis in different cancers, depending on tissue specificity. For example, reduced H3K9 acetylation in prostate and ovarian cancers results in tumour progression, and is associated with a poor prognosis (Seligson et al., 2005, Zhen et al., 2010). However, increased amounts of H3K9ac is associated with a poor prognosis in gastric adenocarcinoma (Park et al., 2008), and decreased H3K9me3 in acute myeloid leukaemia correlates with a better prognosis (Muller-Tidow et al., 2010). This indicates the variation of the different impact of histone PTMs in different cancers, and how important individual study is to identify their role as biomarkers.

With there being so many types of breast cancer (Jaber et al., 2020), PTM of histones is a very important area of study to identify potential biomarkers; as different breast cancer subclasses have distinct gene expression profiles. A study by Elsheikh et al (2009) analysed seven modified histone marks (H3K9ac, H3K18ac, H4K12ac, H4K16ac, H3K4me2, H4K20me3 and H4R3me2) in 880 primary operable invasive breast carcinomas, with normal breast tissue controls. All seven marks were shown in normal tissue, as well as myoepithelial cells, stromal cells and lymphocytes. Moreover, there was positive nuclear staining in breast tumour cells for all the histone marks, but these

varied in intensity. For basal and HER2-positive tumours, reduced detection of the lysine acetylation and arginine methylation histone marks correlated with a large tumour size and poor prognosis. High levels correlated with oestrogen, progesterone and androgen receptor positive tumours.

PTM biomarkers can indicate which of the epigenetic regulatory proteins may be responsible for the modifications on histone tails that are involved in the cancer, and therefore may be potential therapeutic targets. Epigenetic regulatory proteins are known to behave differently in cancer compared with normal tissue. For example, EZH2 is a HKMT which catalyses dimethylation and trimethylation of H3K27 to maintain transcription repression of target genes. When inhibited by 3-deazaneplanocin (DZNep), cell migration, colony formation and genomic instability are lost in breast, colon and prostate cancers, indicating that these epigenetic regulatory proteins have an important oncogenic function (Simó-Riudalbas and Esteller, 2015). Inhibitors of HDACs, such as Romidepsin against class I HDACs in refractory cutaneous T-cell lymphoma, bind to the catalytic pocket of HDACs and prevent substrate binding to the enzyme, leading to re-expression of genes that cause cell cycle arrest and apoptosis (Khan and La Thangue, 2012).

KDM3A is an example of an eraser protein which demethylates transcriptionally repressive H3K9 mono and di-methyl marks, and has a role in ER-positive breast cancer. Depletion of KDM3A is shown to stop recruitment of the ER to the regulatory elements within target gene promoters, therefore reducing ER-target gene expression, such as *pS2* (Wade et al., 2015). KDM3A regulates receptor-target gene transcription by controlling the demethylation of H3K9 at *cis*-regulatory elements of ER-target genes. KDM3A knockdown reduced ER-positive cell proliferation, showing that it is required for ER-positive breast cancer cell growth. Similarly, KDM4B is an eraser protein that demethylates H3K9 tri or di-methylation. Demethylation of H3K9me3 marks allows binding of GATA-3, which is a regulator of *ER* gene expression (Gaughan et al., 2013). This causes upregulation of the *ER*, such that ER-target genes *pS2* and *GREB1* are also upregulated. KDM4B depletion downregulates ER expression. These enzymes show the importance of epigenetic regulators in ER-positive breast cancer, and their potential as targets for reducing ER-positive breast cancer cell growth.

1.6 Epigenetic reader proteins as therapeutic targets

Epigenetic reader proteins recognise histone modifications and direct alterations to the chromatin state, and have recently been identified as a potential source of novel therapeutics. For example, the bromodomain and extra-terminal domain (BET) family of proteins, which consist of BRD2, BRD3 and BRD4 and BRST. Of these proteins, BRD2, BRD3 and BRD4 are epigenetic reader proteins (Deeney et al., 2016). They regulate transcription by binding to acetylated lysines on histones via bromodomains and interact with transcription machinery by recruiting transcription factors and epigenetic regulators. In prostate cancer, the N-terminal regions of BRD2, BRD3 and BRD4 have BD1-BD2 domains that interact with the N-terminus of androgen receptor (Asangani et al., 2014). BET inhibition stops androgen receptor signalling downstream of the receptor. Small molecule inhibitors against BRD4 may also benefit TNBC, as some express the androgen receptor, and they may be effective in TNBC that do not overexpress the androgen receptor. Twist, a transcriptional activator, has histone H4-mimic activity, that binds BRD4 after deacetylation. This interaction is necessary for active WNT5A promoter and mediates tumorigenicity and invasion (Alluri et al., 2014). BET inhibitors inhibit Twist-BRD4 interaction, therefore stopping tumour growth.

As well as TNBC, BRD4 activity is required for proliferation in ER-positive breast cancer. BRD4 regulates ER-induced gene expression by affecting phosphorylation of RNA polymerase II and histone H2B monoubiquitylation (Nagarajan et al., 2014). BRD4 binds to acetylated lysine residues on histones at the transcriptional start site of ER regulated genes, and has therefore been identified as a potential therapeutic target. As ER-positive breast cancer can develop tamoxifen resistance, the epigenetic alterations involved in this are important to understand. BRD3/4 plays a role in tamoxifen resistance by recruiting WHSC1, a H3K36 methyltransferase, to the ESR1 gene promoter, which codes for the ER α and positively regulates its expression. WHSC1 methylates K36 on H3, causing transcription elongation of the ESR1, allowing WHSC1 to maintain oestrogen signalling in ER-positive cells. Inhibiting BRD3 or BRD4 activity with a selective inhibitor called JQ1 compromised the recruitment of WHSC1 to ESR1 promoter, therefore inhibiting its expression (Feng et al., 2014). Tamoxifen resistant ER-positive breast cancer cells have been shown to be more sensitive to the JQ1 treatment than non-resistant cells, showing its potential as an effective second-line therapy.

In conclusion, BRD4 is an example of an epigenetic reader protein that has an active role in breast cancer, that can be therapeutically targeted to stop its activity and reduce breast cancer growth. This means that there are potentially other epigenetic reader proteins that are active in breast cancer, which have undiscovered roles, and could be therapeutic targets.

1.7 CBX2 epigenetic reader protein

Like BRD4, chromobox (CBX) protein 2 (CBX2) is an epigenetic reader protein. CBX2 is a member of the Polycomb group (PcG) complex Polycomb repressor complex 1 (PRC1). The CBX protein within this complex can be one of five (CBX2, CBX4, CBX6, CBX7 and CBX8). As well as a CBX protein, the PRC1 complex comprises of one of six polycomb group factors (PCGF), one of three human polyhomeotic homologs (HPH) and one of two E3-ligase proteins (RING). There are two types of PcG complex, PRC1 and PRC2, that are epigenetic regulatory complexes that modify histones, causing gene silencing (Figure 1.6) (Veneti et al., 2017). The EZH2 sub-unit of the PRC2 complex trimethylates lysine 27 on histone 3 (H3K27me3). This in turn is read and bound by the CBX proteins of the PRC1 polycomb core, that then causes the PRC1 RING protein to monoubiquitinate lysine 119 on histone 2A (H2AK119ub), causing chromatin compaction and gene silencing at the genome loci (Ma et al., 2014). Eight CBX proteins contain an N-terminal chromodomain, which regulate heterochromatin. Five of these, including CBX2, have a C-terminal polycomb repressor box, involved in transcriptional silencing and are the canonical component in PRC1.

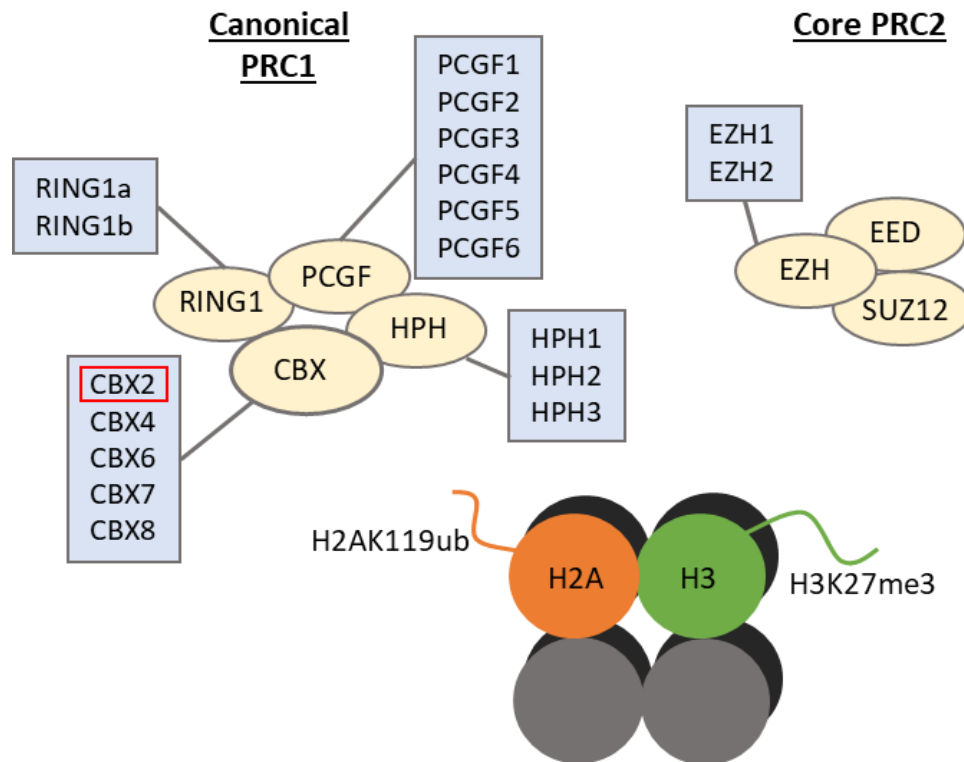


Figure 1.6. Components of the PRC1 and PRC2 complex. Modified from (Di Croce and Helin, 2013).

CBX2 is 532 amino acids long, and its gene is on chromosome 17. It is involved in many cellular processes by regulating gene expression, such as controlling embryonic development, sexual determination, stem cell differentiation, cell cycle and growth, and tumourigenesis (Pethe et al., 2014; Di Costanzo et al., 2018; Gu et al., 2018; Sproll et al., 2018).

The CBX proteins have differential binding to methylated histone tails, with CBX2 being able to bind both H3K27me3 and H3K9me3, unlike CBX4 which has a greater affinity for H3K9me3. The CBX homologs have an AT-hook like motif, or, in terms of CBX2, a DNA-binding motif and an AT-hook, made up of 29 amino acids, which binds to the minor groove of adenine-thymine (AT) rich DNA (Senthilkumar and Mishra, 2009). This enhances the interaction of the protein with DNA or chromatin. The AT-hook contains basic residues which may interact with the chromodomain, preventing the interaction with H3K27me3. The N-terminus of CBX2 is also necessary for targeting it to the chromatin. Moreover, CBX2 within the PRC1 complex can directly compact chromatin, unlike other PcG components, as a result of its highly positively charged region within the C-terminus (Clermont et al., 2014). CBX2 can undergo phosphorylation, likely by

casein kinase II (CK2) (Vandamme et al., 2011). Phosphorylation within the chromodomain can affect the binding specificity of CBX2 for methylated histone H3. If phosphorylation is within the unique serine rich region (SRR) of CBX2, it can increase the binding specificity for H3K27me3 marked nucleosomes (Kawaguchi et al., 2017). CBX2 also has two other specific motifs, these being Cx2.1 containing basic residues and Proline, used in protein biosynthesis, and Cx2.2 which has more serine residues within the C terminal region.

1.7.1 CBX2 and cancer

CBX2 has been implicated in a number of cancers, however its exact role in tumour development and progression is still not well understood. In a study by Clermont et al (2016), CBX2 was shown to be upregulated in metastatic and androgen-independent prostate cancer, increasing in expression and causing a poor prognosis. Inhibiting CBX2 induced cancer cell death in an aggressive and lethal form of prostate cancer, castration resistant prostate cancer. CBX2 inhibition caused up-regulation of PI3K antagonists, therefore resulting in inhibition of the AKT/ PI3K/ mTOR pathways. When this pathway is overactive during cancer, cell apoptosis is reduced and proliferation is enhanced. This research shows that targeting CBX2 could be a potential therapeutic option for aggressive prostate cancers, and also be a novel biomarker due to its overexpression. It also indicates the potential of CBX2 being involved in other types of cancer.

1.7.2 CBX2 in breast cancer

A study by Chen et al (2017) showed CBX2 to be expressed more highly in 455 breast tissues, compared to normal breast tissue. High expression was associated with a large tumour size, lymph node metastasis, a high TNM stage, a positive HER-2 status and shorter overall survival. A further study by Liang et al (2017) has also shown CBX2 to be highly expressed in breast cancer (Figure 1.7). It showed that CBX2 had a higher expression in ER-positive breast cancer, compared with normal tissue. Malignant tumours have displayed a recurrent overexpression of CBX2 with a more malignant phenotype (Parris et al., 2010). High expression of *CBX2* mRNA correlated with a worse relapse free survival. Therefore, these studies show that CBX2 may be a novel breast cancer biomarker due to its overexpression. Furthermore, overexpression of CBX2 also predicts poor survival for the subgroup treated with adjuvant chemotherapy. High

expression of CBX2 meant that patients treated with the chemotherapy drug, Taxol, had a shorter overall survival than patients having treatment without Taxol (Chen et al., 2017). As there was no difference for low expression, patients with high CBX2 expression may not be sensitive to chemotherapy, therefore CBX2 may contribute to chemoresistance in breast cancer. This means that CBX2 could also be a biomarker to identify which patients will benefit from chemotherapy.

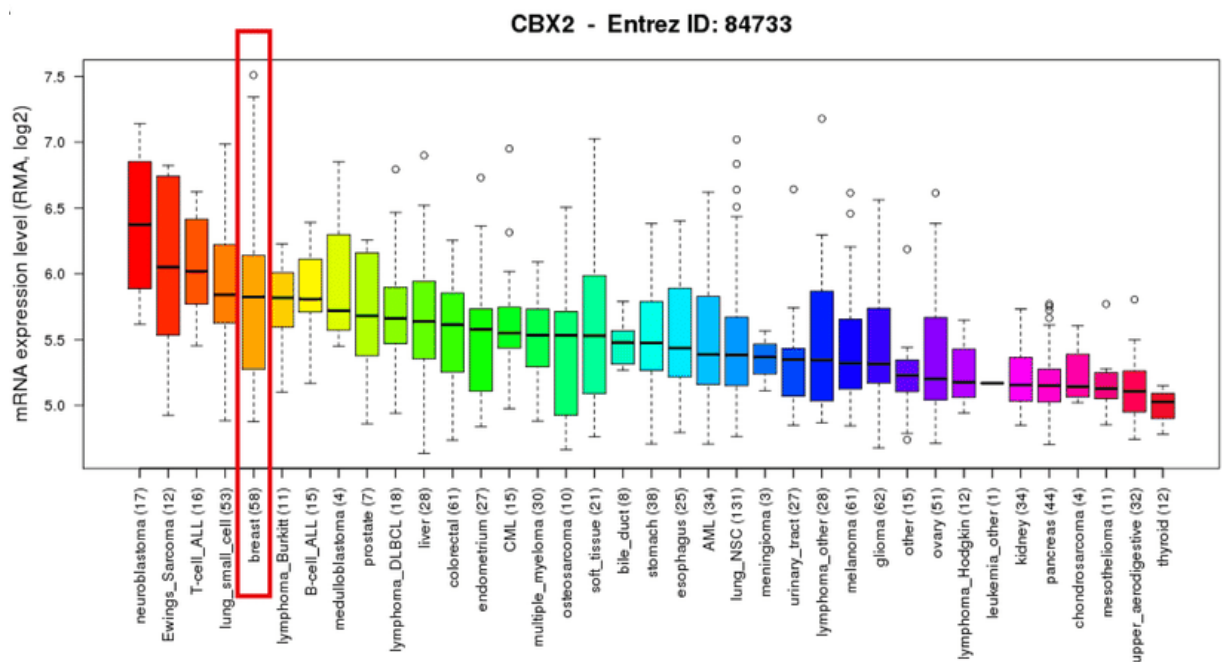


Figure 1.7. mRNA expression of CBX2 is the fifth highest for breast cancer, compared with other types of cancer. Figure from (Liang et al., 2017).

These studies showing overexpression of CBX2, especially in breast cancer, make it a possible biomarker and a potential therapeutic target. The present research validates CBX2 for further study, in order to understand its mechanisms with regards to relevant histone modifications in ER-positive breast cancer and to validate it as a potentially novel therapeutic target.

Chapter 2: Hypothesis

2.1 Hypothesis: CBX2 plays a role in ER-positive breast cancer.

2.2 Objectives:

- To confirm CBX2 knockdown in MCF-7 and T47D cell lines by qPCR and Western blot.
- To observe the effect of CBX2 knockdown on global and local histone modifications by Western blot, specifically H3K27me3, H2AK119ub and H3K27ac.
- To observe the effect of CBX2 on cell death by apoptosis assays, and on cell proliferation by MTS assays.
- To determine the *CBX2* regulated transcriptome by RNA-sequencing of MCF-7 cells following siRNA mediated knockdown of CBX2.
- To analyse the effect of CBX2 knockdown on ER target genes by qPCR, including *pS2 (TFF1)* and *CCND1*.

2.3 Ethical Considerations

This project will use cultured human ER-positive breast cancer cells, MCF-7 and T47D, from the American Type Culture Collection (ATCC). The use of cancer cell lines does not have any direct ethical considerations, however, there are risks in producing them originally. Moreover, risk assessment COSHH forms will be completed to ensure safety in the laboratory.

Chapter 3: Materials and Methods

3.1 Cell Culture

Cell culture is the method of growing cells previously removed from tissue to use in experiments, in the sterile environment of a tissue culture hood (ESCOglobal, UK). MCF-7 and T47D ER-positive breast cancer cell lines, both from ATCC, were grown in RPMI media 1640 (Gibco, UK), supplemented with 10% foetal bovine serum (FBS), 1% glutamine, 1% penicillin and streptomycin (Thermofisher, UK). The cells were most commonly grown in T75 flasks (Sarstedt, Germany) with 12 ml of media, which was changed every three days, or in T175 flasks with 30 ml of media. Cells were incubated in a humidified incubator at 37 °C with 5% CO₂ (Nuair, UK).

3.1.1 Cell trypsinisation

The cells were trypsinised when they reached 80% confluency. Phosphate buffer saline (PBS) was produced from 200 ml of double distilled water (ddH₂O) and one PBS tablet (Fisher Scientific, UK), then sterilised using an autoclave (Prestige medical, UK) so it was suitable for cell culture. Trypsin (Lonza, UK) was diluted 1:30 with PBS. To split the cells, the media was removed, then the flask washed with 8 ml PBS. 3 ml of diluted trypsin was added to the T75, or 5 ml to a T175, then the flask was incubated at 37 °C for 2-5 minutes for the cells to detach. The trypsin was neutralised with 12 ml of media, or 10 ml for a T175 flask. The cells were then centrifuged at 1500 x g (Centrifuge 5702, Eppendorf, UK) for three minutes to pellet the cells, then the media was removed. The cells were resuspended in 5 ml of fresh media, pipetting up and down to mix. For continued cell culture, a fraction of cells were dispensed into fresh tissue culture flasks so that the cells could grow in a sub-confluent environment.

3.1.2 siRNA transfections

Small interfering ribonucleic acids (siRNAs) were used to knockdown *CBX2* mRNA. A non-silencing scrambled siRNA (siSCR) was used as a control. Three individual *CBX2* targeting siRNA were used (siCBX2-1, siCBX2-3 and siCBX2-4) (Table 3.1). Master mixes containing 1:100:2 of siRNA (50 µM stock), basal media, and RNAiMAX lipofectamine reagent (Thermofisher, UK) respectively were created and kept at room temperature for 20 minutes prior to transfection whilst the cells were trypsinised (as described above).

When the cells were resuspended in media, 20 μ l of cell suspension was placed under a coverslip onto a haemocytometer, and counted under the light microscope. The transfection mix was then placed in the centre of each well with the appropriate amount of cells dispensed onto these, depending on the experiment, resulting in a final siRNA concentration of 25 nM.

Table 3.1. The siRNAs used for transfecting, along with the company, catalogue numbers and the sequences.

siRNA	Company	Catalogue Number	Sequence (5'-3')
siRNA SCR	Sigma	HA11411080	UUCUCCGAACGUGUCACGU
siRNA CBX2-1	Sigma	HA11411074	AGGAGGUGCAGAACCGGAA
siRNA CBX2-3	Sigma	HA11411076	GCAAGGGCAAGCUGGAGUA
siRNA CBX2-4	Sigma	HA11411078	CAAGGAAGCUCACUGCCAU

3.1.3 Oestrogen-stimulated experiments

For certain experiments, cells were grown in phenol-red free media (Gibco, UK), containing 10% charcoal-stripped FBS (Hyclone, UK), 1% glutamine and 1% penicillin/streptomycin. 2 ml of MCF-7 cells at a concentration of 7.5×10^4 cells per ml were plated in 6 well plates (Sarstedt, Germany), incubated for 24 hours and then the transfection mixes added, as described above. These were then incubated for a further 48 hours. Certain wells could then be spiked with 1 μ l 17- β -oestradiol to a final concentration of 10 nM, then incubated for 6 hours before extracting RNA for quantitative-PCR analysis (detailed in section 3.4.2).

3.2 Western blot

3.2.1 Protein lysis

After counting, as described in section 3.1.2, 2 ml of cell suspension were transfected with 100 μ l of transfection mix in a 6 well plate then incubated for 72 hours. 7.5×10^4 cells per ml were added for MCF-7 cells, and 1×10^5 per ml for T47D cells. At the point of protein lysis, the media was removed and the wells were washed once with 1 ml PBS. The cells were then incubated in 100-200 μ l (depending on cell confluency) of sodium dodecyl sulphate (SDS) lysis buffer (125mM Tris, 10% v/v glycerol, 2% w/v SDS, pH 6.8). Then the wells were scraped and lysates were added to eppendorf tubes. Protein lysates could then be stored at -20 $^{\circ}$ C for future use in Western blot analysis.

3.2.2 Gel electrophoresis

Proteins within a protein lysate were separated in order of molecular weight by sodium dodecyl sulphate polyacrylamide gel electrophoresis (SDS-PAGE). A 10% running gel was used for knockdown confirmation, and a 15% running gel was used for investigating specific histone modifications (Table 3.2 and 3.3). The running gel was pipetted into 1.5 mm electrophoresis plates within a gel cast (BioRad, UK). 200µl of isopropanol was then added on top of this to ensure the gel set evenly. Once the gel had set, the isopropanol was removed and the stacking gel made and pipetted on top of the running gel, within the glass plates. A 10 or 15 well comb was placed in the stacking gel before it set. Once the complete gel was set, it was placed into an electrophoresis tank (BioRad, UK) with 1× running buffer, made up of 800 ml ddH₂O and 200 ml 5× running buffer (Table 3.4). The protein samples were boiled for 10 minutes, then loaded into the wells. 5 µl of Spectra molecular protein ladder (Thermofisher, UK) was also loaded into a well to confirm separation of proteins and use as a size marker for target proteins. The gels were ran at 140 V for approximately an hour using a powerpack (BioRad, UK).

Table 3.2. The composition of Buffer A and B. pH with hydrochloric acid as required.

	1 L Buffer A (pH 8.8) in H ₂ O	1 L Buffer B (pH 6.8) in H ₂ O
Tris (g)	18.16	6
SDS (g)	0.4	0.4

Table 3.3. The composition of running and stacking gels. The acrylamide and water vary for 15% compared with 10%.

	Running (10 ml total)		Stacking (5 ml total) 6%
	10%	15%	
Acrylamide (33% v/v)	3.3 ml	5 ml	830 µl
ddH ₂ O (ml)	1.67	-	1.6
Buffer A (ml)	5	5	-
Buffer B (ml)	-	-	2.5
APS (µl)	100	100	50
TEMED (µl)	12	12	7.5

Table 3.4. The composition of running buffer, transfer buffer and 10×TBS. All made up to 1 L with ddH₂O.

	5× Running Buffer	10× Transfer Buffer	10× TBS (pH 7.6)
Tris (g)	30	-	24.2
SDS (g)	5	30.28	-
Glycine (g)	144	112.6	-
NaCl (g)	-	-	8.8

3.2.3 Gel transfer

Following gel electrophoresis, the separated proteins were transferred onto a polyvinylidene difluoride (PVDF) membrane (GE Healthcare, UK). This was assembled in a transfer cassette, which was opened with the black side as the base. Two sponges were wet with transfer buffer and placed on the base, followed by two pieces of transfer buffer soaked Whatman paper (GE Healthcare, UK). The gel was removed carefully from the glass plates, and placed face down on the Whatman paper. The PVDF membrane was placed on top of this. This was followed by a further two pieces of Whatman paper soaked in transfer buffer, and then the final two sponges. The sandwich was rolled with a glass roller to ensure there was no bubbles. The cassette was placed into a transfer chamber with 1× transfer buffer, consisting of 900 ml ddH₂O and 10× 100 ml transfer buffer (Table 3.4). An ice pack to prevent overheating and a magnetic stirrer were also placed in the tank. This was ran at 100 V using a powerpack for 1 hour.

3.2.4 Antibody incubation and visualisation

Following the gel transfer, the membrane was washed three times for 10 minutes in tris-buffered saline and tween (TBS-T), containing 900 ml dH₂O, 100 ml 10×TBS and 1 ml Tween (Table 3.4) and then blocked for 1 hour in non-fat dried milk (5 g milk powder (Marvel, UK) to 100 ml TBS-T) to prevent non-specific binding. The membrane was then added to the primary antibody-5% milk solution then incubated at 4 °C overnight on a roller (Antibody concentrations found in Table 3.5). The following day, the membrane was washed three times for 10 minutes in TBS-T. It was then incubated in a secondary antibody, diluted appropriately in 5% milk solution, at room temperature for 1 hour on a roller. The secondary antibody binds to the heavy chains of the primary antibody of

that species. The membrane was then washed twice in TBS-T and once in TBS (900 ml dH₂O, 100 ml 10×TBS). The secondary antibody contains horseradish peroxidase, allowing for detection of the bands by chemiluminescence. An ECL substrate (Bio-Rad, UK) reacts with this, so is used to visualise the bands. ECL was mixed 1:1:2 with substrate one, substrate two and TBS respectively. 1 ml of the mixture was added to the membranes, then placed between parafilm. The membrane was visualised on the ChemiDoc XRS+ (Bio-Rad, UK). Images could then be compared to the molecular weight ladder on ImageLab software to identify the target protein.

Table 3.5. Antibodies used for Western blots, including the type, company and catalogue numbers.

Antibody	Type	Dilution	Species	Company	Catalogue Number
CBX2	Primary	1:5000	Rabbit	Abcam	ab80044
	Secondary	1:5000	Goat anti-rabbit	Abcam	ab97051
Alpha tubulin	Primary	1:10000	Mouse	Proteintech	6603I-I-Ig
	Secondary	1:10000	Goat anti-mouse	Abcam	ab97046
IgG	Primary	1:5000	Rabbit	Diagenode	C15410206
H3K27ac	Primary	1:1000	Rabbit	Diagenode	C15410174
H3K9me1	Primary	1:5000	Rabbit	Diagenode	C15410045
H2AK119ub	Primary	1:20000	Rabbit	Diagenode	C15410002-10
H2A-pan	Primary	1:20000	Rabbit	Diagenode	C15410166-10
H3K27me3	Primary	1:20000	Rabbit	Diagenode	C15410069-10
H3-pan	Primary	1:20000	Rabbit	Diagenode	C15310135-20
Apoptosis cocktail	Primary	1:250	Rabbit and mouse	Diagenode	ab136812
	Secondary	1:100	Rabbit and mouse	Diagenode	ab136812

3.3 RNA extraction

6 well plates were set up as described in section 3.1.3. After a 72 hour incubation, the media was removed and the wells washed in 1 ml of PBS. 500 µl of Ribozol reagent (VWR international, UK) was added to each well to denature the cells and extract the RNA. The plate was incubated on a rocker for 5 minutes and then the wells were scraped and contents transferred to RNase free Eppendorf tubes (Thermofisher, UK). The samples were then incubated at room temperature for 10 minutes.

Following incubation, 200 μl of chloroform was added to each tube to cause phase separation. The tubes were shaken vigorously for 15 seconds and then incubated at room temperature for 2 minutes. The samples were then centrifuged for 15 minutes at 12000 x g, at 4 °C, causing separation of the phases, with the RNA being in a clear aqueous layer above lipid and protein sections. This layer was carefully aspirated into a new RNase-free Eppendorf tube, avoiding aspirating any of the organic layers. 250 μl of isopropanol was added to the tube, shaken and then incubated on ice for 10 minutes. The samples were then centrifuged for 10 minutes at 12000 x g, at 4 °C to produce a pellet. The supernatant was removed without disturbing the pellet. 500 μl of 75% ethanol was added to the tube. This was then vortexed to dislodge the pellet, and then centrifuged at 7500 x g for 5 minutes at 4 °C. This was repeated twice to wash the pellet, removing the supernatant each time. After the final wash, it was ensured that all of the ethanol had been removed by aspirating it as close to the pellet as possible without disturbing it. The pellet was then heated at 37 °C with the lid open to dry any excess ethanol. 30 μl of molecular grade water was added to resuspend the pellet, then was heated to 55 °C for 10 minutes.

Using Z-100 software on a computer, the RNA concentration was determined using a Nanodrop 2000 (Thermo Scientific, UK). The amount of RNA was expressed as ng/ μl , the Ribozol contamination absorbance was the 260:280 nm reading, and the isopropanol or ethanol contamination was the 260:230 nm ratio.

3.4 RT qPCR

3.4.1 Reverse transcription

Once the RNA was extracted, 1 μg of RNA was reverse transcribed into cDNA. The amount of μl of RNA for 1 μg was calculated using the ng/ μl readings from the Nanodrop and molecular grade water added to make a final volume of 12.7 μl . The samples were heated at 55 °C for 5 minutes, then spun down in the centrifuge. Meanwhile, a master mix was made up in an Eppendorf, containing 4 μl of 5Xrt-buffer (Promega, UK), 2 μl of 400 nM dNTPs (Bioline, UK), 1 μl of oligo dT primer (Invitrogen, UK) and 0.3 μl of M-MLV reverse transcriptase enzyme (Promega, UK) per sample. 7.3 μl of master mix was added to each sample. These were then placed on a heat block at 37 °C for 1 hour. The samples were then heated to 100 °C for 5 minutes to inactivate the enzyme. 180 μl of molecular

molecular grade water was added to each sample. The cDNA samples were then ready for qPCR (section 3.4.2).

3.4.2 qPCR

RT qPCR monitors the amplification of a targeted DNA molecule in real time. On ice, a master mix was made containing 5 μ l SYBR Green quickstart master mix (Sigma, UK), 0.4 μ l of appropriate forward and reverse primers (Table 3.6), and 2.2 μ l of molecular grade water per reaction. If a standard curve was required for testing primers with new cDNA, the siSCR cDNA was diluted 1:5, 1:10, 1:20 and 1:50 with molecular grade water. 8 μ l of the master mix was pipetted into the wells of a 96 well qPCR micro-plate (Applied biosystems, UK). 2 μ l of the cDNA sample was then loaded into the top of the wells in triplicate. A negative control of molecular grade water was also used. An adhesive PCR plate cover slip (Applied biosystems, UK) was stuck over the plate, ensuring it was flat with no bubbles, and then the plate was spun down using a centrifuge. Next, the plate was placed into the ABI StepOne machine (ThermoFisher, UK), and set up using the StepOne software as required (Table 3.7). A melt curve was ran to observe dissociation aspects of the double stranded DNA during heating, by fluorescence. Once the qPCR had finished, the amplification of the target genes could be observed on graphs and exported into an Excel file. The CT mean could then be used to calculate the expression fold change of *CBX2* mRNA expression, compared with the siSCR. T tests were ran to test the significance, using Graphpad.

Table 3.6. Primers used in qPCR with the catalogue numbers and companies.

Antibody	Company	Sequence (5'-3')
CBX2 forward primer	IDT	GCT CCA AAG CCA GAC TAA CA
CBX2 reverse primer	IDT	CAG GGA CAG ACA TCC TCA TTT C
RPL13A forward primer	Sigma	CCTGGAGGAGGAGAGGAAA-GAGA
RPL13A reverse primer	Sigma	TTGAGGACCTCTGTGTATT-TGTCAA
CDKN1A forward primer	Sigma	CAGCATGACAGATTTCTACC
CDKN1A reverse primer	Sigma	CAGGGTATGTACATGAGGA-G
CDKN2A forward primer	Sigma	AGCATGGAGCCTTCG
CDKN2A reverse primer	Sigma	ATCATGACCTGGATCGG
pS2 forward primer	Sigma	GTGTCACGCCCTCCCAGT
pS2 reverse primer	Sigma	GGACCCCACGAACGGTG
CCND1 forward primer	Sigma	ACTACCGCCTCACACGCTTC
CCND1 reverse primer	Sigma	AGTCCGGGTCACACTTGAT-CA
GREB1 forward primer	Sigma	CAAAGAATAACCTGTTGGCCCTGC
GREB1 reverse primer	Sigma	GACATGCCTGCGCTCTCATACTTA
P21 forward primer	Sigma	AGCATGGAGCCTTCG
P21 reverse primer	Sigma	ATCATGACCTGGATCGG
P16 forward primer	Sigma	CAGCATGACAGATTTCTACC
P16 reverse primer	Sigma	CAGGGTATGTACATGAGGAG

Table 3.7. qPCR run, repeated for 40 cycles, including the temperature and time at each stage.

Stage	Temperature (°C)	Time (m)
Holding stage	95	10:00
Cycling stage (40 cycles)	95	00:15
	60	01:00

3.5 Immunoprecipitation

Immunoprecipitation is the technique of isolating an antigen using a specific antibody, which is immobilised to magnetic beads. Cells were grown at 1 million cells per 10 cm² plate for 72 hours. Plates were then washed with 10 ml of PBS, then the cells scraped into a 15 ml falcon tube each. These were centrifuged for 3 minutes at 1500 x g, then the supernatant removed.

The cells were resuspended in 1 ml of lysis buffer on ice for 30 minutes to release the proteins from the sample. Lysis buffer was made up of 250 µl Tris pH 7.5, 188 µl 4 M sodium chloride (NaCl), 50 µl NP40 non-ionic surfactant, 4.315 ml water, 5 µl 1 M

dithiothreitol (DTT), 50 µl phenylmethane sulphonyl fluoride (PMSF) made from 17.4 mg PMSF stock and 1 ml methanol, and 50 µl of protease inhibitor.

Lysed samples were then transferred to two Eppendorf tubes. These were centrifuged at full speed for 3 minutes, then the supernatant was retrieved into a separate Eppendorf. 50µl of this was separated and frozen as the input sample. 2 µl of CBX2 antibody was added to one tube, 2 µl of rabbit IgG was added to the other tube as an isotype negative control. The tubes were then covered in parafilm and placed on a rotator at 4 °C for 2 hours. Meanwhile, two Eppendorfs were prepared with 25 µl of Dynabeads (Thermofisher, UK) and 1 ml of Triton X-100. A magnet was used to collect the beads to one side of the Eppendorf tube so the Triton X-100 could carefully be removed. 1 ml of Triton X-100 was added again, and the wash repeated three times. Once washed, the beads were resuspended in 30 µl Triton X-100.

Following the 2 hour incubation of the samples, the Triton X-100 was removed and the beads resuspended in the cell-antibody suspension. These were then incubated overnight on the rotator at 4 °C, allowing the antibodies to bind to the beads. The following day, a magnet was used to recover the beads and the supernatant was transferred to a separate Eppendorf as the flowthrough. The beads were then washed with 1 ml of Triton X-100 three times as previously. All supernatant was removed on the final wash. 20 µl of frozen input and flowthrough was aliquotted into separate tubes with 6 µl of SDS loading buffer. 30 µl of SD was added to the negative control, CBX2 and beads. After boiling at 70 °C for 10 mins, these samples were ready to be loaded on a 10% gel for Western blotting.

3.6 Shrimp Alkaline Phosphatase

This was used to test whether CBX2 was phosphorylated in the ER-positive breast cancer cell lines. Firstly, a 10 ml stock of RIPA buffer was made, containing 375 µl NaCl, 500 µl of 50 mM Tris-HCl (pH 8.0), 100 µl NP40, 50 µg of sodium deoxycholate, 10 µg of SDS and the rest ddH₂O. Then an alkaline phosphatase buffer was made, containing 50 ml 1 M Tris-HCl pH 9.0 and 0.5 M MgCl₂. 1 ml of RIPA buffer was added into two Eppendorf tubes. 10 mM of sodium fluoride was added to each tube, then 10 µl of protease inhibitor was added to one of the tubes. Two pellets, each containing 1 million cells, were lysed in 200 µl of RIPA buffer with the inhibitor, and two pellets were lysed in the

one without. These were incubated on ice for 30 minutes to 1 hour. Then 200 µl of the alkaline phosphatase reaction buffer was added to each tube. 160 U/ml (64 µl) of shrimp alkaline phosphatase (rSAP) was added to one Eppendorf containing the protease inhibitor, and one without it. The four Eppendorf tubes were then incubated at 37 °C for 3 hours. The samples could then be boiled with SDS buffer and ran on a Western blot to compare the molecular weights.

3.7 Calf Intestinal Alkaline Phosphatase Treatment

3.7.1 BCA Assay

Protein samples were prepared using Albumin Standard (BSA) (Thermofisher, UK) in separate Eppendorf tubes, and labelled A to I (Table 3.8).

Table 3.8. Preparation of diluted BSA standards.

Vial	Volume of Diluent (µl)	Volume and Source of BSA (µl)	Final BSA Concentration (µg/ml)
A	0	300 of stock	2000
B	125	375 of stock	1500
C	325	325 of stock	1000
D	175	175 of vial B dilution	750
E	325	325 of vial C dilution	500
F	325	325 of vial E dilution	250
G	325	325 of vial F dilution	125
H	400	100 of vial G dilution	25
I	400	0	0 = blank

Next, the volume of the BCA working reagent (WR) was determined, using the following formula:

$(\# \text{ standards} + \# \text{ unknowns}) \times (\# \text{ replicates}) \times (\text{volume of WR sample}) = \text{total volume of WR required}$

The WR was then prepared by mixing 50:1 BCA reagent A: BCA reagent B, in a falcon tube. As the sample sizes were limited, 10 µl of each unknown sample and standard was pipetted into the wells of a 96 well plate in triplicate. 200 µl of WR was then added into each of these wells. The plate was mixed on a plate shaker for 30 seconds, then it was covered with foil and incubated at 37 °C for 30 minutes. This was then cooled to room

temperature, and the absorbance measured at 595 nm on a spectrophotometer. The readings could be used to calculate the volume of protein required for 20 µg on Excel.

3.7.2 CIP

Meanwhile, 100 ml of calf intestinal alkaline phosphatase (CIP) buffer was made up, containing 2.5 ml of NaCl, 5 ml of Tris-HCl, 2 ml of MgCl₂, 100 µl DTT and the rest ddH₂O. This was pH to 7.9 at 25 °C. Two Eppendorf tubes each containing one million cells were suspended in 50 µl of immunoprecipitation lysis buffer (section 3.5), and left on ice to lyse for 1 hour. Two Eppendorf tubes were prepared with the appropriate volume calculated in the BCA assay. These were resuspended in 1 µg of protein per 10 µl of buffer, in this case, 200 µl of CIP buffer. One unit of CIP per µg of protein was added to one Eppendorf tube. Both samples were then incubated for 1 hour at 37 °C. SDS sample buffer was added so the samples could be ran on a Western blot.

3.8 Nuclear and Cytoplasmic Extraction

This is the method of separating and preparing cytoplasmic and nuclear extracts from cultured cells using the NE-PAR Nuclear and Cytoplasmic Extraction kit (Thermofisher, UK), following manufacturers instructions. 200 µl of CER I was added to two cell pellets each containing 1 million cells. These were vortexed for 15 seconds, and then the contents placed into one Eppendorf tube. This was incubated on ice for 10 minutes. Then, 11 µl of CER II was added to the cell pellet. This was vortexed for 5 seconds, incubated on ice for 1 minute, vortexed a further 5 seconds and then centrifuged for 5 minutes at maximum speed. This caused cell pellet disruption and the release of cytoplasmic contents. The cytoplasmic extract supernatant was transferred to another tube. The pellet was then resuspended in 100 µl of NER and vortexed for 15 seconds every 10 minutes for 40 minutes, keeping on ice in between. After this, the tube was centrifuged at full speed for 10 minutes, releasing the nuclear proteins. The supernatant of this was the nuclear extract, and was transferred to another Eppendorf. The remaining pellet was the chromatin extract. 40 µl of SDS was added to the cytoplasmic extract, 20 µl to the nuclear extract and 50µl to the chromatin. These samples could then be ran on a Western blot.

3.9 MTS Assay

MTS (3-(4,5-dimethylthiazol-2-yl)-5-(3-carboxymethoxyphenyl)-2-(4-sulfophenyl)-2H-tetrazolium) assay (abcam, UK) is a colorimetric method for measuring cell proliferation. MTS produces a formazan product, from the reduction of MTS tetrazolium compound by NAD(P)H dehydrogenases, changing colour in the presence of proliferating cells. Firstly, the cells were trypsinised and counted as in section 3.1.1. 2500 cells were required per well for MCF-7 cells, and transfection mixes were made as in section 3.1.2. In a 96 well plate, a border of 100 μ l cells in full media was placed around the transfected cells. In the centre of this in columns, 5 μ l of transfection mix was placed in each well, and 100 μ l of cells in full media was added. The plates were configured so that each condition (siSCR, siCBX2-3 and si-CBX2-4 transfected cells) were analysed in triplicate wells. This was repeated to have four 96 well plates in total, so they could be read at 24, 48, 72 and 96 hour time points. After incubating for the required number of hours, 10.5 μ l of MTS reagent was added to the central wells to be analysed. The plate was incubated for 3 hours at 37 °C. The plate could then be read on the plate reader (BioTek instruments, UK) at 490 nm, using KC4 software (BioTek instruments, UK) to measure the amount of and therefore the relative number of proliferating cells at each timepoint and in each condition.

3.10 Phase Contrast Microscopy

This was used to take bright field photographs of the cells. Firstly, the Axio Vert-A1 microscope (Zeiss, Germany) was set to bright field. The cells were focussed using the microscope. Then the shutter on the microscope was opened to allow for viewing on the computer, using ZEN software (Zeiss, Germany). The magnification was set to 5 \times , and it was ensured bright field was selected. The software was then set to live and exposure to set in order to view the cells. These could then be photographed and saved with a scale bar added.

3.11 Apoptosis Assay

The cells were plated into three 6 well plates and lysed as in section 3.1.3. The media was removed into a 15 ml falcon, then the wells were washed with PBS. The PBS was then added to the falcon tube, which were then centrifuged for 3 minutes at 1500 x g. The supernatant was removed from the tube, then the cell pellet was lysed along with

the cells adhered to the 6 well plate with SDS, after 24, 48 and 72 hours. The amount of SDS added accounted for the floating cells from the media. These protein lysates are then ran on a 10% gel for a Western blot. Apoptosis cocktail primary and secondary antibodies were used (Table 3.5), containing β -actin, and the apoptosis biomarkers pro-caspase, cleaved caspase 3 and cleaved PARP.

3.12 RNA Sequencing

The cells were transfected and incubated for 72 hours as in section 3.1.2. RNA was extracted from transfected cells using an RNeasy mini kit (Qiagen), following manufacturers instructions. Cells were lysed using 350 μ l per well of Buffer RLT, then the cells were scraped and contents transferred to RNase free Eppendorf tubes. 350 μ l of 70% ethanol was added to each tube, pipetting up and down to mix. 700 μ l of this was then transferred into a spin column within a 2 ml collection tube. These were centrifuged for 15 seconds at 8000 x g. The flowthrough was discarded from the collection tube, ensuring the liquid did not touch the filter of the spin column. Following this, 700 μ l of Buffer RW1 was added to wash the pellet, then the tube was centrifuged again at 8000 x g for 15 seconds. After discarding the flowthrough, 500 μ l of Buffer RPE was added, inverting the tube to cover the sides. This was centrifuged at 8000 x g for 15 seconds, then the flowthrough discarded. 500 μ l of Buffer RPE was added again, then centrifuged at 8000 x g for 2 minutes. The spin column was then placed in a clean tube and centrifuged at maximum speed for 1 minute to dry the membrane. Finally, 30 μ l of RNase-free water was added to the column, directly onto the filter. The column was placed within a 1.5 ml collection tube and centrifuged for 1 minute at 8000 x g. The samples were read on the Nanodrop, as explained in section 3.3.

The samples required were three repeats of siSCR, siCBX2-3 and siCBX2-4, all with 2.0 or above readings for the 260:280 nm and 260:230 nm ratios. These were then aliquoted and sent to Novogene for analysis on dry ice. All of the samples passed the quality control (QC) testing by an Agilent bioanalyser, having RNA integrity numbers (RIN) of over 8.0. Therefore Novogene produced a cDNA library then sequenced the RNA using the Illumina PE150 HiSeq platform. Novogene performed all bioinformatic and QC analysis. The differentially expressed genes were compared to all genes within the KEGG pathway database to see which were involved, and therefore statistically significant.

When this was sent back to the laboratory, Dr Mark Wade conducted further gene set enrichment analysis from this data.

3.13 Statistical analysis

To analyse the statistical significance of three repeats from RT-qPCR data, student's T tests were conducted using Graphpad, testing the differences of the siRNAs relative to the siSCR control.

Chapter 4: Results

4.1 Knockdown of CBX2 confirmed by RT-qPCR

Firstly, it was required to confirm whether the CBX2 targeting siRNAs depleted *CBX2* mRNA. *CBX2* mRNA expression was analysed by qPCR. MCF-7 and T47D cells were transfected with a non-silencing siRNA (siSCR) and three independent CBX2 targeting siRNAs, siCBX2-1, siCBX2-3 and siCBX2-4, then incubated for 72 hours. The RNA was extracted then reverse transcribed to produce cDNA. qPCR was then performed using CBX2 primers and primers for the housekeeping gene RPL13A as a normalising control to test the effect of CBX2 knockdown in at least three independent repeats (Figure 4.1). The expression fold change of *CBX2* mRNA in CBX2 targeting siRNA transfected cells, compared to siSCR, was analysed using students T test. For both cell lines, it was observed that *CBX2* gene expression was significantly lower in the cells transfected with CBX2 targeting siRNAs compared to cells transfected with siSCR ($p < 0.05$).

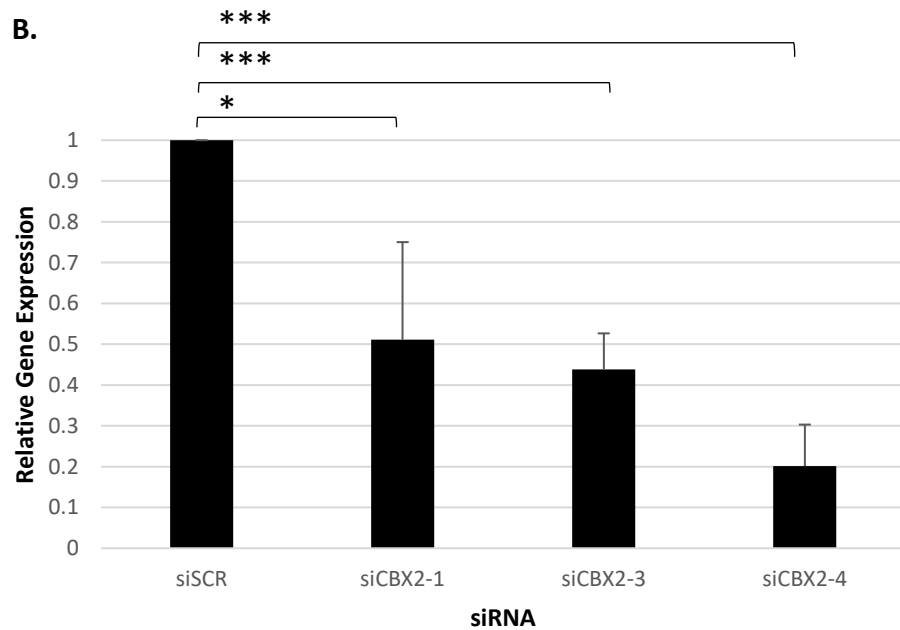
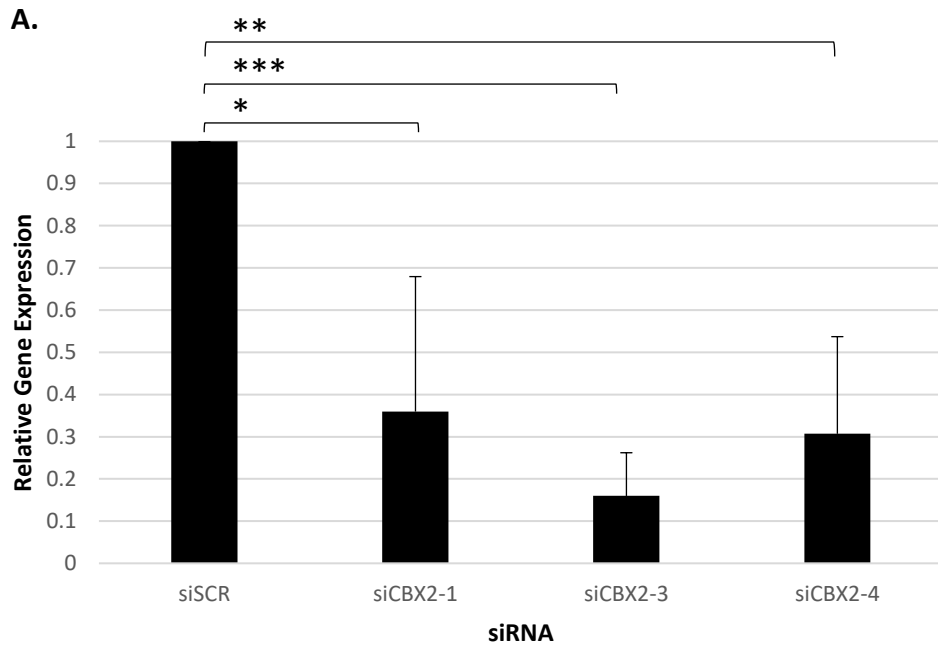


Figure 4.1. Relative *CBX2* mRNA expression in siCBX2-1, 3 and 4 transfected MCF-7 (A) and T47D (B) cells. qPCR data are an average of 3 (T47D) or 4 (MCF-7) repeats \pm SEM and are expressed relative to gene expression in siSCR transfected cells. *P* values were determined by Student's *T* test. A. (4 repeats): * = significant ($p < 0.05$), ** = very significant ($p < 0.01$), *** = extremely significant ($p < 0.001$). B. (3 repeats): * = significant ($p < 0.05$), *** = extremely significant ($p < 0.001$).

4.2 Knockdown of CBX2 confirmed by Western blot

Following confirmation that CBX2 targeting siRNA reduced *CBX2* mRNA levels, the effect of knockdown on CBX2 protein expression was assessed. As above, MCF-7 and T47D cells were transfected using a non-silencing siSCR control and three independent CBX2 targeting siRNAs, siCBX2-1, siCBX2-3 and siCBX2-4, then incubated for 72 hours prior to protein extraction. Western blots were performed to assess CBX2 protein levels, using antibodies specific to CBX2 and alpha tubulin (Figure 4.2; Supplementary Figure 1-5). For both cell lines, it was observed that a protein band at 72 kDa was lost in cells transfected with CBX2 targeting siRNAs, compared to cells transfected with siSCR. The alpha tubulin levels remained consistent for each protein lysate, indicating equal loading and therefore that the 72 kDa band knockdown was genuine.

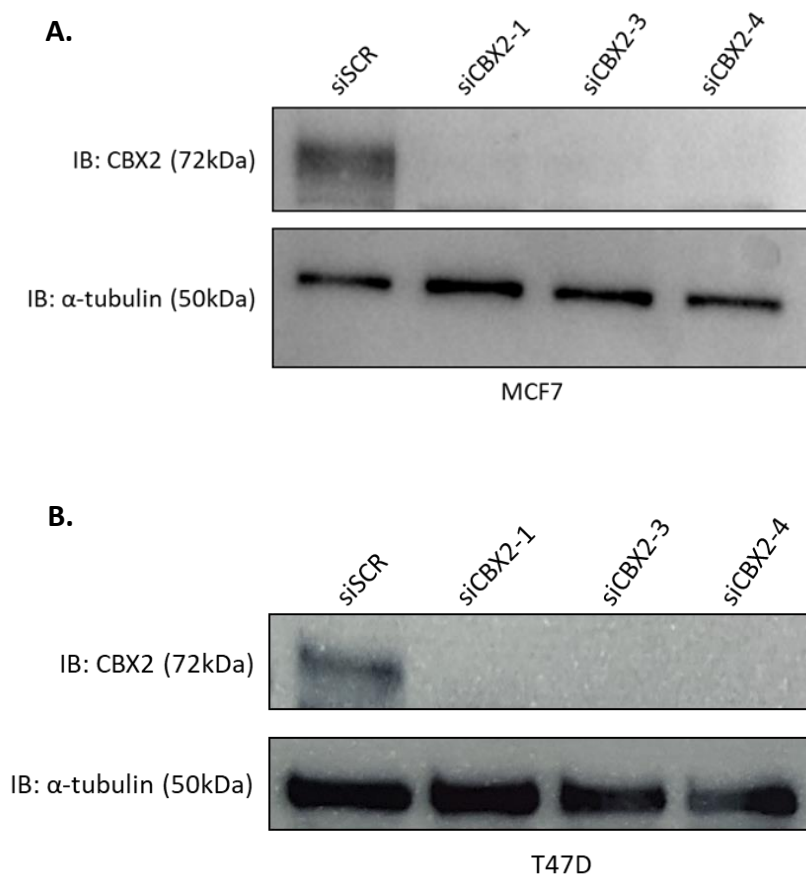


Figure 4.2. Western blot showing CBX2 knockdown in MCF-7 (**A**) and T47D (**B**) cells. Antibody used and molecular weight of protein bands observed is indicated to the left of the blots (IB = Immunoblot). Lysates from cells transfected with different siRNAs (siSCR, siCBX2-1/3/4) are indicated above relevant lanes. Representative images from numerous repeats.

4.3 CBX2 at 72kDa is a phosphorylated form of the protein

It was expected that CBX2 would be observed by Western blot at 56 kDa molecular weight, as was quoted by the manufacturers and is the expected molecular weight of CBX2 (Uniprot.org, n.d.). The previous knockdown Western blot data using three independent siRNAs consistently observed knockdown of a band at 72 kDa. A band at 72 kDa was observed in previous studies by Di Costanzo et al (2018) in K562, U937 and HL-60 leukaemia cells, and it was determined that this was an active phosphorylated form of CBX2. It was therefore investigated whether the 72 kDa band observed in the study is a phosphorylated version of CBX2.

MCF-7 protein lysates were dephosphorylated using shrimp alkaline phosphatase, and compared to a lysate not treated with phosphatase enzyme, on a Western blot. These experiments did not work, with the Westerns consistently failing, possibly due to the amount of buffers used. Therefore, this was repeated using calf intestinal alkaline phosphatase (CIP) to dephosphorylate an MCF-7 protein lysate, compared to an MCF-7 protein lysate not treated with the phosphatase enzyme. Phosphatase treated and control lysates were analysed by Western blot, using antibodies specific for CBX2 and alpha tubulin (Figure 4.3). Alpha tubulin showed equal loading between lysates. In non-CIP treated cells, the CBX2 band was present, albeit faintly, at 72 kDa, however the band for CBX2 in CIP treated cells was lower. Although this result was from a single experiment (due to time constraints), it may indicate that the CBX2 band at 72 kDa was a phosphorylated protein.

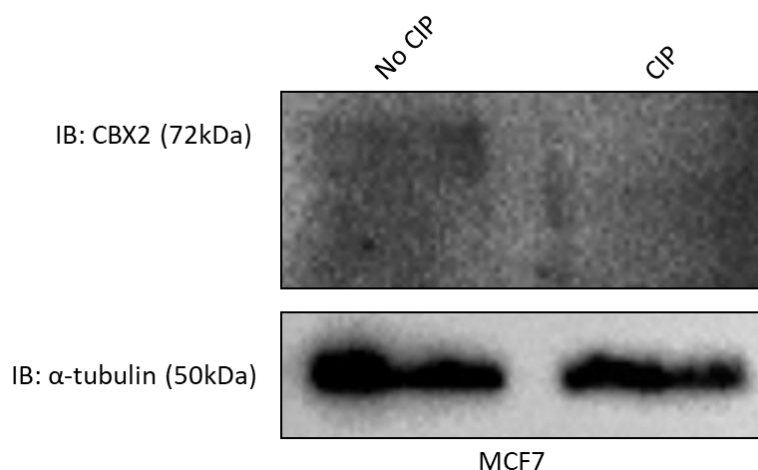


Figure 4.3. Western blot showing CBX2 phosphorylation in MCF-7 cells. Antibodies used (CBX2 and alpha tubulin loading control) indicated to left of blots. Cells incubated with no CIP or CIP indicated above relevant lane.

4.4 CBX2 is localised in the nucleus

The CIP results indicated that CBX2 was phosphorylated at 72 kDa. It is shown in the literature that the phosphorylated version of CBX2 is present in the nucleus compared to the cytoplasm (Kawaguchi et al., 2017). Therefore, CBX2 localisation was investigated to further support the hypothesis that the 72 kDa band identified is genuinely CBX2. MCF-7 and T47D cells were fractionated into cytoplasmic and nuclear components. These were then ran on a Western blot using a CBX2 antibody and alpha tubulin as a known cytoplasmic marker (Figure 4.4; Supplementary Figure 6-8). See Supplementary Figure 9 for a full blot with the molecular marker. In both cell lines, CBX2 appeared at 72 kDa only within the nuclear fraction. Alpha tubulin was present in the cytoplasmic fraction as expected, with only a small amount of crossover to the nuclear fraction, showing that the fractionation was not completely efficient.

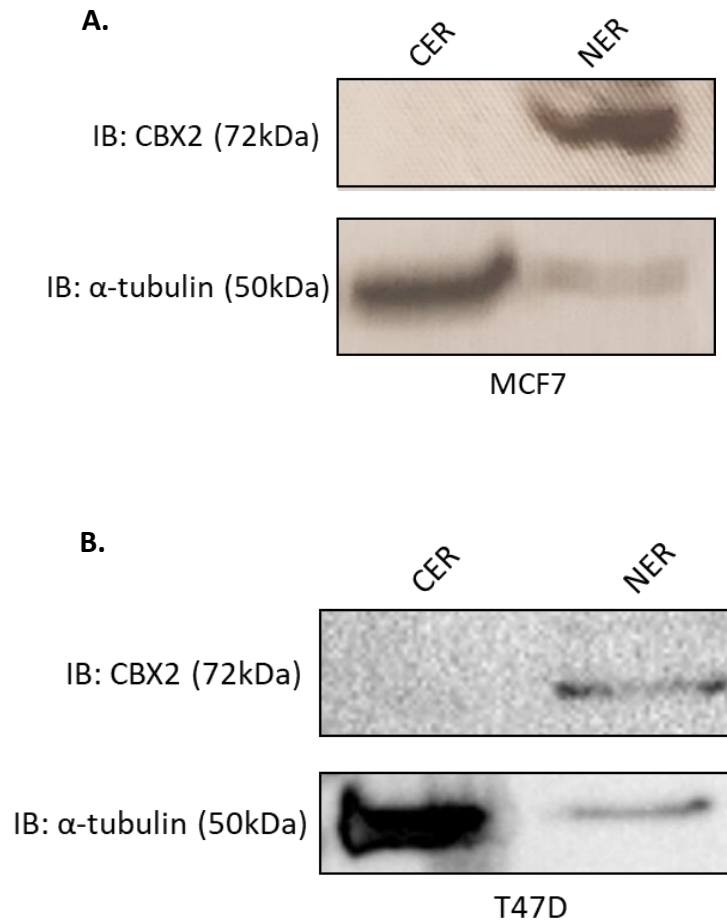


Figure 4.4. Western blot showing CBX2 located in the nucleus and alpha tubulin in the cytoplasm, in MCF-7 (**A**) and T47D (**B**) cells. CER = cytoplasmic extract, NER = nuclear extract.

4.5 CBX2 isolated by immunoprecipitation

Finally, it was determined whether CBX2 could be isolated by immunoprecipitation and whether this would also be detected at 72 kDa. MCF-7 cells were lysed then incubated with either a CBX2 antibody or an IgG negative control. Magnetic beads were used to bind the antibodies, then the proteins were taken out of the lysate and ran on a Western blot (Figure 4.5; Supplementary Figure 10). The membrane was incubated with the CBX2 antibody. CBX2 was shown to be at 72 kDa in the sample incubated with the CBX2 antibody, but not in the IgG control, adding further evidence that the 72 kDa band detected is genuinely CBX2.

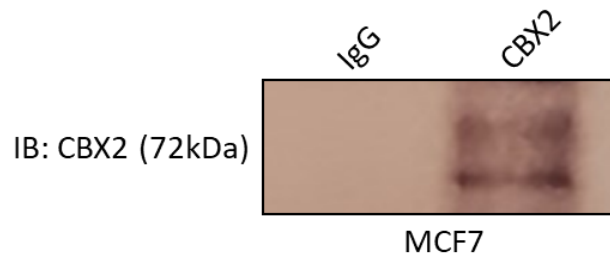


Figure 4.5. Immunoprecipitation Western blot, showing CBX2 in MCF-7 cells. Lysates immunoprecipitated with IgG or CBX2 antibodies are indicated above relevant lanes.

4.6 Effect of CBX2 knockdown on histone modifications

The next investigation was to determine whether CBX2 impacts the relevant histone modifications H2AK119ub, H3K27me3 and H3K27ac. These were investigated because CBX2 recognises and binds to H3K27me3 marks (trimethylated by the PRC2 complex) and recruits the PRC1 complex which ubiquitinates lysine 119 on histone H2A. H3K27ac was investigated because it is a transcriptionally activating mark, and is on the same lysine as the trimethylation mark. If H2AK119ub was to reduce following CBX2 knockdown, this would indicate that the lack of CBX2 is stopping PRC1 function. The effect of CBX2 knockdown on the other two histone modifications is unknown.

Protein lysates were extracted from MCF-7 and T47D cells transfected with the siSCR control and three CBX2 targeting siRNAs (siCBX2-1, siCBX2-3 and siCBX2-4), and analysed by Western blot using antibodies specific for H2AK119ub and its loading control, H2A-pan (Figure 4.6; Supplementary Figure 11-13). H2A-pan was used as a loading control because it looks at the whole histone, rather than a specific modification. siCBX2-4 was consistently low for both H2AK119ub and H2A-pan in T47D cells, but there was little change for the other CBX2 targeting siRNAs compared to the siSCR. The H2A-pan was equal for siSCR, siCBX2-1, and siCBX2-3, indicating that CBX2 had no effect on global H2AK119 ubiquitination in T47D cells. This was also the case for one of the MCF-7 blots. However, for another blot, there was a reduction in H2AK119ub in siCBX2-4 when H2A-pan was equal for all other siRNAs.

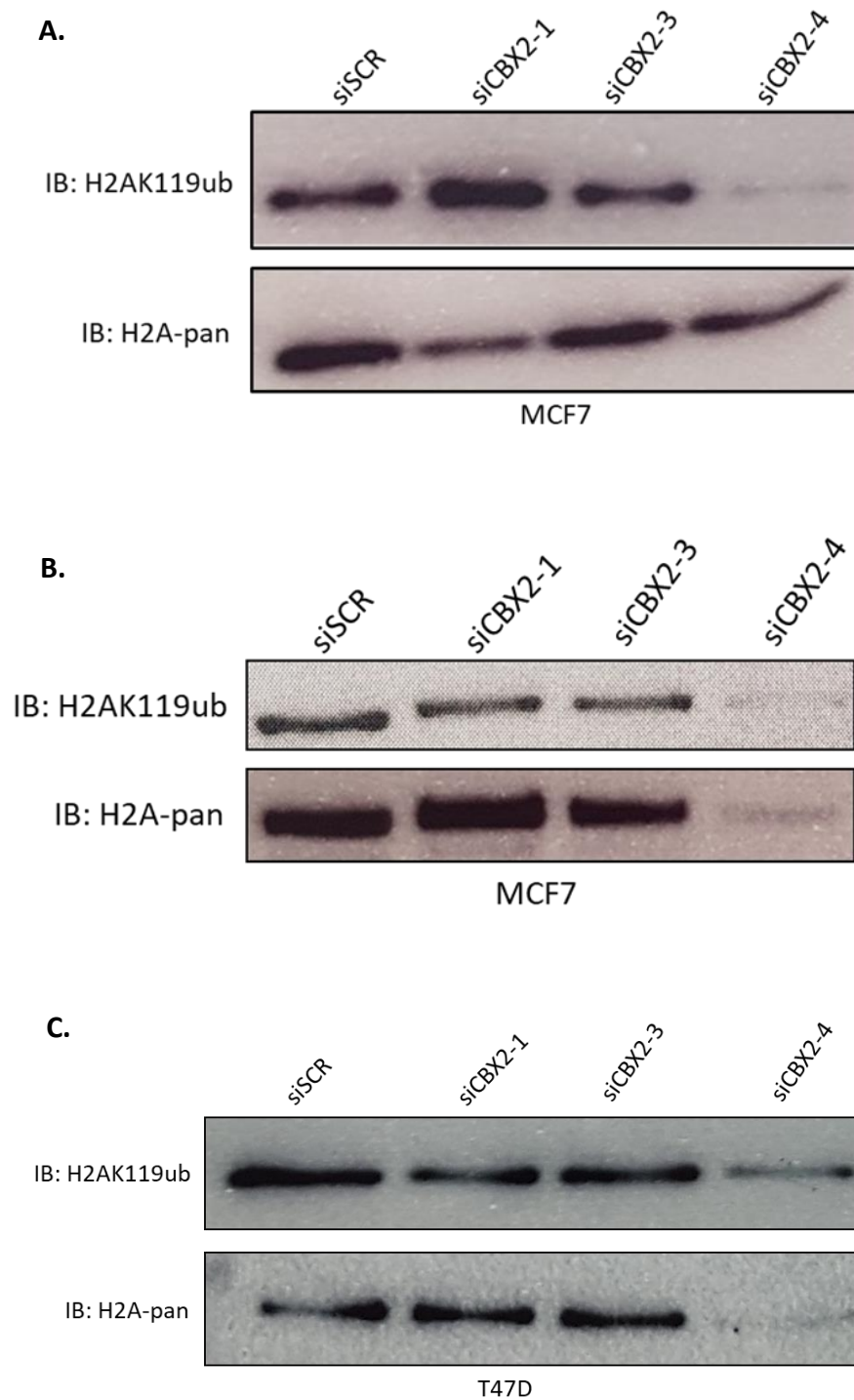


Figure 4.6. Western blot probed for H2AK119ub and a H2A-pan loading control, using MCF-7 (A, B) and T47D (C) cells. Protein lysates transfected with an siSCR control and three knockdown siRNAs (siCBX2-1/3/4) indicated above relevant lanes.

Furthermore, the effect of CBX2 knockdowns on H3K27me3 was investigated. Protein lysates were extracted from MCF-7 and T47D cells transfected with the siSCR control and three CBX2 targeting siRNAs (siCBX2-1, siCBX2-3, siCBX2-4) and analysed by

Western blot, using antibodies specific for H3K27me3 and its loading control, H3-pan (Figure 4.7; Supplementary Figure 14-17). There was little change between the H3-pan loading control and H3K27me3.

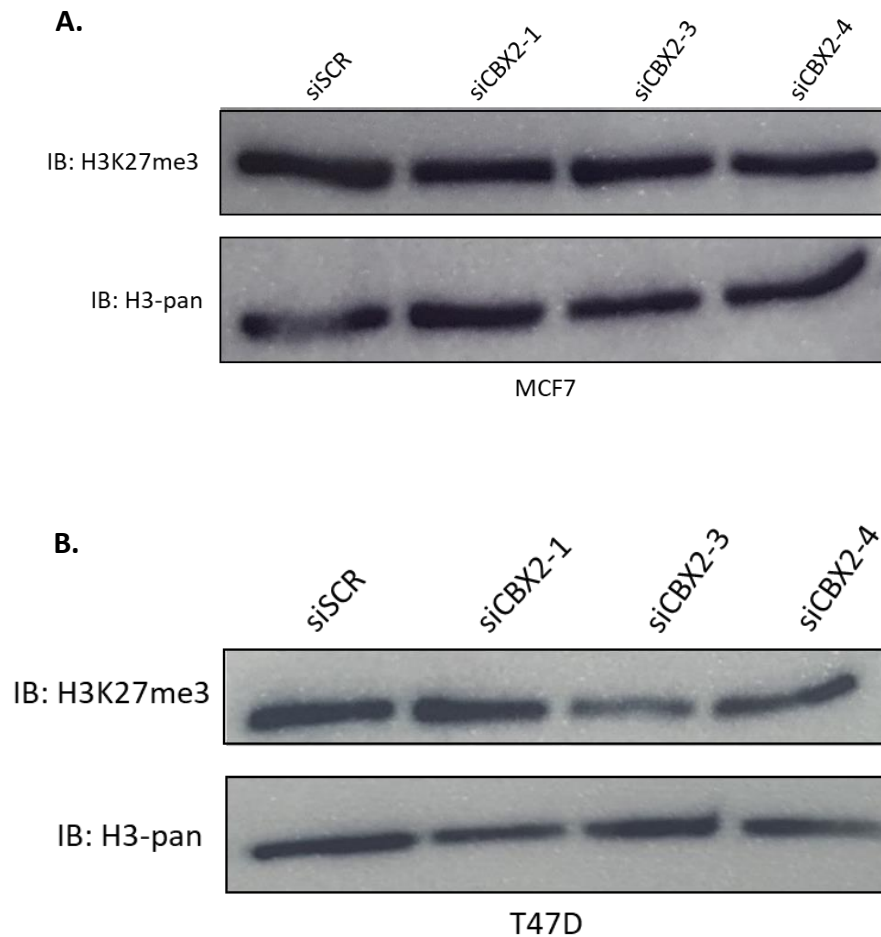


Figure 4.7. Western blot probed for H3K27me3 and a H3-pan control, using MCF-7 (A) and T47D (B) cells, transfected with siSCR control and siCBX2-1, siCBX2-3 and siCBX2-4 (indicated above lanes).

The final mark assessed was H3K27ac. Protein lysates from MCF-7 and T47D cells were analysed by Western blot, using antibodies specific for H3K27ac and its loading control, H3-pan (Figure 4.8; Supplementary Figure 18-21). CBX2 knockdown decreased H3K27 acetylation while the loading of the H3-pan was fairly equal across the repeats.

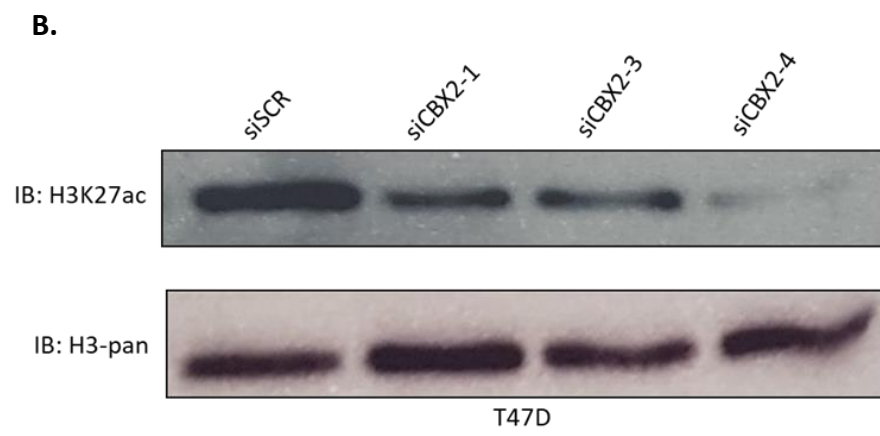
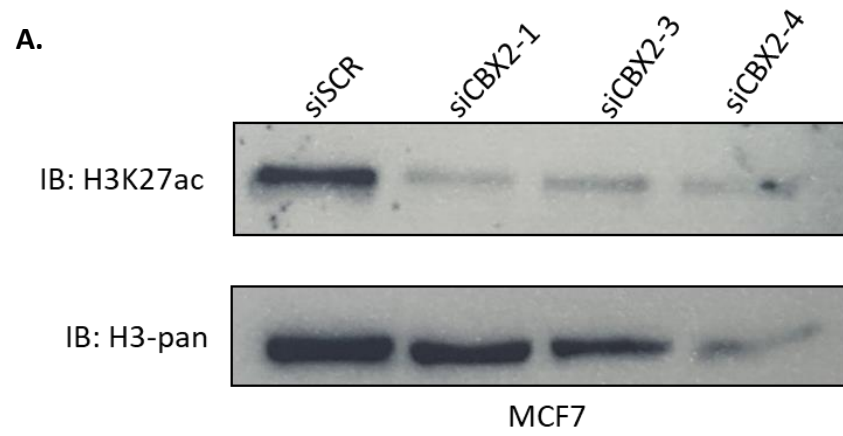


Figure 4.8. Western blot showing the effect of CBX2 knockdown on H3K27ac and its loading control, H3-pan, in MCF-7 (A) and T47D (B) cells. siRNA transfections indicated above relevant lanes.

4.7 CBX2 knockdown reduces cell growth

Unpublished data from the group show that there is a decrease in cell number 72 hours post transfection with CBX2 targeting siRNA, compared with siSCR transfected cells. The reason why there is a decrease in cell number was investigated with two phenotypic experiments, with the knowledge of MCF-7 (Sutherland et al., 1983) and T47D (ATCC, 2012) doubling times. The first was an MTS assay which investigated whether CBX2 knockdown has an impact on cell proliferation. MCF-7 cells were transfected in 96 well plates with siSCR, siCBX2-3 and siCBX2-4, then incubated with MTS reagent. MTS plates were read after 24, 48 and 72 hours. After 48 hours, the growth of the siCBX2-3 and 4 transfected cells slowed compared with the siSCR, though not significantly ($p>0.05$) (Figure 4.9). This was also tested once in T47D cells, but did not work due to the slow growth rate of these cells (Supplementary Figure 22).

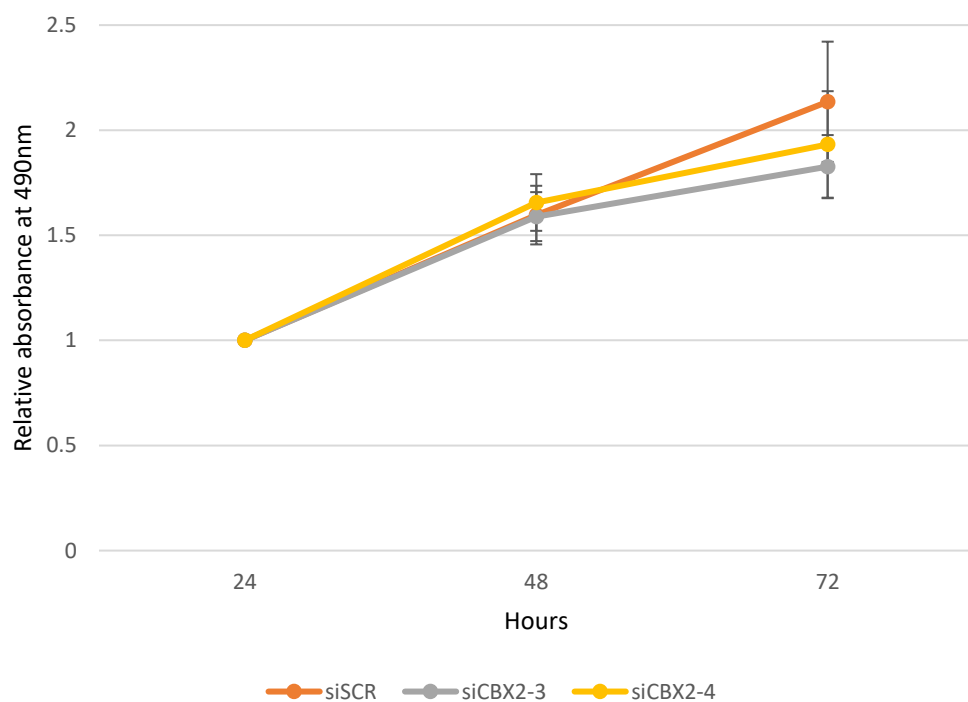


Figure 4.9. MTS assay graph showing effect of CBX2 knockdown on cell proliferation in MCF-7 cells, measured at 490nm. Cells transfected with siCBX2-3 and 4 compared with the siSCR, over three time points (24, 48, 72 hours), with three repeats. Data normalised to 1 at 24-hour time point; 48- and 72-hour time points relative to absorbance at 24 hours. Error bars +/- SEM.

To further support that CBX2 knockdown reduces cell proliferation rate, cells were photographed by phase-contrast microscopy. MCF-7 and T47D cells were transfected using the siSCR control and the three CBX2 targeting siRNAs, siCBX2-1/3/4, then

incubated for 72 hours. The cells were then imaged with a phase-contrast microscope with bright-field setting (Figure 4.10; Supplementary Figure 23). See Supplementary Figure 24 for cells at a larger magnification. It can be observed that cell numbers decreased in the siRNA knockdowns compared to the siSCR. The morphology of the cells also changed upon knockdown as both cell lines became rounder, indicating that cells were potentially dying.

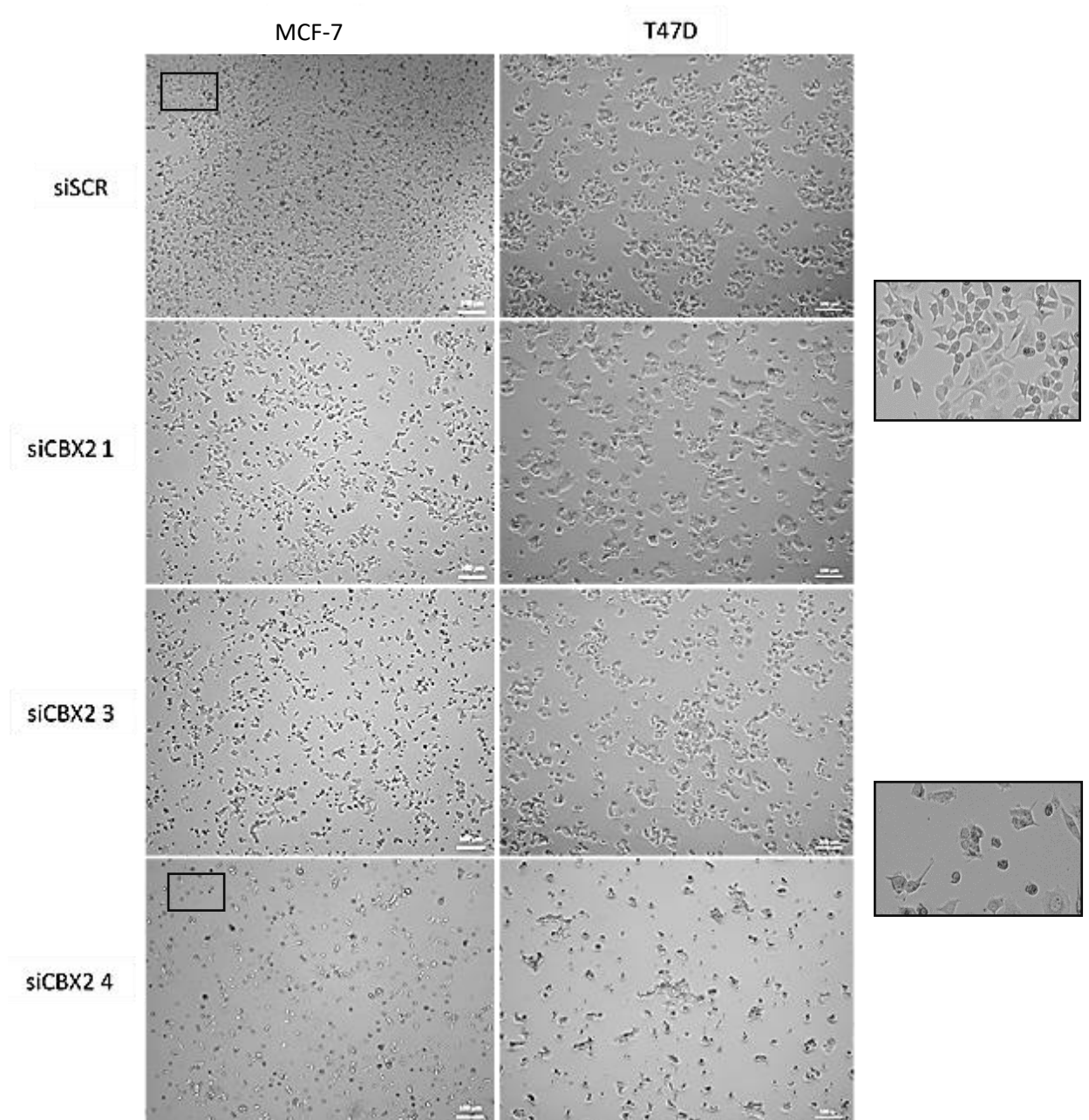


Figure 4.10. Microscopy images of MCF-7 and T47D cells, transfected with siSCR and siCBX2-1/3/4. Scale bar size: 100 μ m. MCF-7 cells decreased in number and became rounder compared with the siSCR, especially in siCBX2-4, as indicated by the magnified boxes. T47D cells also decreased in number and became rounder and slightly larger compared with the siSCR.

4.8 CBX2 causes cell apoptosis

After showing results indicating that CBX2 knockdown reduces cell proliferation, and the fact cells seemed to be dying when viewing them down the microscope, a second phenotypic experiment was undertaken to investigate the effect of CBX2 knockdown on cell death. Western blot analysis for markers of apoptosis were performed on siSCR and siCBX2-1/3/4 transfected MCF-7 cells after 24, 48 and 72 hour incubation. Protein lysates were run on a Western blot, using an apoptosis cocktail antibody, containing the apoptosis markers pro-caspase, cleaved caspase 3, cleaved PARP, and a β -actin loading control (Figure 4.11; Supplementary Figure 25). This was also tested in T47D cells (Supplementary Figure 26), but did not work, potentially due to these cells having a longer doubling time. CBX2 knockdown was also confirmed in MCF-7 cells using the CBX2 antibody. The apoptosis marker, cleaved PARP, was shown to increase after 48 hours in siCBX2-3 and siCBX2-4, indicating that CBX2 does indeed cause cell death. Beta-actin was equal across the lysates.

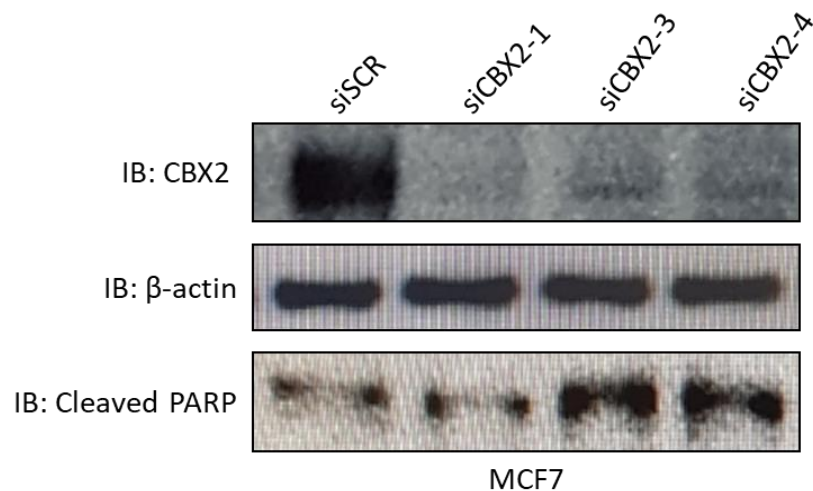


Figure 4.11. Western blots showing CBX2 knockdown effect on cell apoptosis in MCF-7 cells. Antibodies on left: CBX2, a beta-actin loading control and the apoptosis marker cleaved PARP. Cells transfected with siSCR, and siCBX2-1/3/4, indicated above relevant lanes.

4.9 RNA-Sequencing

4.9.1 RNA-Seq samples passed QC

Following phenotypic experiments analysing the decrease in cells after CBX2 knockdown, RNA-Seq was used to analyse the effect of CBX2 knockdown on the MCF-7 gene expression profile. This enabled genes to be identified which CBX2 may regulate. The company Novogene analysed the RNA integrity (RIN) of triplicate RNA samples extracted from MCF-7 cells, transfected with siSCR, siCBX2-3 and siCBX2-4 for quality control (Table 4.1). All RIN numbers were above 8.0, indicating the RNA quality was good enough for sequencing.

Table 4.1. Each sample with the RIN number. ER = ER-positive, SCR = siSCR, CB3 = siCBX2-3, CB4 = siCBX2-4, 1,2,3 = number of repeats.

Sample Name	RIN
ER SCR 1	9.8
ER SCR 2	9.7
ER SCR 3	9.3
ER CB3 1	9.9
ER CB3 2	9.9
ER CB3 3	9
ER CB4 1	9.5
ER CB4 2	9.7
ER CB4 3	8.6

Following sequencing, Novogene then quality checked the data to see if the gene expression profiles of the biological replicates were similar to each other, using Pearson correlation coefficient between the samples. Triplicate samples from the same experimental condition were most similar to each other (Figure 4.12), therefore indicating that no mix up in samples had occurred and that experimental conditions were consistent between the replicates.

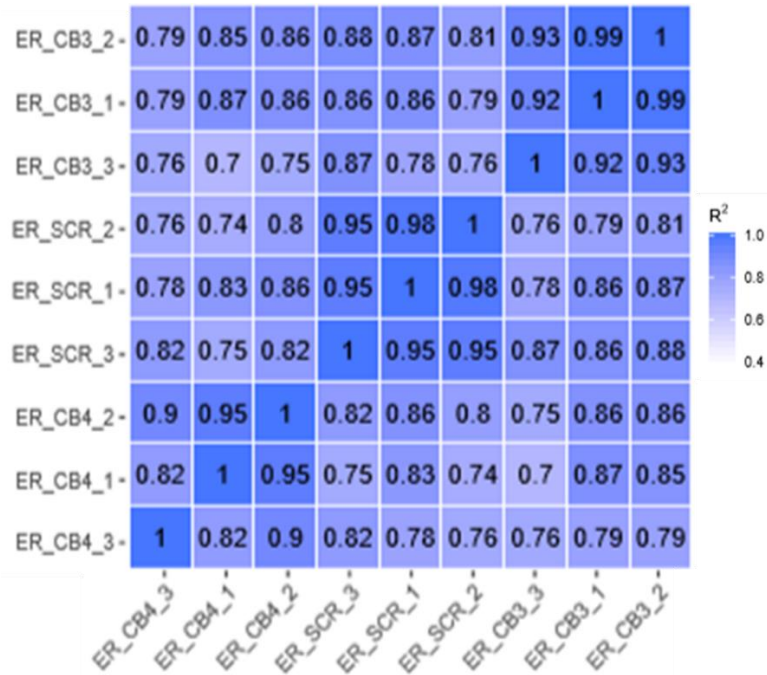


Figure 4.12. A Pearson correlation coefficient between triplicates of RNA samples (siSCR, siCBX2-3, siCBX2-4). Each is compared, using an R^2 number to represent biological similarity. All compared siRNA triplicates above 0.8, therefore significant.

4.9.2 Cluster heat map

After confirming that the quality of the RNA samples, Novogene analysed all of the genes within the siSCR, siCBX2-3 and siCBX2-4 RNA samples once the replicates were combined. These were plotted on a cluster heat map to view the overall expression profiles (Figure 4.13). This shows how similar the profiles are for each transfection condition, with siSCR and siCBX2-3 transfected cell transcriptomes being more similar to each other than siCBX2-4.

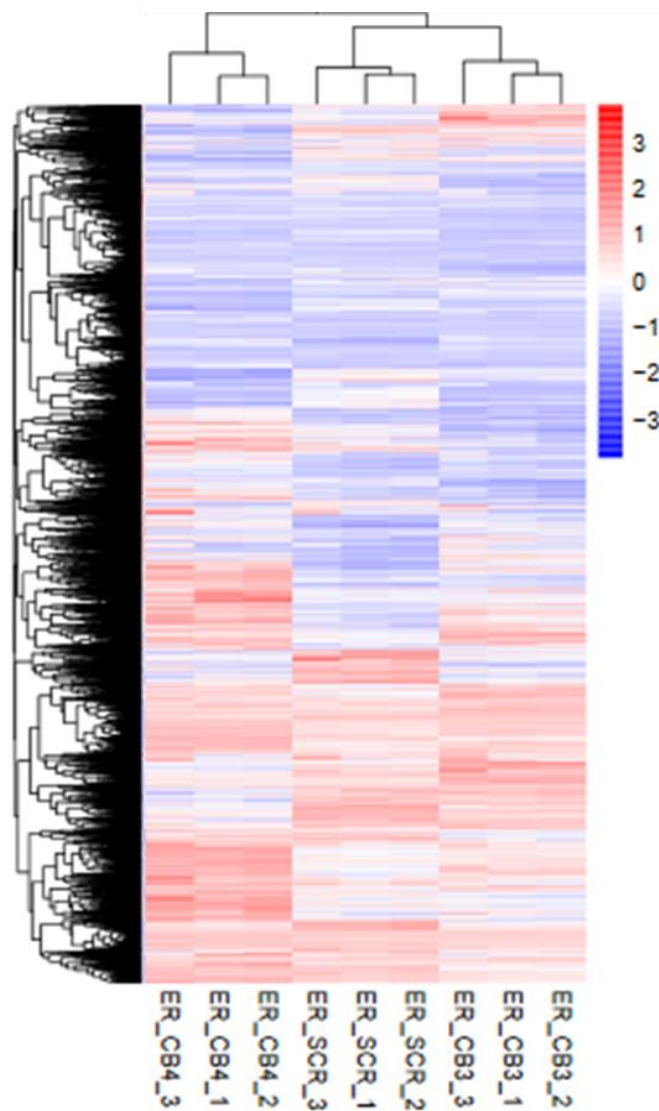


Figure 4.13. Cluster heat map showing gene expression in siSCR, siCBX2-3 and siCBX2-4 repeat samples (individual samples indicated along the bottom). Blue = low expression, red = high expression, white = medium. Cluster analysis along the top shows that siSCR and siCBX2-3 samples are most closely related.

4.9.3 More genes are upregulated

Initial analysis was done to compare gene expression profiles of cells transfected with siSCR and siCBX2-4. The number of significantly differentially regulated genes, following CBX2 knockdown was analysed (Figure 4.14), presenting this on a volcano plot. This showed there being more genes significantly upregulated (4280) than downregulated (2776), following CBX2 knockdown.

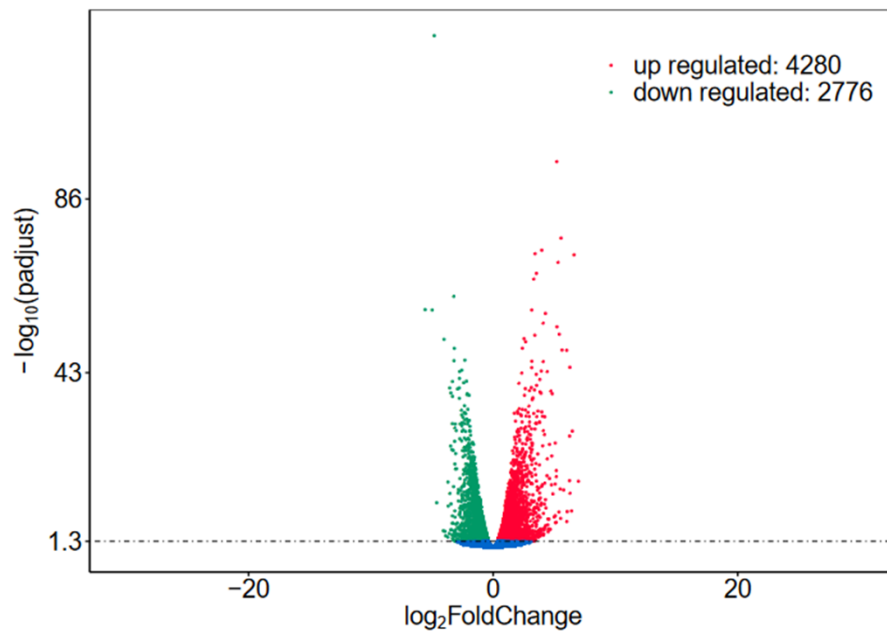


Figure 4.14. A volcano plot showing 4280 genes being significantly up regulated and 2776 genes significantly down regulated in siCBX2-4 compared with siSCR ($p < 0.05$). Each dot represents a different gene. The X-axis is the \log_2 of the fold change between the siCBX2-4 and siSCR. The higher up the Y-axis the plot is, the more significant the difference in expression for that particular gene.

4.9.4 Top 20 enriched pathways

After showing the general gene expression profiles, specific pathways enriched for differentially regulated genes were identified. The CBX2 differentially expressed genes were compared to all genes in a KEGG pathway database using gene ontology. This then produced a list of the top 20 pathways enriched for genes differentially regulated, following CBX2 knockdown (Figure 4.15). Highlighted pathways that CBX2 is involved in include the cell cycle, pathways in cancer, and the p53 signalling pathway.

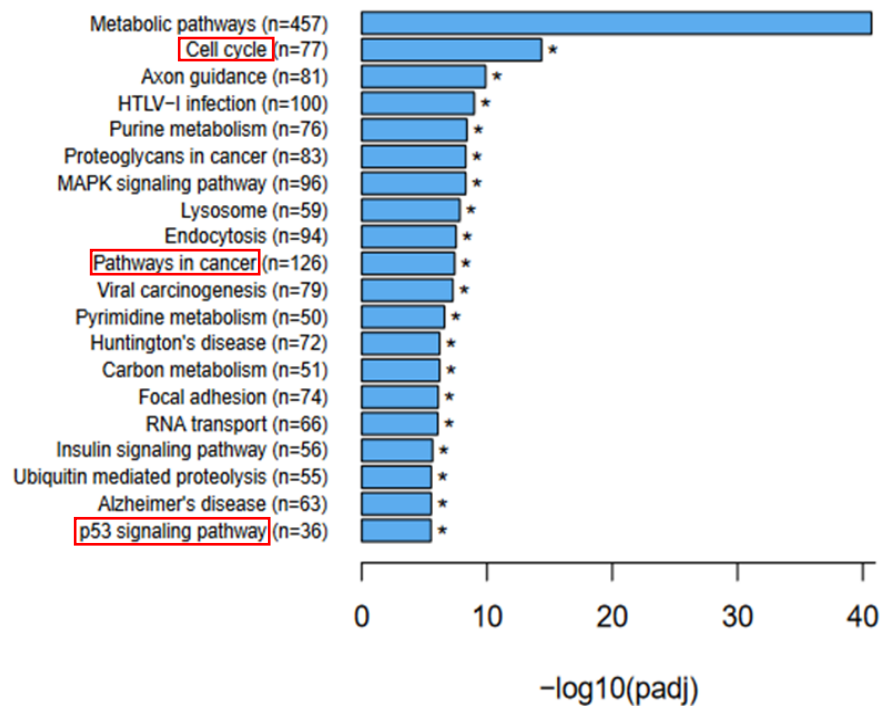


Figure 4.15. The top 20 pathways that CBX2 is significantly involved in, with the number of genes regulated in each pathway ($p < 0.05$). Pathways of interest highlighted within red boxes. X-axis - \log_{10} = adjusted p value, Y-axis = 20 enriched pathways. n = number of genes differentially expressed that belong to that pathway.

4.9.5 CBX2 in the cell cycle

As the cell cycle was one of the top enriched pathways from the KEGG pathway database, this was investigated in greater detail. In the cell cycle diagram (Figure 4.16), the genes boxed in red were upregulated, following CBX2 knockdown, including *GSK3B*, *p15* and *p16*, and genes in green were down regulated by CBX2 knockdown, such as *Cyclin D*, *CDK1* and *CDK2*. *GSK3B* is an inhibitor of cell cycle regulatory genes, so this being upregulated may be a reason a reduction in cell growth is seen upon knocking down CBX2. *p16* is a tumour suppressor gene which may slow cell progression from the G1 to S phase, so this being upregulated means cells cannot progress through the cell cycle. Furthermore, many of the cells downregulated, such as *CDK1*, are involved in promoting the cell cycle cycle. Without these, the cells cannot progress through mitosis. These result in cell death, as shown in the phenotypic experiments.

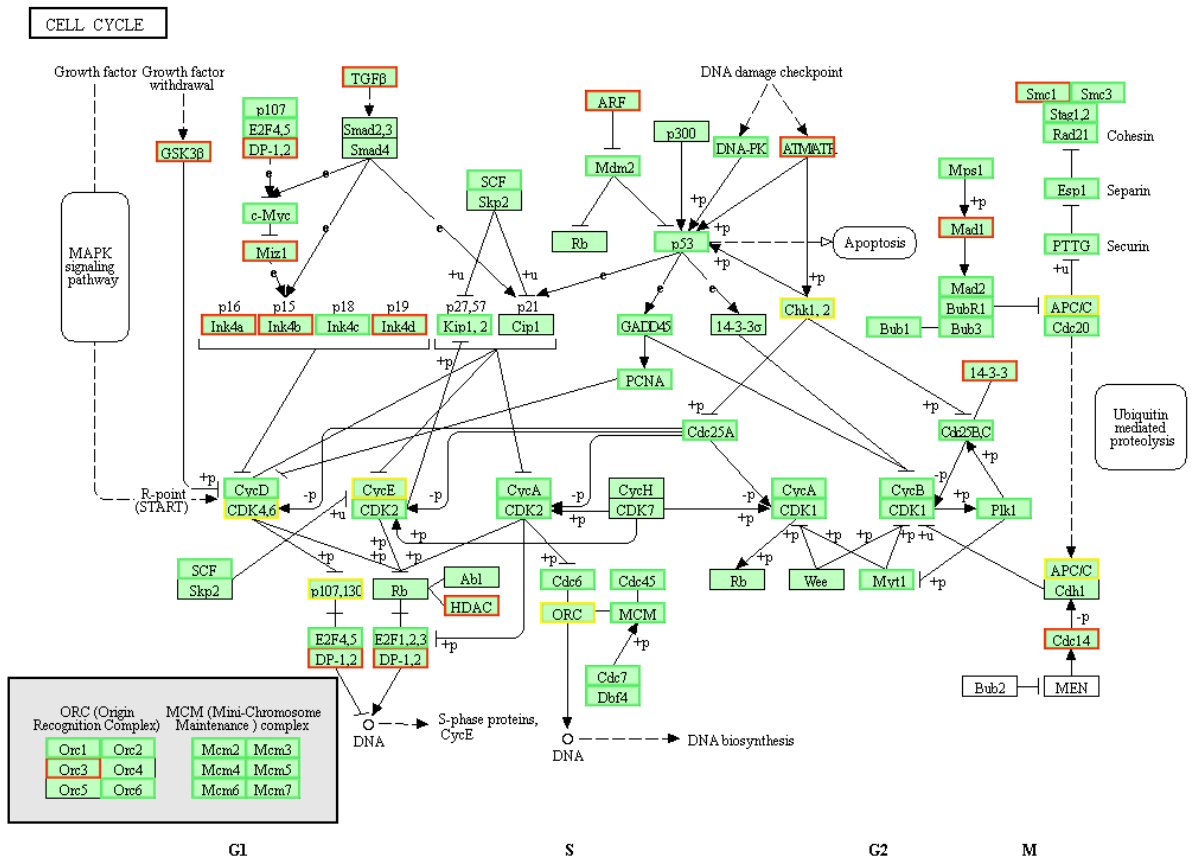


Figure 4.16. The genes involved in the cell cycle, within G1, S, G2 and M phases. Genes in red are upregulated, and genes in green are down regulated. Yellow boxes indicate genes within this group which are both up- and downregulated.

4.9.6 Gene Set Enrichment Analysis

After identifying cell cycle genes regulated by CBX2, Dr Wade also undertook gene set enrichment analysis to look for pathways enriched in upregulated or downregulated genes, following CBX2 knockdown. This identified the G2 to M checkpoint hallmark gene set (Figure 4.17). Significantly upregulated genes are in red at one side, and significantly downregulated genes following CBX2 knockdown are at the other side in blue. The analysis shows that following CBX2 knockdown, a significant amount of downregulated genes were associated with the G2/M checkpoint. This means that the cells are unable to progress through mitosis, so cell growth is slowed, which correlates with the phenotypic analysis.

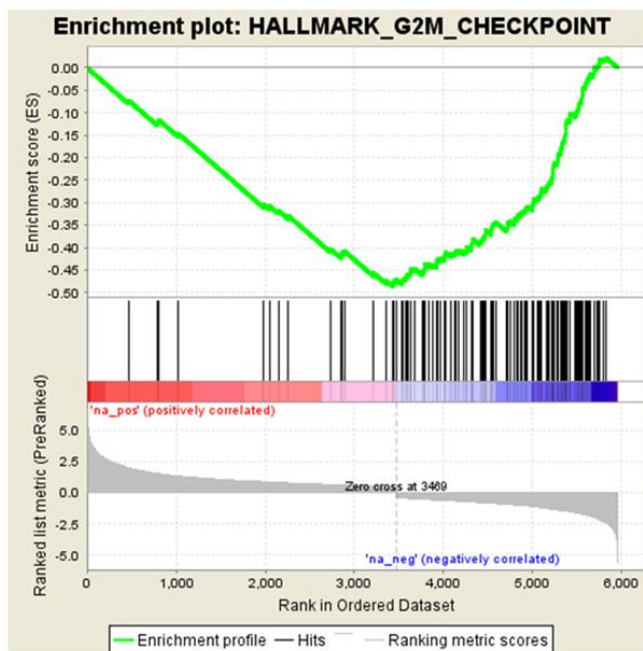


Figure 4.17. Genes significantly upregulated (red) or down regulated (blue) at the G2 to M checkpoint.

Gene set enrichment analysis also identified MYC target gene signature (Figure 4.18). MYC is a proto-oncogene which regulate genes involved in cell proliferation. Many genes were significantly downregulated in this gene set, meaning cell proliferation may be slowed with CBX2 knockdown, validating what was previously shown.

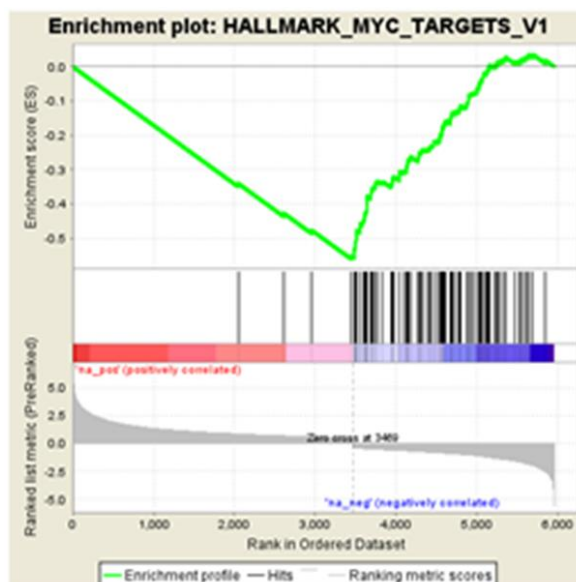


Figure 4.18. Genes significantly upregulated in red and significantly downregulated in blue within MYC target genes.

Gene set enrichment analysis also identified that genes downregulated following CBX2 knockdown were also enriched in E2F target gene signature (Figure 4.19). E2F promotes the cell cycle. The majority of these genes were also downregulated, again further validating that CBX2 is required for cell growth.

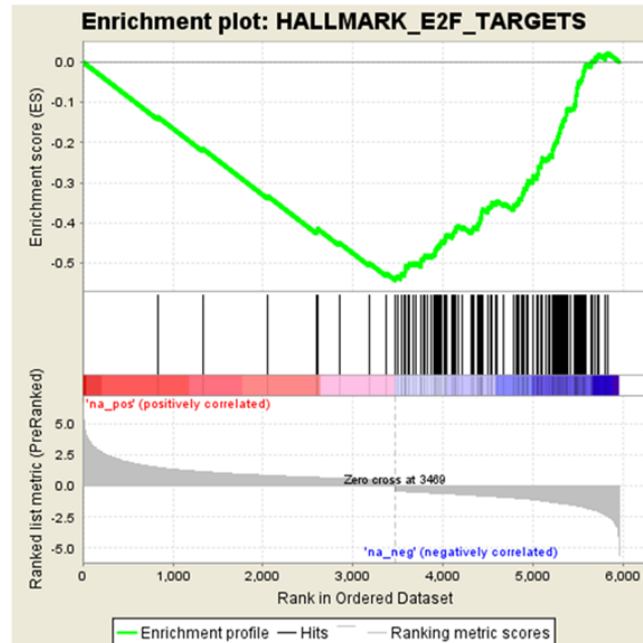


Figure 4.19. E2F target genes significantly upregulated (red) or downregulated (blue).

The final hallmark gene set observed by gene set enrichment analysis was the late oestrogen response (Figure 4.20). As MCF-7 is an ER-positive breast cancer cell line, it was interesting to see the effect of CBX2 knockdown on the oestrogen response. Some of the genes involved in this gene signature were upregulated, but most were downregulated following CBX2 knockdown, as with the other hallmark gene sets. This suggests that CBX2 is affecting oestrogen signalling.

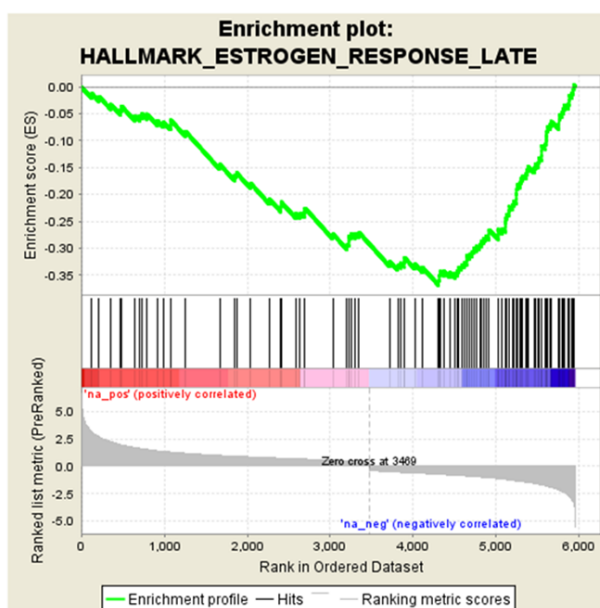


Figure 4.20. Genes significantly upregulated (red) or downregulated (blue) in the late oestrogen response.

4.10 pS2 and CCND1 expression decreases with CBX2 knockdown

Following on from investigating the involvement of CBX2 in specific pathways in the RNA-Seq data, the effect of CBX2 on *p16* and *p21* was investigated by qPCR. Despite showing these to be significantly upregulated in the RNA-Seq data, the qPCR on the cell knockdowns did not work. These samples had been shown that CBX2 had knocked down, but the *p16* and *p21* primers did not amplify, meaning their impact on CBX2 transcription could not be concluded.

ER-target genes were also investigated by qPCR because the ER gene set was identified to be downregulated following CBX2 knockdown by the RNA-Seq analysis. This used siSCR and two CBX2 targeting siRNAs (siCBX2-3 and siCBX2-4) transfected in cells grown in full media, with *pS2* (*TFF1*) and *Cyclin D1* (*CCND1*) primers for qPCR (Figure 4.21 for *pS2* and Figure 4.22 for *CCND1*). Significance was calculated using a T-test. For cells transfected with siCBX2-3 and 4, *pS2* gene expression decreased in both cell lines compared with siSCR. *CCND1* was downregulated in MCF-7 cells following knockdown, but not in T47D cells. To test the affect of the ER-target genes and the oestrogen response, *pS2* and *CCND1* gene expressions were also analysed in siSCR, siCBX2-3 and siCBX2-4 transfected cells in oestrogen and non-oestrogen stimulated conditions

(Supplementary Figure 27-29). These experiments did not work so further optimisation is required.

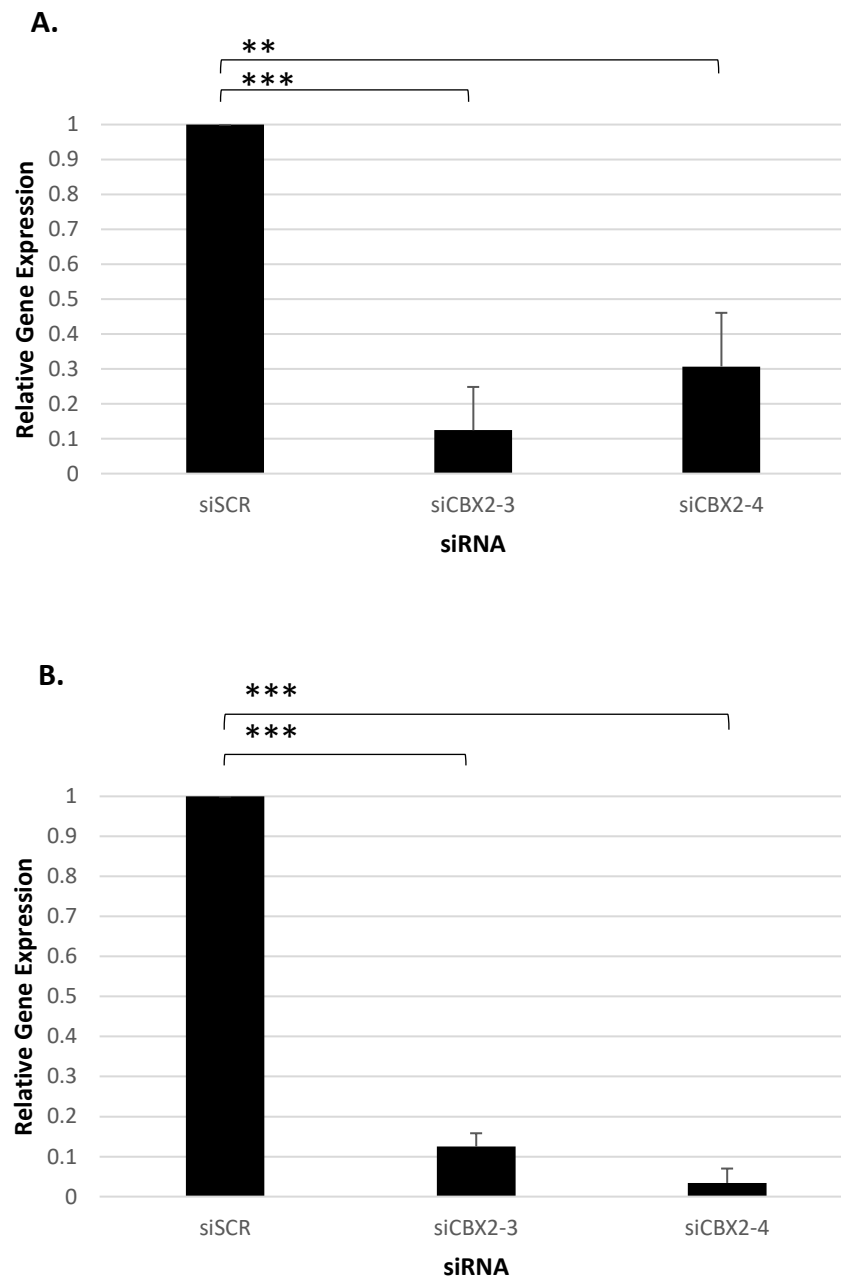


Figure 4.21. Relative *pS2* mRNA expression in siCBX2-3 and 4 transfected MCF-7 (A) and T47D (B) cells. qPCR data are an average of 3 repeats \pm SEM and are expressed relative to gene expression in siSCR transfected cells. *P* values were determined by Student's *T* test. **A:** ** = very significant ($p < 0.01$), *** = extremely significant ($p < 0.001$). **B:** *** = extremely significant ($p < 0.001$ for both knockdown siRNAs).

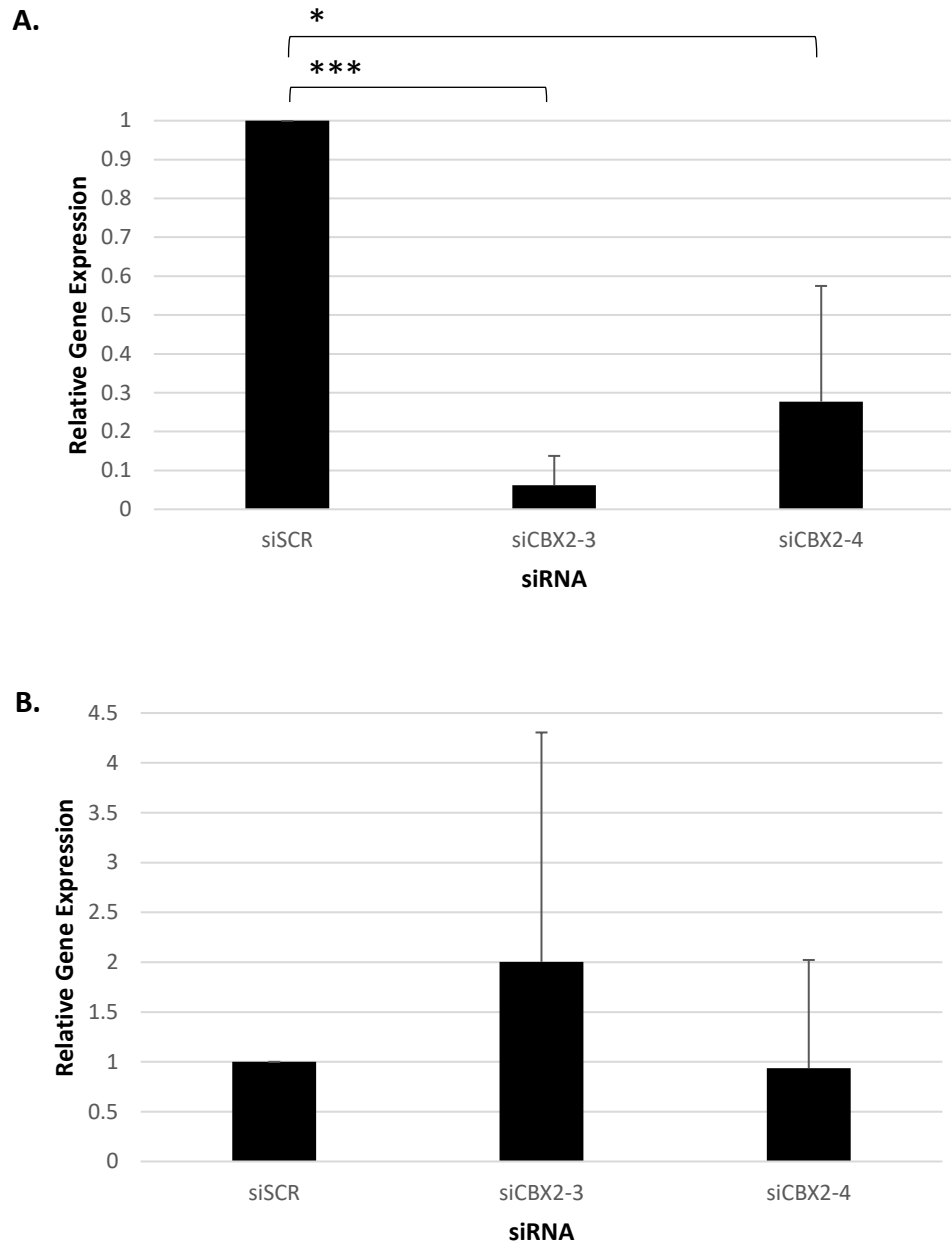


Figure 4.22. Relative *CCND1* mRNA expression in siCBX2-3 and 4 transfected MCF-7 (A) and T47D (B) cells. qPCR data are an average of 3 repeats \pm SEM and are expressed relative to gene expression in siSCR transfected cells. *P* values were determined by Student's *T* test. A. * = significant ($p < 0.05$), *** = extremely significant ($p < 0.001$).

Chapter 5: Discussion

As CBX2 has already been established as a possible therapeutic target in other types of cancer, the aim of this study was to begin to assess the role of CBX2 in ER-positive breast cancer. It is very important to identify new drug targets against ER-positive breast cancer because of the therapeutic resistance to existing treatments, such as Tamoxifen and Fulvestrant, as discussed in the introduction. CBX2 is a potential target as although it is mostly shown to be upregulated in basal and HER2 positive breast cancers, when compared to normal tissue, it is also upregulated in ER-positive breast cancer (Chan et al., 2018). Moreover, it has been previously shown that CBX2 knockdown in basal and HER2 positive breast cancers impedes breast cancer growth (Piqué et al., 2019). In this study, the knockdown of CBX2 was shown to affect ER-positive cell growth, and that CBX2 has a role in regulating oncogenic signalling pathways and ER-signalling, suggesting that CBX2 also has a role in regulating ER-positive breast cancer growth. Another important aspect of CBX2 as a potential therapeutic target is that it has a chromodomain which has been shown can be pharmacologically targeted (Stuckey et al., 2016). UNC3866 is a chromodomain inhibitor, but is most potent at binding CBX4 or CBX7. This shows that it is possible to target chromodomains and therefore potentially CBX2. Understanding the role of CBX2 in ER-positive breast cancer and the mechanisms in which it promotes tumour growth is therefore important to fully validate its potential as a future therapeutic target.

5.1 CBX2 is phosphorylated in ER-positive breast cancer cells

The first aim of the project was to confirm CBX2 knockdown, using three CBX2 targeting siRNAs, siCBX2-1, siCBX2-3 and siCBX2-4. Three independent siRNAs targeting different sites within *CBX2* mRNA were used to mitigate the risk that observed results were due to siRNA off target effects. Knockdown was proved at both mRNA level by qPCR, and protein level by Western blot.

After showing CBX2 knockdown, it was found that CBX2 was consistently observed at 72 kDa. This was apparent in the standard Western blot analysis and also after immunoprecipitation. The CBX2 band is expected at approximately 56 kDa, according to antibody data sheets (abcam.com, n.d., rndsystems.com, n.d.). This is the expected molecular weight due to the number of amino acids (Genecards.org, n.d., Uniprot.org,

n.d.). Further to this, a paper by Zheng et al (2019) identified CBX2 to be at 56 kDa in both MCF-7 and MDA-MB-231 breast cancer cells.

A recent study by Kawaguchi et al (2017) conducted protein dephosphorylation experiments using SAP in HEK293T embryonic kidney cells, showing that CBX2 at 72 kDa is a phosphorylated form of the protein. When lysates were treated with rSAP, the CBX2 band was observed at a lower molecular weight, indicating that the observed 72 kDa form of CBX2 is phosphorylated. This research supports findings by Hatano et al (2010), which also identified CBX2 at 72 kDa. This study used numerous cell lines, including F9 embryonal carcinoma cells, and showed that treatment with the phosphatase CIP reduced the molecular weight of CBX2, again indicating that CBX2 at 72 kDa is a phosphorylated form. Multiple papers on CBX2 do not state the molecular weight (Wheeler et al., 2018, Zhen et al., 2010). These therefore may have observed CBX2 at 72 kDa, but it cannot be concluded.

In an attempt to confirm whether CBX2 observed in this study is phosphorylated, as the literature suggests, the SAP dephosphorylation method was used. It was repeated numerous times using protein lysate from 1 million cells, but rarely showed any bands. It was then tried either using more cells, up to 6 million, or less lysis buffer, in order to concentrate the protein sample. A large volume of protein lysate was added to each well to maximise the amount of protein. The blots still appeared either blank, or such a high exposure was required that the blots were too dark to see any bands. A different dephosphorylation method was then tried instead by using CIP. Although the bands observed on the subsequent Western blot were also fairly faint, it was clear that there was a difference between the bands observed for lysates treated with and without CIP. The band from the lysate not treated with CIP was still observed at 72 kDa, however this band height was lower in the CIP treated lysate, suggesting that the 72 kDa band is a phosphorylated version of CBX2. Due to time restraints, only one repeat of this was obtained, though this positive result is supported by the literature.

The study by Kawaguchi et al (2017) also showed, using nucleosome pull-down assays, that the phosphorylation of CBX2 is critical for its transition to the nucleus from the cytoplasm, and its nucleosome binding specificity to H3K27me3, and therefore its transcriptional regulatory activity. This shows that the 72 kDa version of CBX2 is the active form of the protein as it is present in the nucleus, unlike the unphosphorylated

protein seen at 56 kDa. This study also showed that the active 72 kDa form of CBX2 is present *in vivo*. In the present study, CBX2 was also shown to be in the nuclear fraction, which is a novel result for the ER-positive cell lines. There were sometimes issues with obtaining a clean fractionation, shown by alpha tubulin being present in small amounts in the nuclear fraction. This is likely due to pipetting errors when separating the fractions after centrifugation. In the future, a nuclear marker should also be included, such as PARP, to further validate that CBX2 is in the nuclear fraction. A comparison between the mechanisms involving phosphorylated and non-phosphorylated CBX2 would be an interesting future study in ER-positive breast cancer, as would the investigation into the proteins responsible for CBX2 phosphorylation and therefore activation.

In summary, evidence suggests that CBX2 is found in a phosphorylated, and therefore active state in the ER-breast cancer cell line models used in this study. The results observed following CBX2 knockdown in this study are therefore potentially reflective of what would be seen *in vivo*, which is important for its validation as a potential therapeutic target.

5.2 CBX2 impacts certain histone modifications

Next, the effect of CBX2 knockdown on relevant histone modifications that CBX2 is known to interact with was investigated. Lysine 119 on histone H2A is ubiquitinated by E3 ligase upon CBX2 reading H3K27me3 and recruiting the PRC1 complex. Therefore, it was expected that CBX2 knockdown would result in a reduction of H2AK119ub, which would indicate that the CBX2-associated PRC1 complex is active in the ER-positive cell lines. When probing for H2AK119ub in lysates from cells transfected with CBX2 targeting siRNA knockdowns, siCBX2-4 consistently reduced the mark whereas the other siRNAs did not. Despite this result, there was sometimes a faint H2A-pan loading control band for siCBX2-4, in comparison to equal loading for the other siRNAs. As the loading was not equal for all repeats, it cannot be conclusively concluded whether CBX2 is having an effect on global H2AK119ub levels. The fact only siCBX2-4 showed an effect may suggest that a threshold level of CBX2 knockdown is required that only siCBX2-4 reached. Conversely, it may suggest that siCBX2-4 has off-target effects, especially considering the effect on H2A-pan on some occasions. The lack of consistency between knockdown and effect on H2AK119ub levels may also be explained by the fact that numerous CBX proteins exist and the different PRC1 complex compositions are thought to regulate

different genes (Ma et al., 2014). Therefore, knocking down just one CBX protein may not result in global H2AK119ub changes. Although global changes were not consistently altered by knockdown, CBX2 may still be affecting H2AK119 ubiquitination at specific genes. Further study is therefore needed to investigate H2AK119ub ubiquitination marks at specific genomic loci.

Furthermore, the CBX2 knockdown lysates and siSCR were probed for H3K27me3. The PRC2 complex causes the trimethylation of lysine 27 on histone 3, then CBX2 reads this mark and recruits the PRC1 complex. As not much change was seen with the siSCR or CBX2 targeting siRNAs compared to the H3-pan loading control, CBX2 may just read this mark rather than influence it.

Another histone mark investigated was H3K27ac because it is transcriptionally activating, and on the same lysine as the trimethylation mark. H3K27ac decreased in the knockdown siRNAs compared to the siSCR, with an equal H3-pan loading control. This is surprising because CBX2 is known to be a transcriptional repressor. If CBX2 is knocked down, the effect on a transcriptionally activating mark may be expected to increase, rather than decrease. This novel result suggests that CBX2 may be affecting either a HAT or a HDAC, possibly via *CCND1* expression. *CCND1* mRNA was shown to be downregulated when CBX2 is knocked down. *CCND1* associates with p300/CBP-associated factor, which has histone acetylase activity to enhance transcriptional activity (Takahashi-Yanaga and Sasaguri, 2008). This suggests that *CCND1* via CBX2 expression may be affecting enzyme activity which regulate HATs or HDACs influencing H3K27ac. More investigation is needed into this. Another reason for this affect may be that CBX2 is affecting a gene upstream of this mark, which has caused this decrease in H3K27ac further downstream. If CBX2 is regulating a gene upstream, the knockdown of CBX2 may cause an increase in a previously regulated TSG or a decrease in the expression of an oncogene, which has caused this decrease in H3K27ac. The genes involved in this require further investigation.

The Western blots conducted for the histone modification experiments required numerous repeats due to the variable results achieved when using the histone modification antibodies. The blots often came up blank. Moreover, there were some problems with the ChemiDoc machine used to read the Western blots, and the computer attached had a virus, meaning this was out of action for a while. This resulted

in densitometry not being able to be performed on the Western blots, as some of the images could not be saved. In the future, densitometry should be conducted on the Western blots to semi-quantify them.

5.3 CBX2 knockdown inhibits cell growth

Previous research from the group has identified that CBX2 knockdown causes a reduction in breast cancer cell number (data not yet published). Cell proliferation was measured in this study using an MTS assay as an alternative growth assay. When plating, a border of media was placed around the wells being analysed to ensure more accurate results, as the outer wells had more exposure to the external environment and therefore temperature differences. siCBX2-3 and 4 were used to knockdown CBX2 in this analysis. After 48 hours, it was shown that the CBX2 depleted MCF-7 cells slowed in growth, whereas the non-transfected or siSCR cells continued growing, although this difference was not significant. Cells transfected with siSCR, siCBX2-1, siCBX2-3 and siCBX2-4 were also observed by microscopy. This showed a large difference between the CBX2 targeting siRNA knockdowns in comparison to the siSCR, especially in siCBX2-4. The morphology was different, with cells being more round and larger, as well as an obvious decrease in cell number. The microscopy would suggest that the MTS may be under representing the effect of knockdown on cell proliferation, meaning other techniques should also be used, such as using a luminescence based assay which measures the amount of ATP to determine presence of metabolically active cells (Morten et al., 2016). The MTS experiment was also tested using T47D cells, but these are much slower growing than MCF-7, so the T47D MTS showed very little growth of any cells. In the future, the plating process could be tested using forward transfections rather than the reverse transfections used to see if this makes a difference to the recovery time of the cells after transfection. Also, the T47D MTS could be recorded over a longer period of time or in larger wells to be able to observe cell proliferation.

Overall, this data suggests that CBX2 is required for ER-positive breast cancer cell growth. This conclusion is supported by Zheng et al (2019), whose paper was published during this project, observing that CBX2 knockdown inhibits MCF-7 breast cancer cell proliferation *in vitro*, using a cell counting kit. They also showed that tumorigenesis was suppressed in xenografts of MCF-7 breast cancer cells when CBX2 was silenced, shown by an EDU staining assay, meaning CBX2 may be a regulator of ER-positive breast tumour

growth. Their study only used one shRNA sequence however, therefore the results are not as accurate as if multiple shRNAs/siRNAs had been used to reduce the risk of results being due to off target effects. This present study used three siRNAs, therefore reliably supports their conclusion.

The effect of knocking down CBX2 on cell apoptosis was also investigated in this study. Previously in the laboratory, MCF-7 and T47D cells were shown, using flow cytometry, to have cell cycle arrest in the G1 phase of the cell cycle, and an increase in cell number in the sub-G1 phase of the cell cycle, indicating apoptosis (data not shown). In hematopoietic stem cells CD34+, CD38+ and CB cells, van der boom et al (2013) showed that, upon CBX2 knockdown, cell apoptosis was observed. They suggested that, also due to decrease in cell proliferation upon knockdown, CBX2 knockdown affects the cell cycle and apoptosis. A study by Mao et al (2019) showed that CBX2 knockdown decreased proliferation in Huh7 and Bel-7402 hepatocellular carcinoma cells. This was by their RNA-Seq data showing CBX2 was involved in the Hippo pathway, specifically its knockdown inhibiting WTIP protein, causing phosphorylation of Yes-associated protein (YAP), and thereby affecting cell proliferation and apoptosis. An clonogenic survival assay then showed CBX2 knockdown decreased proliferation of these cells. Apoptotic cells were detected by Annexin V-PI dual staining. Furthermore, a study by Clermont et al (2016) observed LNCaP and C4-2 prostate cancer cells undergoing morphological changes in the CBX2 targeting siRNA treated cells, but not in the cells treated with a non-targeting siRNA. Cells became larger, and after three days post transfection, stopped proliferating and began detaching from the plate. This was further investigated using an MTT assay and by analysing caspase 3/7 activity, which was shown to increase, indicating cell apoptosis. As CBX2 knockdown has been shown to cause cell apoptosis in other cancers, it was important to show whether CBX2 knockdown causes cell apoptosis in ER-positive breast cancer. The resulting Western blot analysis showed the apoptosis marker cleaved PARP increased in siCBX2-3 and siCBX2-4, compared to the siSCR control. This result, alongside observations of apparent dead cells in the CBX2 targeted siRNA transfected cells down the microscope, indicates that CBX2 knockdown causes cell death in a model of ER-positive breast cancer.

5.4 Gene expression analysis

RNA from siSCR, siCBX2-3 and siCBX2-4 transfected MCF-7 cells was sent to Novogene in triplicate for RNA sequencing, in order to analyse the gene expression regulatory role of CBX2 in ER-positive breast cancer cells. On the cluster heat map, the siSCR and siCBX2-3 were more similar to each other than the siCBX2-3 and siCBX2-4. This could be due to siCBX2-4, in comparison to siCBX2-3, having alternatively-spliced variants, or off-target effects. The data from this experiment was returned just prior to submission of this thesis and therefore preliminary analysis so far has only been undertaken by Dr Wade on the comparison between siSCR and siCBX2-4 transfected cells. The next stage will be to validate this data by qPCR.

The main pathways that CBX2 was shown to regulate, identified by RNA-Seq, were the cell cycle, pathways in cancer and the *p53* pathway. The cell cycle pathway is of particular relevance to this study due to the observations of CBX2 knockdown on cell growth, so this pathway was analysed in greater detail. Multiple genes involved in cell cycle regulation were shown to be downregulated following CBX2 knockdown. *CCND1*, which was downregulated, promotes G1-S transition (Wang et al., 2018). The downregulation of this gene upon CBX2 knockdown means that the CDKs it regulates are also downregulated, meaning the cell cannot progress through the cell cycle. *CDK1* is a protein kinase which is activated when it binds to *Cyclin B1* and the Thr161 residue on its T-loop is phosphorylated (Chow et al., 2011). This allows rapid entry of cells into mitosis. As *CDK1* is downregulated when CBX2 is knocked down, cells are unable to progress through mitosis, so will apoptose. *CDK2* is a cell cycle regulator which is involved in G1/S and G2/M transitions, meaning it is necessary for the cells to progress through the cell cycle, in order to replicate their DNA (Bačević et al., 2017). A study by Neganova et al (2011) in human embryonic stem cells showed that the downregulation of *CDK2* triggers the G1 checkpoint by the ATM-CHK2-p53-p21 pathway, causes G1 arrest, and therefore cell apoptosis. This was shown by flow cytometry. It also was shown to cause upregulation of *p21* and *p27*, which inhibit the cell cycle, and result in the DNA damage response, shown by a comet assay. *p27* was also shown to be upregulated in this RNA-Seq data. As *CDK2* was downregulated upon CBX2 knockdown, this means cells cannot progress past the G1 checkpoint, so cell apoptosis occurs. *GSK3B* was also shown to be upregulated upon CBX2 knockdown. When phosphorylated, it is

an inhibitor of cell cycle regulatory genes downstream, regulating ubiquitination and proteolysis of signaling proteins and transcription factors (Xu et al., 2009). The upregulation of this gene may therefore mean inhibition of important regulatory genes, so the cell cycle is arrested and cells apoptose.

As well as the cyclin and CDK genes, the RNA-Seq data showed *p15* and *p16* to be upregulated when CBX2 was knocked down. It was previously shown that CBX2 binds to the promotor of *CDKN2A* and *CDKN2B* in proliferating fibroblasts, and that it turns off *p14*, *p15* and *p16*, causing downregulation of these genes and cancer progression (Jangal et al., 2019). Using transcriptomic analysis of CBX2 expression, it was also shown that when CBX2 was upregulated, *p15* was downregulated in multiple cancers (Clermont et al., 2014). *p16* causes inhibition of *CCND1*, resulting in G1 cell cycle arrest, which may be why *CCND1* was shown to be downregulated in this study (Romagosa et al., 2011). *p21* was also shown to be upregulated in hematopoietic stem cells (van den Boom et al., 2013), this being caused by downregulation of CDK2, which was observed. These genes were therefore investigated in MCF-7 cells, using *p16* and *p21* primers for qPCR with an siSCR and CBX2 targeting siRNA knockdowns. The qPCR didn't work for *p16*, but it was later seen in the literature that MCF-7 cells did not express *p16* (Craig et al., 1998, Karimi-Busheri et al., 2010). As it is significantly upregulated when CBX2 is knocked down (as shown by the RNA-Seq analysis), MCF-7 cells not expressing *p16* could possibly be due to CBX2 being present. This requires further investigation. Another likely reason is the primers not amplifying in qPCR for both *p16* and *p21*. This could be due to qPCR not being sensitive enough, as RNA-Seq is a much more sensitive process for detecting gene expression. The qPCR should also be tested with new *p16* and *p21* primers, with time to optimise these.

These genes being regulated differently in the cell cycle with CBX2 knockdown all prevent the cells from being able to progress through the cell cycle, therefore the cells apoptose. This correlates with the phenotypic results from this study, indicating that CBX2 could be potentially targeted at its chromodomain to cause apoptosis of ER-positive breast cancer cells.

After identifying particular genes involved in the cell cycle that are regulated by CBX2, Dr Wade undertook gene set enrichment analysis to look for pathways enriched in upregulated or downregulated genes after CBX2 knockdown. This identified the G2 to

M checkpoint, MYC target genes, E2F target genes and the late oestrogen response hallmark gene sets. Many of the genes in these hallmark gene sets overlap with the ones discussed in the cell cycle. In all of these gene sets, most of the genes were downregulated. This is because CBX2 may be repressing genes upstream, such as *p15* and *p16*, causing this repression downstream. *CDK1* is involved in the G2 to M checkpoint, and was shown to be downregulated, as previously discussed. Furthermore, MYC target genes include cyclins and CDKs such as *CDK2*, *CDK1* and *Cyclin B*. They also include E2F transcription factors (Bretones et al., 2015). *p16*, shown to be upregulated in the RNA-Seq analysis, has been proven in the U-2 OS osteosarcoma cell line by *in silico* microarray analysis to repress various E2F genes such as *MCM5*, *RRM1*, *BLM* and *BTG3*, therefore potentially accounting for the E2F target gene downregulation (Vernell et al., 2003).

Furthermore, the majority of genes regulated by the ER were shown to be downregulated following CBX2 knockdown in the RNA-Seq data, indicating that CBX2 may play a role in ER signalling. The ER target genes *CCND1* and *pS2* were investigated by qPCR and shown to decrease with CBX2 knockdown, which correlates with the data observed by RNA-Seq. The next stage of this was to test the ER-target genes in cells grown in oestrogen stimulated media, since the cells are dependent on oestrogen to grow. It was expected that, upon stimulation with oestrogen, the ER-target genes should increase in comparison to cells without oestrogen stimulation. This qPCR did not work, so new oestrogen was added to non-transfected cells, then a forward transfection technique used rather than the usual reverse, since the phenol-free media and transfection mix was too damaging for the cells to adhere properly. Repeats of these did not work either, and there was not time to optimise the experiment by testing different incubation times and amounts of oestrogen. This is a future experiment to test.

5.5 Conclusions and Future Perspectives

The main findings of this research is that CBX2 is involved in the regulation of specific cell cycle genes and ER-target genes, many of which regulate cell growth. This means that CBX2 may be important for cell cycle regulation, though the extent of this needs further investigation, and the RNA-Seq data requires validating by qPCR. Another discovery is that CBX2 knockdown reduces the transcriptionally activating mark, H3K27ac, though further research in to the reasons for this is required.

In the future, the use of a second CBX2 antibody will aid in validating the results. Repeats of some experiments such as CIP, and further optimisation of experiments such as non-oestrogen and oestrogen stimulated cells are required in multiple ER-positive cell lines. Furthermore, techniques such as chromatin immunoprecipitation (ChIP) could potentially provide more specific locations in the genome that are associated with different histone modifications regulated by CBX2 associated PRC1 complexes, which could be correlated to RNA-Seq data to identify genes directly regulated by CBX2. Further to this, the RNA-Seq data may reveal possible alternatively-spliced variants of CBX2, which may indicate why specific siRNAs for CBX2 have different genotypic consequences. The results from these ER-positive cell lines could be compared to other breast cancer cell lines, such as TNBC and HER2 positive. ChIP analysis of H2AK119ub in CBX2 expressing and depleted cells could also be conducted to identify genomic loci directly regulated by CBX2-associated PRC1 complexes. Other experiments such as co-immunoprecipitation could be used to analyse CBX2 interacting with the ER. Rescue experiments using a wild-type and chromodomain mutant version of CBX2 could also be performed to see if genotypic and phenotypic changes observed by CBX2 knockdown could be reversed and therefore identify whether effects are due to the epi-reader role which CBX2 has, and not another function, therefore indicating whether the chromodomain of CBX2 should be pharmacologically targeted. Furthermore, experimentation *in vivo* will be required for further validation of the role of CBX2, such as patient-derived xenografts and clinical samples, due to the limitations of using cell lines, including their lack of heterogeneity and no microenvironment influence. A long-term goal will be therapeutically targeting the chromodomain of CBX2, as similar chromodomains have previously been shown to be pharmacologically targeted.

Chapter 6: References

- Abcam.com. (n.d.). *Anti-CBX2 antibody (ab80044) | Abcam*. [online] Available at: <https://www.abcam.com/cbx2-antibody-ab80044.html> [Accessed 2 Sep. 2019].
- Abdel-Hafiz, H.A., 2017. Epigenetic Mechanisms of Tamoxifen Resistance in Luminal Breast Cancer. *Diseases* 5. <https://doi.org/10.3390/diseases5030016>
- Aguilera, A., García-Muse, T., 2013. Causes of genome instability. *Annu. Rev. Genet.* 47, 1–32. <https://doi.org/10.1146/annurev-genet-111212-133232>
- Ahmed, S., Sami, A., Xiang, J., 2015. HER2-directed therapy: current treatment options for HER2-positive breast cancer. *Breast Cancer* 22, 101–116. <https://doi.org/10.1007/s12282-015-0587-x>
- Alluri, P.G., Asangani, I.A., Chinnaiyan, A.M., 2014. BETs abet Tam-R in ER-positive breast cancer. *Cell research* 24, 899–900. <https://doi.org/10.1038/cr.2014.90>
- Asangani, I.A., Dommeti, V.L., Wang, X., Malik, R., Cieslik, M., Yang, R., Escara-Wilke, J., Wilder-Romans, K., Dhanireddy, S., Engelke, C., Iyer, M.K., Jing, X., Wu, Y.-M., Cao, X., Qin, Z.S., Wang, S., Feng, F.Y., Chinnaiyan, A.M., 2014. Therapeutic targeting of BET bromodomain proteins in castration-resistant prostate cancer. *Nature* 510, 278–282. <https://doi.org/10.1038/nature13229>
- ATCC. SOP: Thawing, Propagation and Cryopreservation of NCI-PBCF-HTB133 (T-47D), n.d. 24.
- Bačević, K., Lossaint, G., Achour, T.N., Georget, V., Fisher, D., Dulić, V., 2017. Cdk2 strengthens the intra-S checkpoint and counteracts cell cycle exit induced by DNA damage. *Scientific Reports* 7. <https://doi.org/10.1038/s41598-017-12868-5>
- Badeaux, A.I., Shi, Y., 2013. Emerging roles for chromatin as a signal integration and storage platform. *Nat. Rev. Mol. Cell Biol.* 14, 211–224. <https://doi.org/10.1038/nrm3545>
- Bannister, A.J., Kouzarides, T., 2011. Regulation of chromatin by histone modifications. *Cell Research* 21, 381–395. <https://doi.org/10.1038/cr.2011.22>
- Biswas, S., Rao, C.M., 2018. Epigenetic tools (The Writers, The Readers and The Erasers) and their implications in cancer therapy. *Eur. J. Pharmacol.* 837, 8–24. <https://doi.org/10.1016/j.ejphar.2018.08.021>
- Björnström, L., Sjöberg, M., 2005. Mechanisms of estrogen receptor signaling: convergence of genomic and nongenomic actions on target genes. *Mol. Endocrinol.* 19, 833–842. <https://doi.org/10.1210/me.2004-0486>

- Brehove, M., Wang, T., North, J., Luo, Y., Dreher, S.J., Shimko, J.C., Ottesen, J.J., Luger, K., Poirier, M.G., 2015. Histone core phosphorylation regulates DNA accessibility. *J. Biol. Chem.* 290, 22612–22621. <https://doi.org/10.1074/jbc.M115.661363>
- Bretones, G., Delgado, M.D., León, J., 2015. Myc and cell cycle control. *Biochimica et Biophysica Acta (BBA) - Gene Regulatory Mechanisms* 1849, 506–516. <https://doi.org/10.1016/j.bbagr.2014.03.013>
- Bulut, N., Altundag, K., 2015. Does estrogen receptor determination affect prognosis in early stage breast cancers? *Int J Clin Exp Med* 8, 21454–21459.
- Cancer Genome Atlas Network, 2012. Comprehensive molecular portraits of human breast tumours. *Nature* 490, 61–70. <https://doi.org/10.1038/nature11412>
- Cancer Research UK. (2015). *Breast cancer statistics*. [online] Available at: <https://www.cancerresearchuk.org/health-professional/cancer-statistics/statistics-by-cancer-type/breast-cancer> [Accessed 28 Nov. 2018].
- Chan, H.L., Beckedorff, F., Zhang, Y., Garcia-Huidobro, J., Jiang, H., Colaprico, A., Bilbao, D., Figueroa, M.E., LaCava, J., Shiekhhattar, R., Morey, L., 2018. Polycomb complexes associate with enhancers and promote oncogenic transcriptional programs in cancer through multiple mechanisms. *Nat Commun* 9, 3377. <https://doi.org/10.1038/s41467-018-05728-x>
- Chang, M., 2012. Tamoxifen resistance in breast cancer. *Biomol Ther (Seoul)* 20, 256–267. <https://doi.org/10.4062/biomolther.2012.20.3.256>
- Chen, W.Y., Zhang, X.Y., Liu, T., Liu, Y., Zhao, Y.S., Pang, D., 2017. Chromobox homolog 2 protein: A novel biomarker for predicting prognosis and Taxol sensitivity in patients with breast cancer. *Oncology Letters* 13, 1149–1156. <https://doi.org/10.3892/ol.2016.5529>
- Chow, J.P.H., Poon, R.Y.C., Ma, H.T., 2011. Inhibitory Phosphorylation of Cyclin-Dependent Kinase 1 as a Compensatory Mechanism for Mitosis Exit. *Molecular and Cellular Biology* 31, 1478–1491. <https://doi.org/10.1128/MCB.00891-10>
- Clermont, P.-L., Crea, F., Chiang, Y.T., Lin, D., Zhang, A., Wang, J.Z.L., Parolia, A., Wu, R., Xue, H., Wang, Y., Ding, J., Thu, K.L., Lam, W.L., Shah, S.P., Collins, C.C., Wang, Y., Helgason, C.D., 2016. Identification of the epigenetic reader CBX2 as a potential drug target in advanced prostate cancer. *Clin Epigenetics* 8, 16. <https://doi.org/10.1186/s13148-016-0182-9>
- Clermont, P.-L., Sun, L., Crea, F., Thu, K.L., Zhang, A., Parolia, A., Lam, W.L., Helgason, C.D., 2014. Genotranscriptomic meta-analysis of the Polycomb gene CBX2 in human cancers: initial

evidence of an oncogenic role. *British Journal of Cancer* 111, 1663–1672. <https://doi.org/10.1038/bjc.2014.474>

Colleoni, M., Sun, Z., Price, K.N., Karlsson, P., Forbes, J.F., Thürlimann, B., Gianni, L., Castiglione, M., Gelber, R.D., Coates, A.S., Goldhirsch, A., 2016. Annual Hazard Rates of Recurrence for Breast Cancer During 24 Years of Follow-Up: Results from the International Breast Cancer Study Group Trials I to V. *J. Clin. Oncol.* 34, 927–935. <https://doi.org/10.1200/JCO.2015.62.3504>

Craig, C., Kim, M., Ohri, E., Wersto, R., Katayose, D., Li, Z., Choi, Y.H., Mudahar, B., Srivastava, S., Seth, P., Cowan, K., 1998. Effects of adenovirus-mediated p16INK4A expression on cell cycle arrest are determined by endogenous p16 and Rb status in human cancer cells. *Oncogene* 16, 265–272. <https://doi.org/10.1038/sj.onc.1201493>

Dai, X., Li, T., Bai, Z., Yang, Y., Liu, X., Zhan, J., Shi, B., 2015. Breast cancer intrinsic subtype classification, clinical use and future trends. *Am J Cancer Res* 5, 2929–2943.

Deeney, J.T., Belkina, A.C., Shirihai, O.S., Corkey, B.E., Denis, G.V., 2016. BET Bromodomain Proteins Brd2, Brd3 and Brd4 Selectively Regulate Metabolic Pathways in the Pancreatic β -Cell. *PLOS ONE* 11, e0151329. <https://doi.org/10.1371/journal.pone.0151329>

Di Costanzo, A., Del Gaudio, N., Conte, L., Dell'Aversana, C., Vermeulen, M., de Thé, H., Migliaccio, A., Nebbioso, A., Altucci, L., 2018. The HDAC inhibitor SAHA regulates CBX2 stability via a SUMO-triggered ubiquitin-mediated pathway in leukemia. *Oncogene* 37, 2559–2572. <https://doi.org/10.1038/s41388-018-0143-1>

Di Croce, L., Helin, K., 2013. Transcriptional regulation by Polycomb group proteins. *Nature Structural & Molecular Biology* 20, 1147–1155. <https://doi.org/10.1038/nsmb.2669>

Elsheikh, S.E., Green, A.R., Rakha, E.A., Powe, D.G., Ahmed, R.A., Collins, H.M., Soria, D., Garibaldi, J.M., Paish, C.E., Ammar, A.A., Grainge, M.J., Ball, G.R., Abdelghany, M.K., Martinez-Pomares, L., Heery, D.M., Ellis, I.O., 2009. Global Histone Modifications in Breast Cancer Correlate with Tumor Phenotypes, Prognostic Factors, and Patient Outcome. *Cancer Research* 69, 3802–3809. <https://doi.org/10.1158/0008-5472.CAN-08-3907>

Feng, Q., Wang, H., Ng, H.H., Erdjument-Bromage, H., Tempst, P., Struhl, K., Zhang, Y., 2002. Methylation of H3-Lysine 79 Is Mediated by a New Family of HMTases without a SET Domain. *Current Biology* 12, 1052–1058. [https://doi.org/10.1016/S0960-9822\(02\)00901-6](https://doi.org/10.1016/S0960-9822(02)00901-6)

Feng, Q., Zhang, Z., Shea, M.J., Creighton, C.J., Coarfa, C., Hilsenbeck, S.G., Lanz, R., He, B., Wang, L., Fu, X., Nardone, A., Song, Y., Bradner, J., Mitsiades, N., Mitsiades, C.S., Osborne, C.K., Schiff,

R., O'Malley, B.W., 2014. An epigenomic approach to therapy for tamoxifen-resistant breast cancer. *Cell Research* 24, 809–819. <https://doi.org/10.1038/cr.2014.71>

Gaughan, L., Stockley, J., Coffey, K., O'Neill, D., Jones, D.L., Wade, M., Wright, J., Moore, M., Tse, S., Rogerson, L., Robson, C.N., 2013. KDM4B is a master regulator of the estrogen receptor signalling cascade. *Nucleic Acids Res.* 41, 6892–6904. <https://doi.org/10.1093/nar/gkt469>

Genecards.org. (n.d.). *CBX2 Gene - GeneCards | CBX2 Protein | CBX2 Antibody*. [online] Available at: <https://www.genecards.org/cgi-bin/carddisp.pl?gene=CBX2> [Accessed 2 Sep. 2019].

Gillette, T.G., Hill, J.A., 2015. Readers, writers, and erasers: chromatin as the whiteboard of heart disease. *Circ. Res.* 116, 1245–1253. <https://doi.org/10.1161/CIRCRESAHA.116.303630>

Gu, X., Wang, X., Su, D., Su, X., Lin, L., Li, S., Wu, Q., Liu, S., Zhang, P., Zhu, X., Jiang, X., 2018. CBX2 Inhibits Neurite Development by Regulating Neuron-Specific Genes Expression. *Front Mol Neurosci* 11, 46. <https://doi.org/10.3389/fnmol.2018.00046>

Gucalp, A., Traina, T.A., 2016. Targeting the androgen receptor in triple-negative breast cancer. *Curr Probl Cancer* 40, 141–150. <https://doi.org/10.1016/j.currprobcancer.2016.09.004>

Hanahan, D., Weinberg, R.A., 2000. The hallmarks of cancer. *Cell* 100, 57–70.

Hatano, A., Matsumoto, M., Higashinakagawa, T., Nakayama, K.I., 2010. Phosphorylation of the chromodomain changes the binding specificity of Cbx2 for methylated histone H3. *Biochem. Biophys. Res. Commun.* 397, 93–99. <https://doi.org/10.1016/j.bbrc.2010.05.074>

Hilton, H.N., Clarke, C.L., Graham, J.D., 2018. Estrogen and progesterone signalling in the normal breast and its implications for cancer development. *Mol. Cell. Endocrinol.* 466, 2–14. <https://doi.org/10.1016/j.mce.2017.08.011>

Hon, J.D.C., Singh, B., Sahin, A., Du, G., Wang, J., Wang, V.Y., Deng, F.-M., Zhang, D.Y., Monaco, M.E., Lee, P., 2016. Breast cancer molecular subtypes: from TNBC to QNBC. *Am J Cancer Res* 6, 1864–1872.

Huisinga, K.L., Brower-Toland, B., Elgin, S.C.R., 2006. The contradictory definitions of heterochromatin: transcription and silencing. *Chromosoma* 115, 110–122. <https://doi.org/10.1007/s00412-006-0052-x>

Jaber, M.I., Song, B., Taylor, C., Vaske, C.J., Benz, S.C., Rabizadeh, S., Soon-Shiong, P., Szeto, C.W., 2020. A deep learning image-based intrinsic molecular subtype classifier of breast tumors reveals tumor heterogeneity that may affect survival. *Breast Cancer Res* 22. <https://doi.org/10.1186/s13058-020-1248-3>

- Jangal, M., Lebeau, B., Witcher, M., 2019. Beyond EZH2: is the polycomb protein CBX2 an emerging target for anti-cancer therapy? *Expert Opin. Ther. Targets* 23, 565–578. <https://doi.org/10.1080/14728222.2019.1627329>
- Jenuwein, T., 2001. Translating the Histone Code. *Science* 293, 1074–1080. <https://doi.org/10.1126/science.1063127>
- Karimi-Busheri, F., Rasouli-Nia, A., Mackey, J.R., Weinfeld, M., 2010. Senescence evasion by MCF-7 human breast tumor-initiating cells. *Breast Cancer Res.* 12, R31. <https://doi.org/10.1186/bcr2583>
- Karsli-Ceppioglu, S., Dagdemir, A., Judes, G., Ngollo, M., Penault-Llorca, F., Pajon, A., Bignon, Y.-J., Bernard-Gallon, D., 2014. Epigenetic mechanisms of breast cancer: an update of the current knowledge. *Epigenomics* 6, 651–664. <https://doi.org/10.2217/epi.14.59>
- Kawaguchi, T., Machida, S., Kurumizaka, H., Tagami, H., Nakayama, J., 2017. Phosphorylation of CBX2 controls its nucleosome-binding specificity. *The Journal of Biochemistry* 162, 343–355. <https://doi.org/10.1093/jb/mvx040>
- Kenemans, P., Verstraeten, R.A., Verheijen, R.H.M., 2004. Oncogenic pathways in hereditary and sporadic breast cancer. *Maturitas* 49, 34–43. <https://doi.org/10.1016/j.maturitas.2004.06.005>
- Khan, S.A., 2015. Global histone post-translational modifications and cancer: Biomarkers for diagnosis, prognosis and treatment? *World Journal of Biological Chemistry* 6, 333. <https://doi.org/10.4331/wjbc.v6.i4.333>
- Khan, O., La Thangue, N.B., 2012. HDAC inhibitors in cancer biology: emerging mechanisms and clinical applications. *Immunology and Cell Biology* 90, 85–94. <https://doi.org/10.1038/icb.2011.100>
- Kishimoto, M., Fujiki, R., Takezawa, S., Sasaki, Y., Nakamura, T., Yamaoka, K., Kitagawa, H., Kato, S., 2006. Nuclear receptor mediated gene regulation through chromatin remodeling and histone modifications. *Endocr. J.* 53, 157–172.
- Kouzarides, T., 2007. Chromatin Modifications and Their Function. *Cell* 128, 693–705. <https://doi.org/10.1016/j.cell.2007.02.005>
- Lawrence, M., Daujat, S., Schneider, R., 2016. Lateral Thinking: How Histone Modifications Regulate Gene Expression. *Trends in Genetics* 32, 42–56. <https://doi.org/10.1016/j.tig.2015.10.007>

- Lee, E.Y.H.P., Muller, W.J., 2010. Oncogenes and tumor suppressor genes. *Cold Spring Harb Perspect Biol* 2, a003236. <https://doi.org/10.1101/cshperspect.a003236>
- Legube, G., Trouche, D., 2003. Regulating histone acetyltransferases and deacetylases. *EMBO reports* 4, 944–947. <https://doi.org/10.1038/sj.embor.embor941>
- Liang, Y.-K., Lin, H.-Y., Chen, C.-F., Zeng, D., 2017. Prognostic values of distinct CBX family members in breast cancer. *Oncotarget* 8, 92375–92387. <https://doi.org/10.18632/oncotarget.21325>
- Lipovka, Y., Konhilas, J.P., 2016. The complex nature of oestrogen signalling in breast cancer: enemy or ally? *Biosci. Rep.* 36. <https://doi.org/10.1042/BSR20160017>
- Ma, R., Zhang, Y., Sun, T., Cheng, B., 2014. Epigenetic regulation by polycomb group complexes: focus on roles of CBX proteins. *Journal of Zhejiang University SCIENCE B* 15, 412–428. <https://doi.org/10.1631/jzus.B1400077>
- Mao, J., Tian, Y., Wang, C., Jiang, K., Li, R., Yao, Y., Zhang, R., Sun, D., Liang, R., Gao, Z., Wang, Q., Wang, L., 2019. CBX2 Regulates Proliferation and Apoptosis via the Phosphorylation of YAP in Hepatocellular Carcinoma. *J Cancer* 10, 2706–2719. <https://doi.org/10.7150/jca.31845>
- Marmorstein, R., Zhou, M.-M., 2014. Writers and Readers of Histone Acetylation: Structure, Mechanism, and Inhibition. *Cold Spring Harbor Perspectives in Biology* 6, a018762–a018762. <https://doi.org/10.1101/cshperspect.a018762>
- Martin, M., López-Tarruella, S., 2016. Emerging Therapeutic Options for HER2-Positive Breast Cancer. *American Society of Clinical Oncology Educational Book* 36, e64–e70. https://doi.org/10.14694/EDBK_159167
- Meas, R., Mao, P., 2015. Histone ubiquitylation and its roles in transcription and DNA damage response. *DNA Repair* 36, 36–42. <https://doi.org/10.1016/j.dnarep.2015.09.016>
- Morten, B.C., Scott, R.J., Avery-Kiejda, K.A., 2016. Comparison of Three Different Methods for Determining Cell Proliferation in Breast Cancer Cell Lines. *J Vis Exp.* <https://doi.org/10.3791/54350>
- Muller-Tidow, C., Klein, H.-U., Hascher, A., Isken, F., Tickenbrock, L., Thoennissen, N., Agrawal-Singh, S., Tschanter, P., Disselhoff, C., Wang, Y., Becker, A., Thiede, C., Ehninger, G., zur Stadt, U., Koschmieder, S., Seidl, M., Muller, F.U., Schmitz, W., Schlenke, P., McClelland, M., Berdel, W.E., Dugas, M., Serve, H., on behalf of the Study Alliance Leukemia, 2010. Profiling of histone H3 lysine 9 trimethylation levels predicts transcription factor activity and survival in acute myeloid leukemia. *Blood* 116, 3564–3571. <https://doi.org/10.1182/blood-2009-09-240978>

Nagarajan, S., Hossan, T., Alawi, M., Najafova, Z., Indenbirken, D., Bedi, U., Taipaleenmäki, H., Ben-Batalla, I., Scheller, M., Loges, S., Knapp, S., Hesse, E., Chiang, C.-M., Grundhoff, A., Johnsen, S.A., 2014. Bromodomain Protein BRD4 Is Required for Estrogen Receptor-Dependent Enhancer Activation and Gene Transcription. *Cell Reports* 8, 460–469. <https://doi.org/10.1016/j.celrep.2014.06.016>

Nardone, A., De Angelis, C., Trivedi, M.V., Osborne, C.K., Schiff, R., 2015. The changing role of ER in endocrine resistance. *Breast* 24 Suppl 2, S60-66. <https://doi.org/10.1016/j.breast.2015.07.015>

Neganova, I., Vilella, F., Atkinson, S.P., Lloret, M., Passos, J.F., von Zglinicki, T., O'Connor, J.-E., Burks, D., Jones, R., Armstrong, L., Lako, M., 2011. An Important Role for CDK2 in G1 to S Checkpoint Activation and DNA Damage Response in Human Embryonic Stem Cells. *STEM CELLS* 29, 651–659. <https://doi.org/10.1002/stem.620>

Nilsson, S., Mäkelä, S., Treuter, E., Tujague, M., Thomsen, J., Andersson, G., Enmark, E., Pettersson, K., Warner, M., Gustafsson, J.-Å., 2001. Mechanisms of Estrogen Action. *Physiological Reviews* 81, 1535–1565. <https://doi.org/10.1152/physrev.2001.81.4.1535>

Osborne, C.K., Schiff, R., Fuqua, S.A., Shou, J., 2001. Estrogen receptor: current understanding of its activation and modulation. *Clin. Cancer Res.* 7, 4338s–4342s; discussion 4411s–4412s.

Osborne, C.K., Wakeling, A., Nicholson, R.I., 2004. Fulvestrant: an oestrogen receptor antagonist with a novel mechanism of action. *Br. J. Cancer* 90 Suppl 1, S2-6. <https://doi.org/10.1038/sj.bjc.6601629>

Park, Y.S., Jin, M.Y., Kim, Y.J., Yook, J.H., Kim, B.S., Jang, S.J., 2008. The Global Histone Modification Pattern Correlates with Cancer Recurrence and Overall Survival in Gastric Adenocarcinoma. *Annals of Surgical Oncology* 15, 1968–1976. <https://doi.org/10.1245/s10434-008-9927-9>

Parris, T.Z., Danielsson, A., Nemes, S., Kovacs, A., Delle, U., Fallenius, G., Mollerstrom, E., Karlsson, P., Helou, K., 2010. Clinical Implications of Gene Dosage and Gene Expression Patterns in Diploid Breast Carcinoma. *Clinical Cancer Research* 16, 3860–3874. <https://doi.org/10.1158/1078-0432.CCR-10-0889>

Participation, E., n.d. Human Tissue Act 2004 [WWW Document]. URL <http://www.legislation.gov.uk/ukpga/2004/30/contents> (accessed 08.06.19).

Perou, C.M., Sørli, T., Eisen, M.B., van de Rijn, M., Jeffrey, S.S., Rees, C.A., Pollack, J.R., Ross, D.T., Johnsen, H., Akslén, L.A., Fluge, O., Pergamenschikov, A., Williams, C., Zhu, S.X., Lønning,

- P.E., Børresen-Dale, A.L., Brown, P.O., Botstein, D., 2000. Molecular portraits of human breast tumours. *Nature* 406, 747–752. <https://doi.org/10.1038/>
- Pethe, P., Nagvenkar, P., Bhartiya, D., 2014. Polycomb group protein expression during differentiation of human embryonic stem cells into pancreatic lineage in vitro. *BMC Cell Biology* 15, 18. <https://doi.org/10.1186/1471-2121-15-18>
- Pietras, R.J., Marquez-Garban, D.C., 2007. Membrane-Associated Estrogen Receptor Signaling Pathways in Human Cancers. *Clinical Cancer Research* 13, 4672–4676. <https://doi.org/10.1158/1078-0432.CCR-07-1373>
- Piqué, D.G., Montagna, C., Grealley, J.M., Mar, J.C., 2019. A novel approach to modelling transcriptional heterogeneity identifies the oncogene candidate CBX2 in invasive breast carcinoma. *Br. J. Cancer*. <https://doi.org/10.1038/s41416-019-0387-8>
- rndsystems.com. (n.d.). *Human Cbx2 Antibody*. [online] Available at: https://www.rndsystems.com/products/human-cbx2-antibody-880833_mab8098 [Accessed 2 Sep. 2019].
- Roger, P., Sahla, M.E., Mäkelä, S., Gustafsson, J.A., Baldet, P., Rochefort, H., 2001. Decreased expression of estrogen receptor beta protein in proliferative preinvasive mammary tumors. *Cancer Res.* 61, 2537–2541.
- Romagosa, C., Simonetti, S., López-Vicente, L., Mazo, A., Lleonart, M.E., Castellvi, J., Ramon y Cajal, S., 2011. p16(Ink4a) overexpression in cancer: a tumor suppressor gene associated with senescence and high-grade tumors. *Oncogene* 30, 2087–2097. <https://doi.org/10.1038/onc.2010.614>
- Rossetto, D., Avvakumov, N., Côté, J., 2012. Histone phosphorylation: A chromatin modification involved in diverse nuclear events. *Epigenetics* 7, 1098–1108. <https://doi.org/10.4161/epi.21975>
- Ruijter, A.J.M. de, Gennip, A.H. van, Caron, H.N., Kemp, S., Kuilenburg, A.B.P. van, 2003. Histone deacetylases (HDACs): characterization of the classical HDAC family. *Biochemical Journal* 370, 737–749. <https://doi.org/10.1042/bj20021321>
- Sadowski, M., Sarcevic, B., 2010. Mechanisms of mono- and poly-ubiquitination: Ubiquitination specificity depends on compatibility between the E2 catalytic core and amino acid residues proximal to the lysine. *Cell Division* 5, 19. <https://doi.org/10.1186/1747-1028-5-19>

- Seligson, D.B., Horvath, S., Shi, T., Yu, H., Tze, S., Grunstein, M., Kurdistani, S.K., 2005. Global histone modification patterns predict risk of prostate cancer recurrence. *Nature* 435, 1262–1266. <https://doi.org/10.1038/nature03672>
- Senthilkumar, R., Mishra, R.K., 2009. Novel motifs distinguish multiple homologues of Polycomb in vertebrates: expansion and diversification of the epigenetic toolkit. *BMC Genomics* 10, 549. <https://doi.org/10.1186/1471-2164-10-549>
- Simó-Riudalbas, L., Esteller, M., 2015. Targeting the histone orthography of cancer: drugs for writers, erasers and readers: Histone orthography of cancer. *British Journal of Pharmacology* 172, 2716–2732. <https://doi.org/10.1111/bph.12844>
- Singla, H., Ludhiadch, A., Kaur, R.P., Chander, H., Kumar, V., Munshi, A., 2017. Recent advances in HER2 positive breast cancer epigenetics: Susceptibility and therapeutic strategies. *Eur J Med Chem* 142, 316–327. <https://doi.org/10.1016/j.ejmech.2017.07.075>
- Song, F., Zhang, J., Li, S., Wu, J., Jin, T., Qin, J., Wang, Y., Wang, M., Xu, J., 2017. ER-positive breast cancer patients with more than three positive nodes or grade 3 tumors are at high risk of late recurrence after 5-year adjuvant endocrine therapy. *Onco Targets Ther* 10, 4859–4867. <https://doi.org/10.2147/OTT.S142698>
- Sproll, P., Eid, W., Gomes, C.R., Mendonca, B.B., Gomes, N.L., Costa, E.M.-F., Biason-Lauber, A., 2018. Assembling the jigsaw puzzle: CBX2 isoform 2 and its targets in disorders/differences of sex development. *Molecular Genetics & Genomic Medicine* 6, 785–795. <https://doi.org/10.1002/mgg3.445>
- Sterner, D.E., Berger, S.L., 2000. Acetylation of histones and transcription-related factors. *Microbiol. Mol. Biol. Rev.* 64, 435–459.
- Stuckey, J.I., Dickson, B.M., Cheng, N., Liu, Y., Norris, J.L., Cholensky, S.H., Tempel, W., Qin, S., Huber, K.G., Sagum, C., Black, K., Li, F., Huang, X.-P., Roth, B.L., Baughman, B.M., Senisterra, G., Pattenden, S.G., Vedadi, M., Brown, P.J., Bedford, M.T., Min, J., Arrowsmith, C.H., James, L.I., Frye, S.V., 2016. A cellular chemical probe targeting the chromodomains of Polycomb repressive complex 1. *Nat. Chem. Biol.* 12, 180–187. <https://doi.org/10.1038/nchembio.2007>
- Sutherland, R.L., Hall, R.E., Taylor, I.W., 1983. Cell proliferation kinetics of MCF-7 human mammary carcinoma cells in culture and effects of tamoxifen on exponentially growing and plateau-phase cells. *Cancer Res.* 43, 3998–4006.
- Takahashi-Yanaga, F., Sasaguri, T., 2008. GSK-3 β regulates cyclin D1 expression: A new target for chemotherapy. *Cellular Signalling* 20, 581–589. <https://doi.org/10.1016/j.cellsig.2007.10.018>

- Tecalco-Cruz, A.C., Pérez-Alvarado, I.A., Ramírez-Jarquín, J.O., Rocha-Zavaleta, L., 2017. Nucleocytoplasmic transport of estrogen receptor alpha in breast cancer cells. *Cell. Signal.* 34, 121–132. <https://doi.org/10.1016/j.cellsig.2017.03.011>
- Thomas, M.P., Potter, B.V.L., 2013. The structural biology of oestrogen metabolism. *J. Steroid Biochem. Mol. Biol.* 137, 27–49. <https://doi.org/10.1016/j.jsbmb.2012.12.014>
- Toy, W., Shen, Y., Won, H., Green, B., Sakr, R.A., Will, M., Li, Z., Gala, K., Fanning, S., King, T.A., Hudis, C., Chen, D., Taran, T., Hortobagyi, G., Greene, G., Berger, M., Baselga, J., Chandarlapaty, S., 2013. ESR1 ligand-binding domain mutations in hormone-resistant breast cancer. *Nat. Genet.* 45, 1439–1445. <https://doi.org/10.1038/ng.2822>
- Tropberger, P., Schneider, R., 2013. Scratching the (lateral) surface of chromatin regulation by histone modifications. *Nature Structural & Molecular Biology* 20, 657–661. <https://doi.org/10.1038/nsmb.2581>
- Turner, N.C., Neven, P., Loibl, S., Andre, F., 2017. Advances in the treatment of advanced oestrogen-receptor-positive breast cancer. *Lancet* 389, 2403–2414. [https://doi.org/10.1016/S0140-6736\(16\)32419-9](https://doi.org/10.1016/S0140-6736(16)32419-9)
- Uniprot.org. (n.d.). *CBX2 - Chromobox protein homolog 2 - Homo sapiens (Human) - CBX2 gene & protein*. [online] Available at: <https://www.uniprot.org/uniprot/Q14781> [Accessed 2 Sep. 2019].
- Upadhyay, A.K., Cheng, X., 2011. Dynamics of histone lysine methylation: structures of methyl writers and erasers. *Prog Drug Res* 67, 107–124.
- Vandamme, J., Völkel, P., Rosnoblet, C., Le Faou, P., Angrand, P.-O., 2011. Interaction proteomics analysis of polycomb proteins defines distinct PRC1 complexes in mammalian cells. *Mol. Cell Proteomics* 10, M110.002642. <https://doi.org/10.1074/mcp.M110.002642>
- van den Boom, V., Rozenveld-Geugien, M., Bonardi, F., Malanga, D., van Gosliga, D., Heijink, A.M., Viglietto, G., Morrone, G., Fusetti, F., Vellenga, E., Schuringa, J.J., 2013. Nonredundant and locus-specific gene repression functions of PRC1 paralog family members in human hematopoietic stem/progenitor cells. *Blood* 121, 2452–2461. <https://doi.org/10.1182/blood-2012-08-451666>
- Veeraraghavan, J., Tan, Y., Cao, X.-X., Kim, J.A., Wang, X., Chamness, G.C., Maiti, S.N., Cooper, L.J.N., Edwards, D.P., Contreras, A., Hilsenbeck, S.G., Chang, E.C., Schiff, R., Wang, X.-S., 2014. Recurrent ESR1-CCDC170 rearrangements in an aggressive subset of oestrogen receptor-positive breast cancers. *Nat Commun* 5, 4577. <https://doi.org/10.1038/ncomms5577>

- Veneti, Z., Gkouskou, K.K., Eliopoulos, A.G., 2017. Polycomb Repressor Complex 2 in Genomic Instability and Cancer. *Int J Mol Sci* 18. <https://doi.org/10.3390/ijms18081657>
- Vernell, R., Helin, K., Müller, H., 2003. Identification of target genes of the p16INK4A-pRB-E2F pathway. *J. Biol. Chem.* 278, 46124–46137. <https://doi.org/10.1074/jbc.M304930200>
- Wade, M.A., Jones, D., Wilson, L., Stockley, J., Coffey, K., Robson, C.N., Gaughan, L., 2015. The histone demethylase enzyme KDM3A is a key estrogen receptor regulator in breast cancer. *Nucleic Acids Res.* 43, 196–207. <https://doi.org/10.1093/nar/gku1298>
- Wahba, H.A., El-Hadaad, H.A., 2015. Current approaches in treatment of triple-negative breast cancer. *Cancer Biol Med* 12, 106–116. <https://doi.org/10.7497/j.issn.2095-3941.2015.0030>
- Wang, Q., He, G., Hou, M., Chen, L., Chen, S., Xu, A., Fu, Y., 2018. Cell Cycle Regulation by Alternative Polyadenylation of CCND1. *Sci Rep* 8, 6824. <https://doi.org/10.1038/s41598-018-25141-0>
- Weake, V.M., Workman, J.L., 2008. Histone Ubiquitination: Triggering Gene Activity. *Molecular Cell* 29, 653–663. <https://doi.org/10.1016/j.molcel.2008.02.014>
- Wheeler, L.J., Watson, Z.L., Qamar, L., Yamamoto, T.M., Post, M.D., Berning, A.A., Spillman, M.A., Behbakht, K., Bitler, B.G., 2018. CBX2 identified as driver of anoikis escape and dissemination in high grade serous ovarian cancer. *Oncogenesis* 7, 92. <https://doi.org/10.1038/s41389-018-0103-1>
- Williams, C., Lin, C.-Y., 2013. Oestrogen receptors in breast cancer: basic mechanisms and clinical implications. *Ecancermedicalsecience* 7, 370. <https://doi.org/10.3332/ecancer.2013.370>
- Wu, S., Zhu, W., Thompson, P., Hannun, Y.A., 2018. Evaluating intrinsic and non-intrinsic cancer risk factors. *Nat Commun* 9, 3490. <https://doi.org/10.1038/s41467-018-05467-z>
- Xu, C., Kim, N.-G., Gumbiner, B.M., 2009. Regulation of protein stability by GSK3 mediated phosphorylation. *Cell Cycle* 8, 4032–4039. <https://doi.org/10.4161/cc.8.24.10111>
- Yang, X.-J., Seto, E., 2007. HATs and HDACs: from structure, function and regulation to novel strategies for therapy and prevention. *Oncogene* 26, 5310–5318. <https://doi.org/10.1038/sj.onc.1210599>
- Yao, H., He, G., Yan, S., Chen, C., Song, L., Rosol, T.J., Deng, X., 2017. Triple-negative breast cancer: is there a treatment on the horizon? *Oncotarget* 8, 1913–1924. <https://doi.org/10.18632/oncotarget.12284>

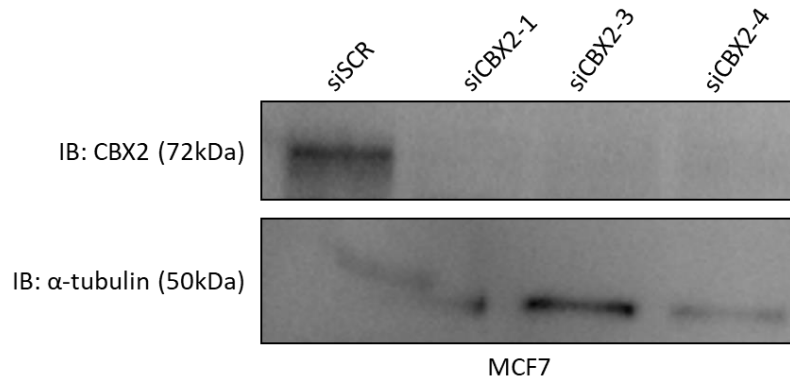
Yeo, S.K., Guan, J.-L., 2017. Breast Cancer: Multiple Subtypes within a Tumor? *Trends Cancer* 3, 753–760. <https://doi.org/10.1016/j.trecan.2017.09.001>

Yersal, O., Barutca, S., 2014. Biological subtypes of breast cancer: Prognostic and therapeutic implications. *World J Clin Oncol* 5, 412–424. <https://doi.org/10.5306/wjco.v5.i3.412>

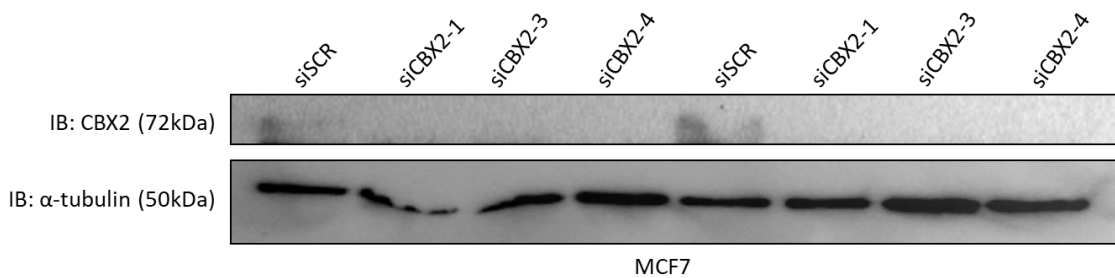
Zhen, L., Gui-lan, L., Ping, Y., Jin, H., Ya-li, W., 2010. The Expression of H3K9Ac, H3K14Ac, and H4K20TriMe in Epithelial Ovarian Tumors and the Clinical Significance: *International Journal of Gynecological Cancer* 20, 82–86. <https://doi.org/10.1111/IGC.0b013e3181ae3efa>

Zheng, S., Lv, P., Su, J., Miao, K., Xu, H., Li, M., 2019. Overexpression of CBX2 in breast cancer promotes tumor progression through the PI3K/AKT signaling pathway. *Am J Transl Res* 11, 1668–1682.

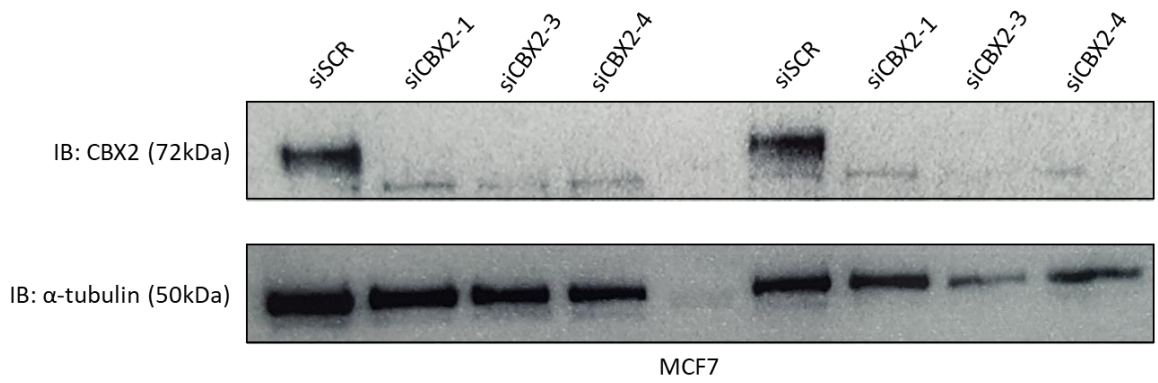
Appendices



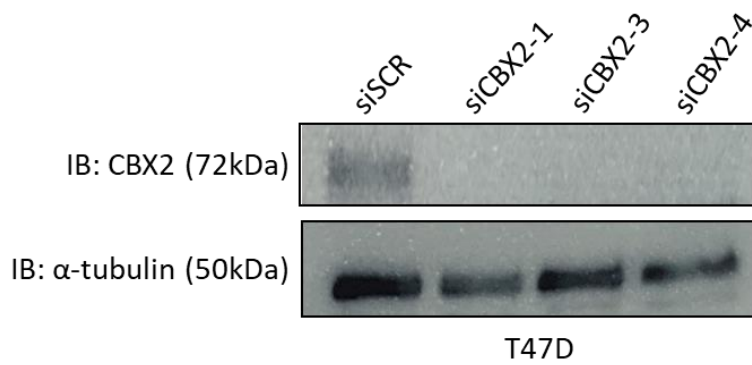
Supplementary Figure 1. Membrane showing CBX2 knockdown and the alpha tubulin loading control on MCF-7 cells. The first blot shows CBX2 knockdown in the CBX2 targeting siRNAs (siCBX2-1/3/4) compared to the control siSCR. The second blot is the loading control, which hasn't transferred adequately in the first two wells.



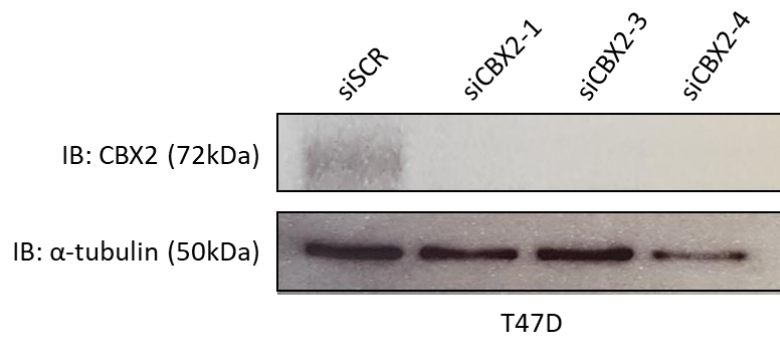
Supplementary Figure 2. Membrane showing CBX2 knockdown and the alpha tubulin loading control on MCF-7 cells. The first blot shows CBX2 knockdown in the CBX2 targeting siRNAs compared to the siSCR control for two sets of protein lysates. These don't appear as strong as in other blots, possibly due to picture resolution. The second blot is the loading control, which possibly had a bubble in between the first and second bands but is otherwise equal.



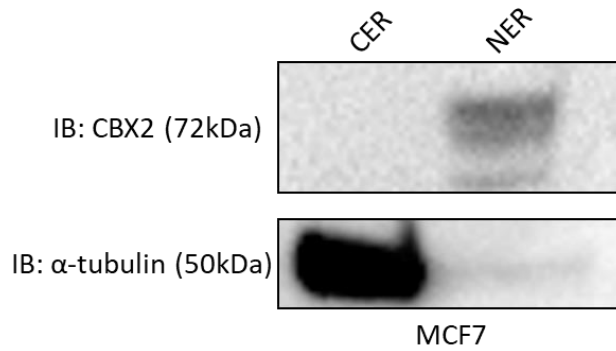
Supplementary Figure 3. Membrane showing CBX2 knockdown and the loading control on MCF-7 cells. The first blot shows CBX2 knockdown in the CBX2 targeting siRNAs compared to the control siSCR for two sets of protein lysates. The second blot is the alpha tubulin loading control, which is equal other than being lower in the second siCBX2-3.



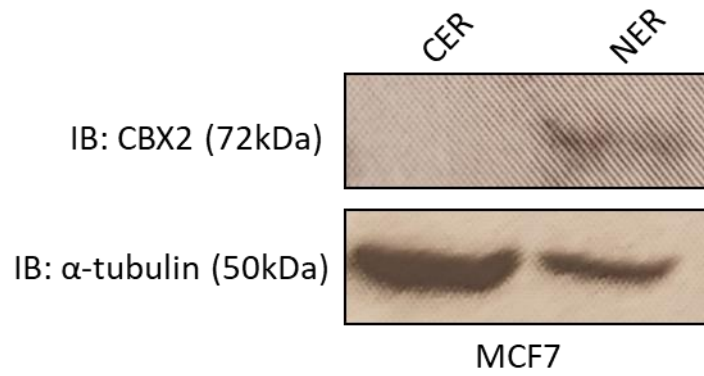
Supplementary Figure 4. Membrane showing CBX2 knockdown and the alpha tubulin loading control on T47D cells. The first blot shows CBX2 knockdown in the CBX2 targeting siRNAs compared to the control siSCR for two sets of protein lysates. The second blot is the loading control, which is equal across.



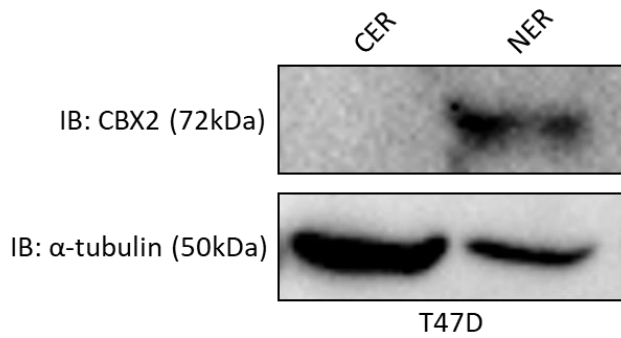
Supplementary Figure 5. Membrane showing CBX2 knockdown and the alpha tubulin loading control on T47D cells. The first blot shows CBX2 knockdown in the CBX2 targeting siRNAs compared to the control siSCR. The second blot is fairly equal for alpha tubulin, with a bit less in siCBX2-4.



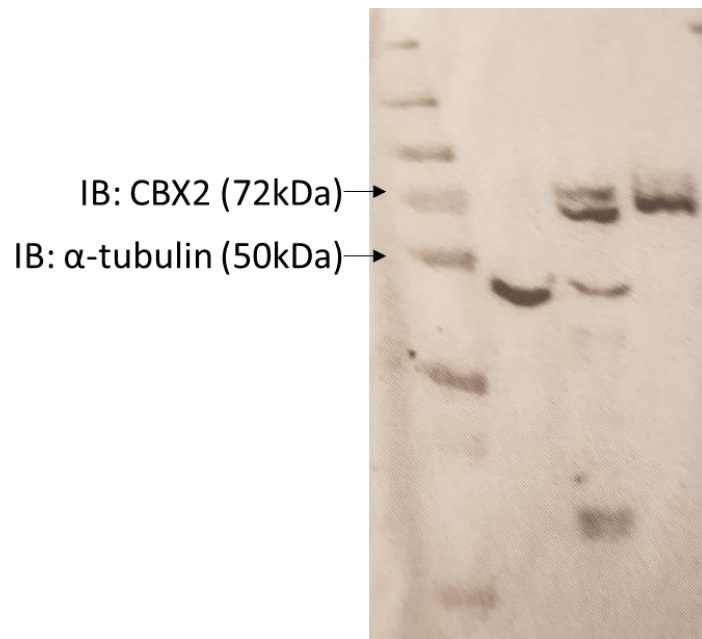
Supplementary Figure 6. Western blot membrane showing CBX2 presence in the nucleus and alpha tubulin control in the cytoplasmic extract, in MCF-7 cells. CER = cytoplasmic extract, NER = nuclear extract.



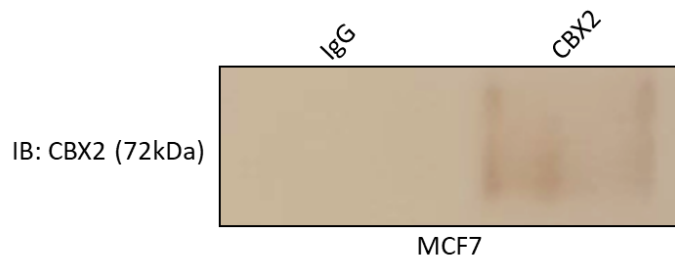
Supplementary Figure 7. Western blot membrane showing CBX2 presence in the nucleus and alpha tubulin control in the cytoplasmic extract, in MCF-7 cells. This fractionation was not as precise as some alpha tubulin is in the nuclear extract.



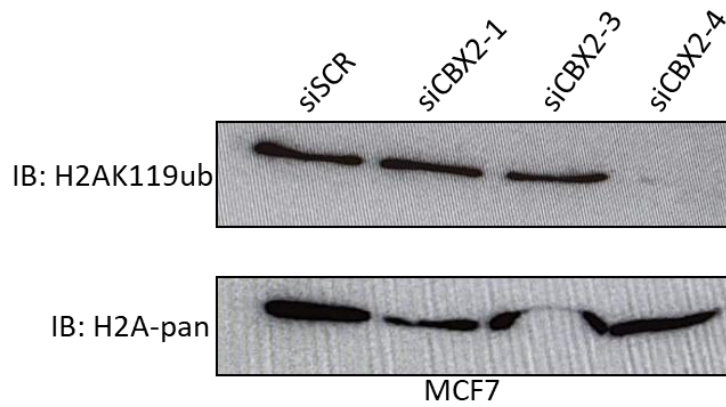
Supplementary Figure 8. Western blot membrane showing CBX2 presence in the nucleus and alpha tubulin control in the cytoplasmic extract, in T47D cells. There is some cross contamination of alpha tubulin in the nuclear fraction.



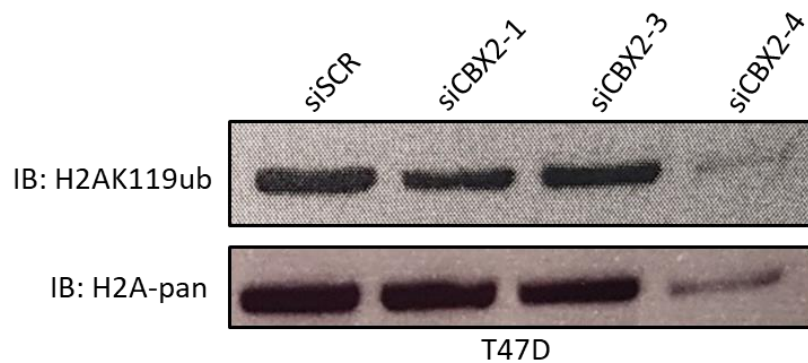
Supplementary Figure 9. Western blot membrane in MCF-7 cells showing CBX2 molecular weight at 72kDa, in comparison to alpha tubulin at the 50kDa molecular marker.



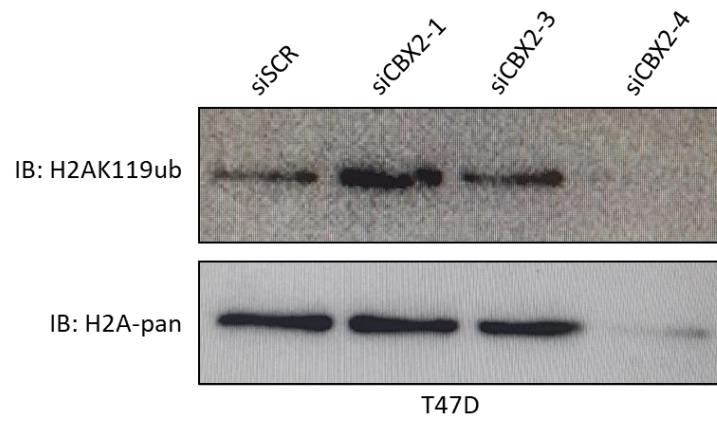
Supplementary Figure 10. Immunoprecipitation membrane showing CBX2 in the CBX2 lane but not IgG, at 72kDa in MCF-7 cells.



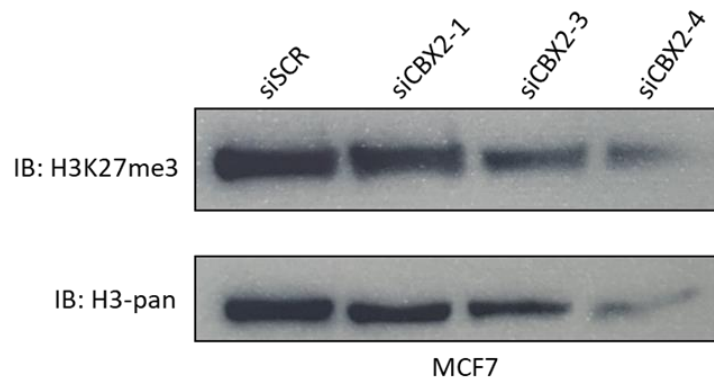
Supplementary Figure 11. A membrane showing the effect of CBX2 knockdown in CBX2 targeting siRNAs (siCBX2-1/3/4) compared to a non-silencing siSCR control, on H2AK119ub and its loading control, H2A-pan in MCF-7 cells. H2AK119ub is a lot less in siCBX2-4. It is difficult to conclude with the H2A-pan comparison as there appears to have been a bubble in the 3rd well.



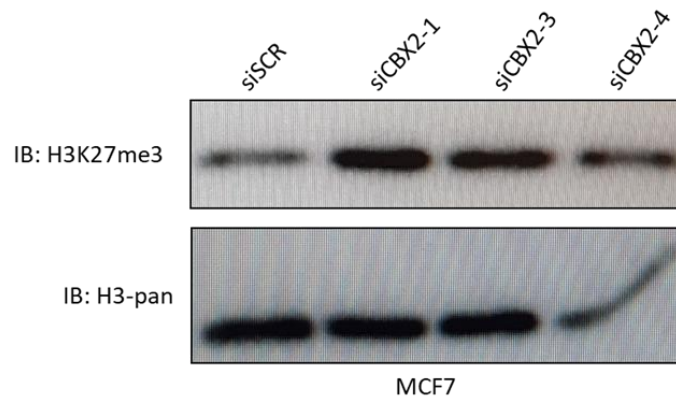
Supplementary Figure 12. A membrane showing the effect of CBX2 knockdown, by CBX2 targeting siRNAs and siSCR, on H2AK119ub and its loading control, H2A-pan in T47D cells. H2AK119ub is a lot less in siCBX2-4, for both the loading control and the histone mark. The loading and comparison between siSCR and siCBX2-1 and 3 is equal otherwise.



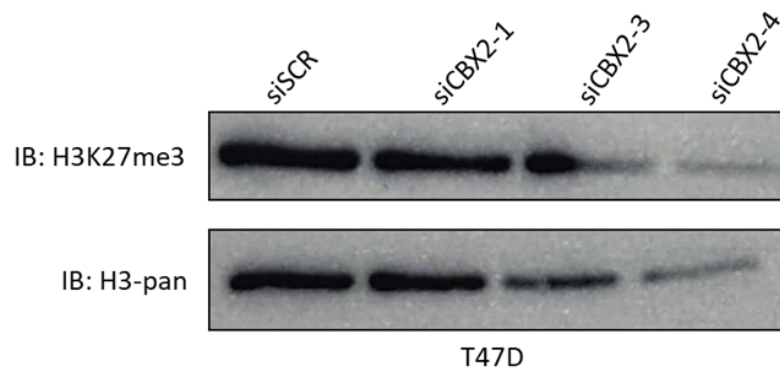
Supplementary Figure 13. A membrane showing the effect of CBX2 knockdown in in CBX2 targeting siRNAs and siSCR control, with H2AK119ub and H2A-pan antibodies, in T47D cells. H2AK119ub is a lot less in siCBX2-4 for both H2AK119ub and H2A-pan, but is also low in the H2AK119ub siSCR, which may be a transfer issue.



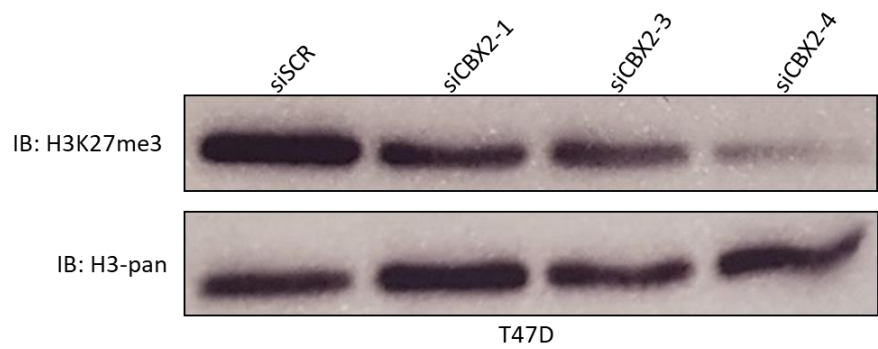
Supplementary Figure 14. A membrane showing the effect of CBX2 knockdown by CBX2 targeting siRNAs compared to a siSCR control, on H3K27me3 and H3-pan loading control, in MCF-7 cells. siCBX2-4 is lower for both blots, which may be due to a loading issue.



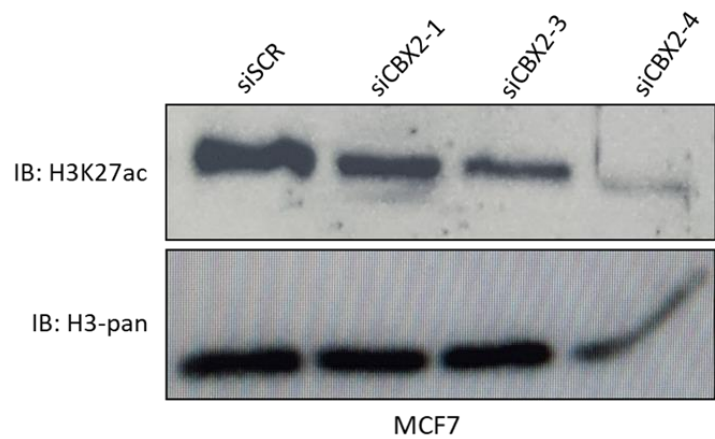
Supplementary Figure 15. A membrane showing the effect of CBX2 knockdown by CBX2 targeting siRNAs compared to a siSCR control, on H3K27me3 and H3-pan loading control, in MCF-7 cells. H3K27me3 is less in the siSCR compared to H3-pan.



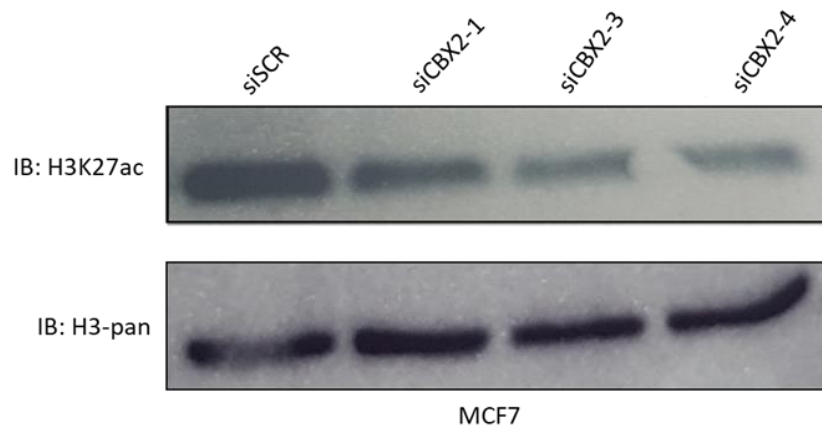
Supplementary Figure 16. A membrane showing the effect of CBX2 knockdown by CBX2 targeting siRNAs compared to a siSCR control, on H3K27me3 and H3-pan loading control, in T47D cells. There is less siCBX2-4 in both membranes, so this may have been a loading issue.



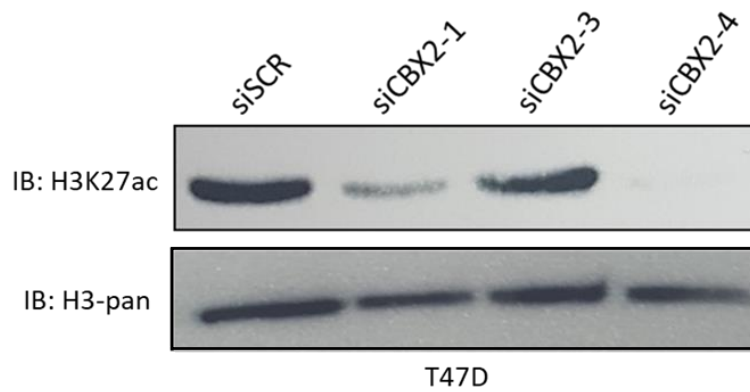
Supplementary Figure 17. A membrane showing the effect of CBX2 knockdown by CBX2 targeting siRNAs compared to a siSCR control, using H3K27me3 and H3-pan antibodies, in T47D cells. H3K27me3 is less in CBX2-4 compared with the loading control.



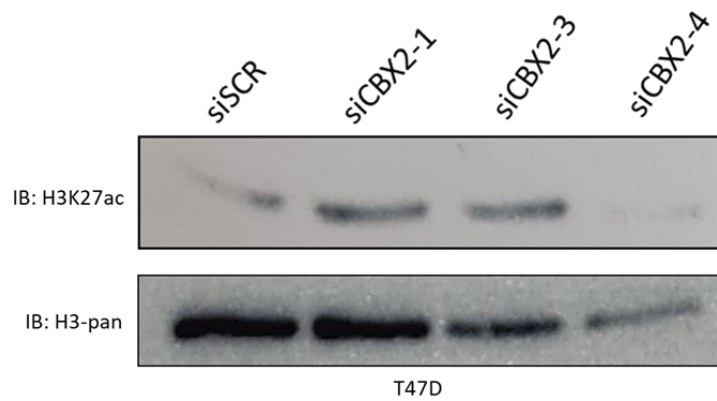
Supplementary Figure 18. A membrane showing the effect of CBX2 knockdown by CBX2 targeting siRNAs compared with an siSCR control on H3K27ac and its loading control, H3-pan in MCF-7 cells. H3K27ac less in the siRNAs compared with the siSCR. It is difficult to tell in siCBX2-4 for H3-pan whether there is even loading as this has spread.



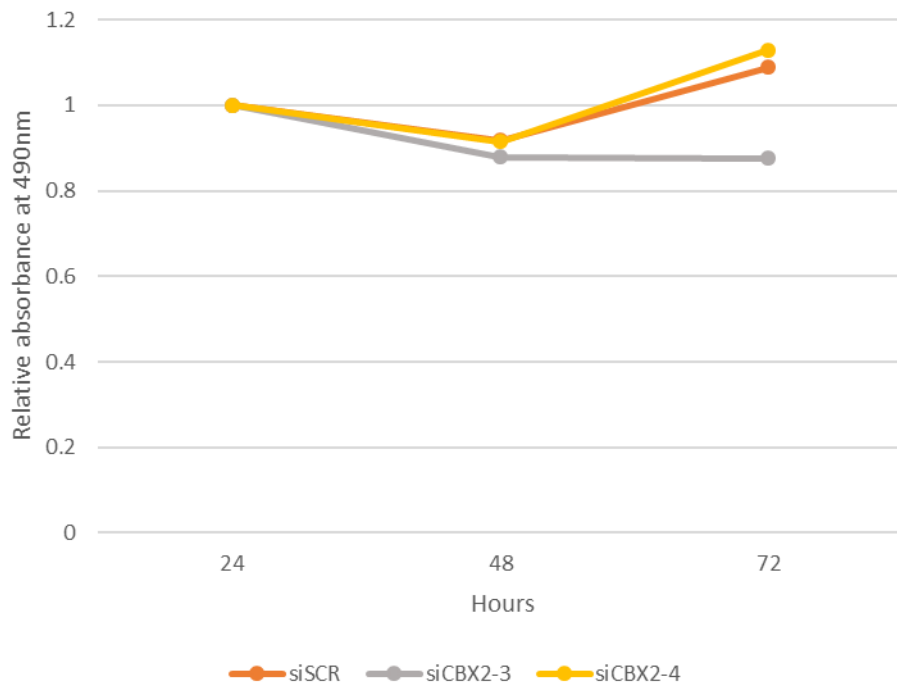
Supplementary Figure 19. A membrane showing the effect of CBX2 knockdown by CBX2 targeting siRNAs compared with an siSCR control on H3K27ac and its loading control, H3-pan in MCF-7 cells. H3K27ac is slightly less in the knockdown siRNAs compared with the siSCR. This is especially as it appears there is less siSCR loaded according to the H3-pan blot.



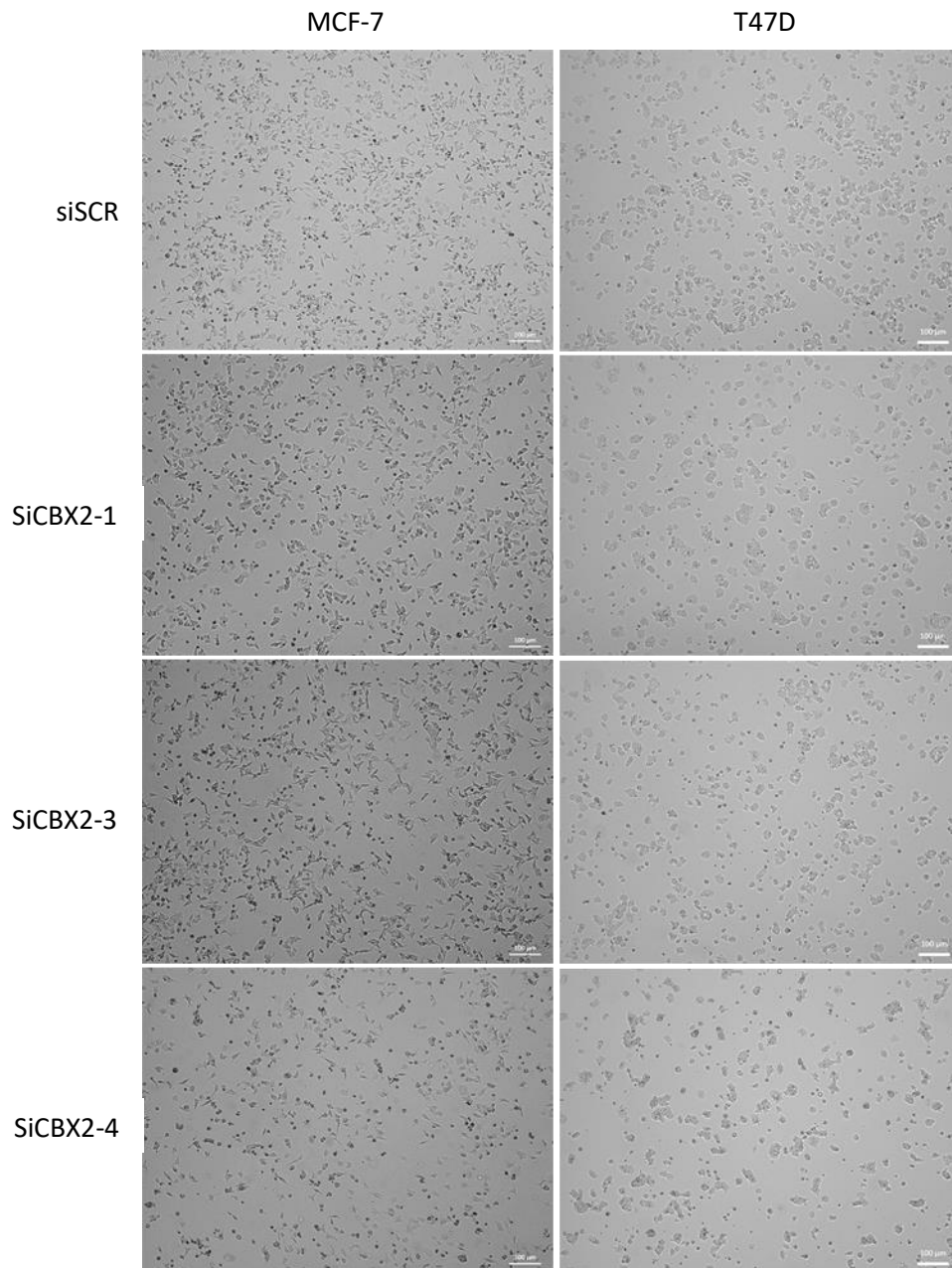
Supplementary Figure 20. A membrane showing the effect of CBX2 knockdown by CBX2 targeting siRNAs compared with an siSCR control on H3K27ac and its loading control, H3-pan in T47D cells. H3K27ac is a lot less in siCBX2-1 and siCBX2-4 compared with the siSCR and loading control, but not in siCBX2-3.



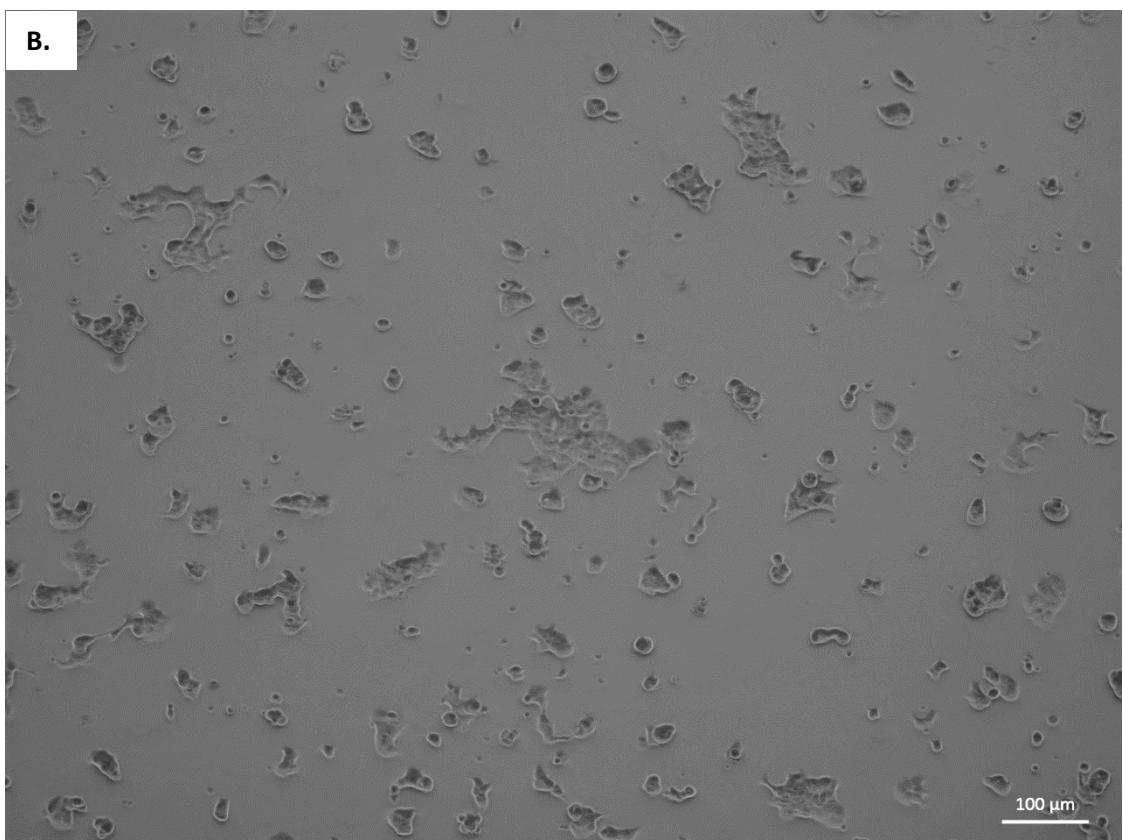
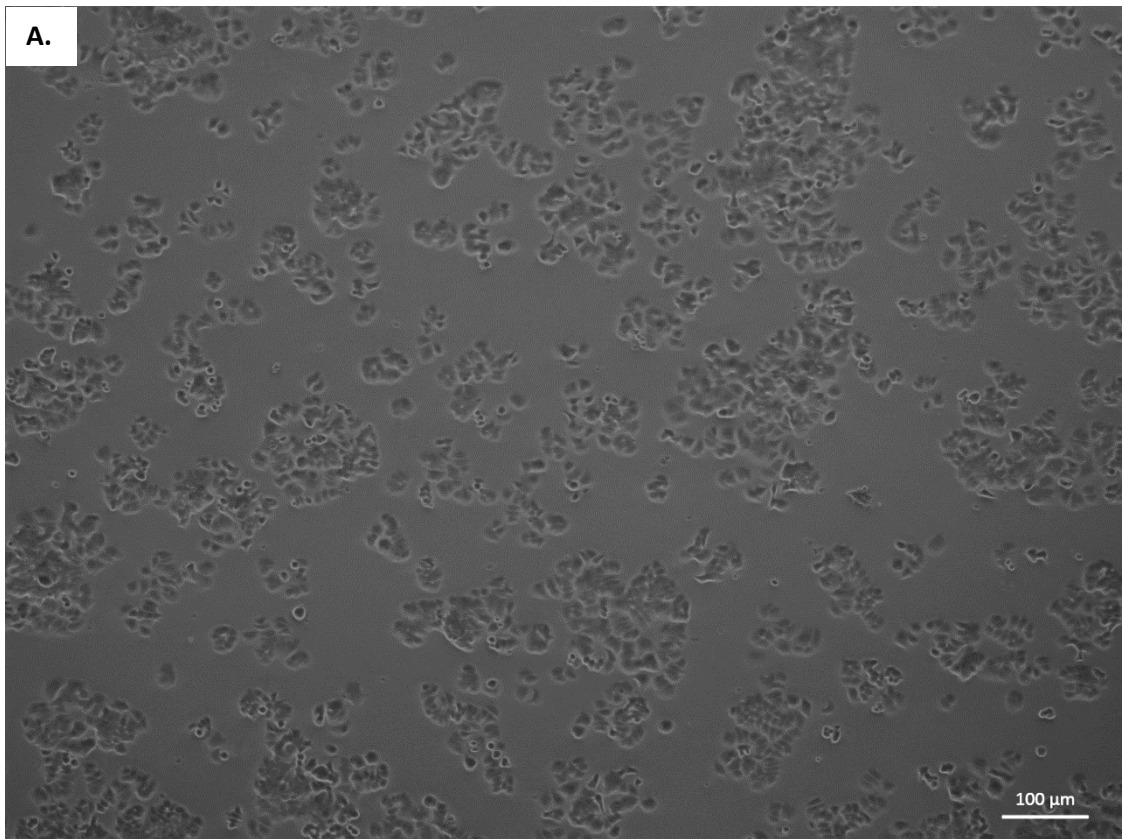
Supplementary Figure 21. A membrane showing the effect of CBX2 knockdown by CBX2 targeting siRNAs compared with an siSCR control on H3K27ac and its loading control, H3-pan in T47D cells. It is difficult to see whether H3K27ac has decreased compared to the siSCR as it hasn't transferred properly. The loading control also seems to have had a transfer issue at the siCBX2-4 end.



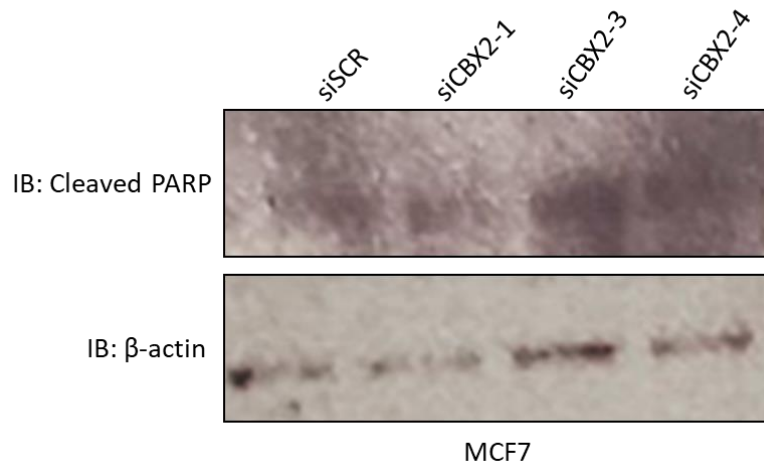
Supplementary Figure 22. An MTS graph showing the siSCR, siCBX2-3 and siCBX2-4 transfected T47D cells, incubated over a 72-hour period. This experiment did not work as expected.



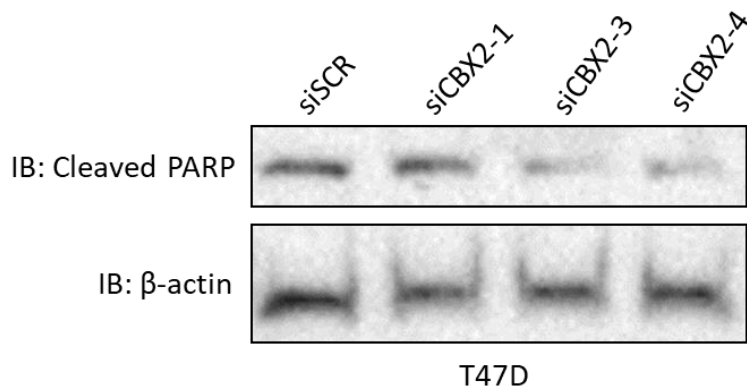
Supplementary Figure 23. Microscopy images of MCF-7 and T47D cells, transfected with siSCR and siCBX2-1/3/4. Scale bar size: 100 μm . MCF-7 cells decreased in number and became rounder compared with the siSCR, especially in siCBX2-4. T47D cells also decreased in number and became rounder and slightly larger compared with the siSCR.



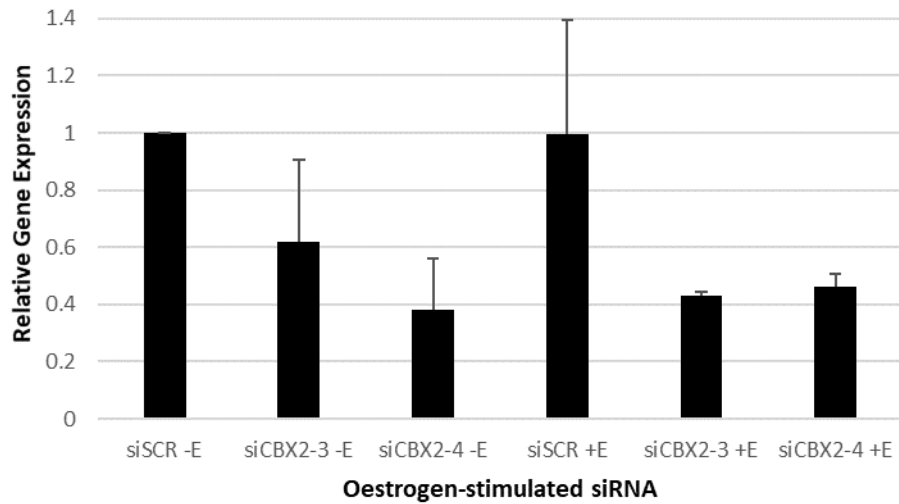
Supplementary Figure 24. Larger microscopy images of T47D cells, transfected with siSCR (A) and siCBX2-4 (B). Scale bar size: 100 μ m.



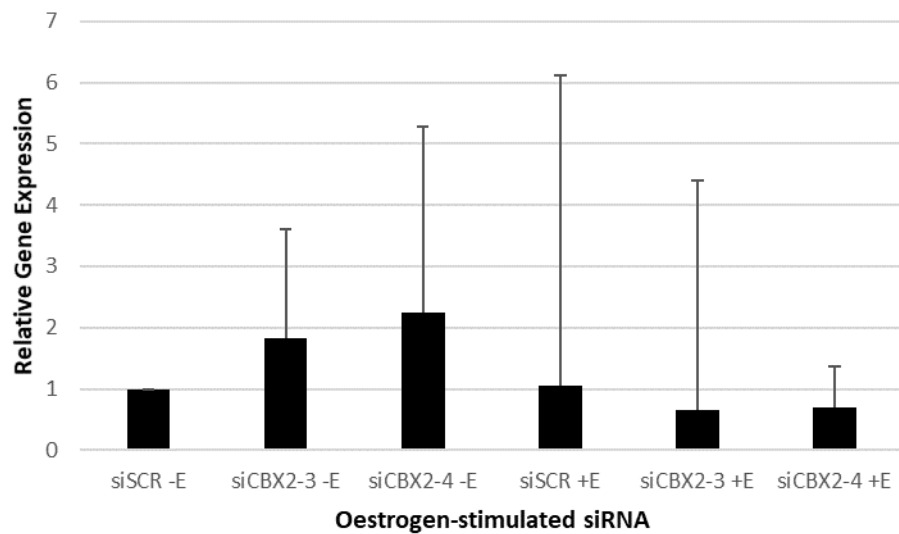
Supplementary Figure 25. Western blots showing the apoptosis marker cleaved PARP and Beta-actin loading control in MCF-7 cells, at 48-hour incubation with siSCR and siCBX2-1/3/4. The blot did not transfer adequately, so the bands are quite faint for beta-actin and difficult to distinguish for cleaved PARP.



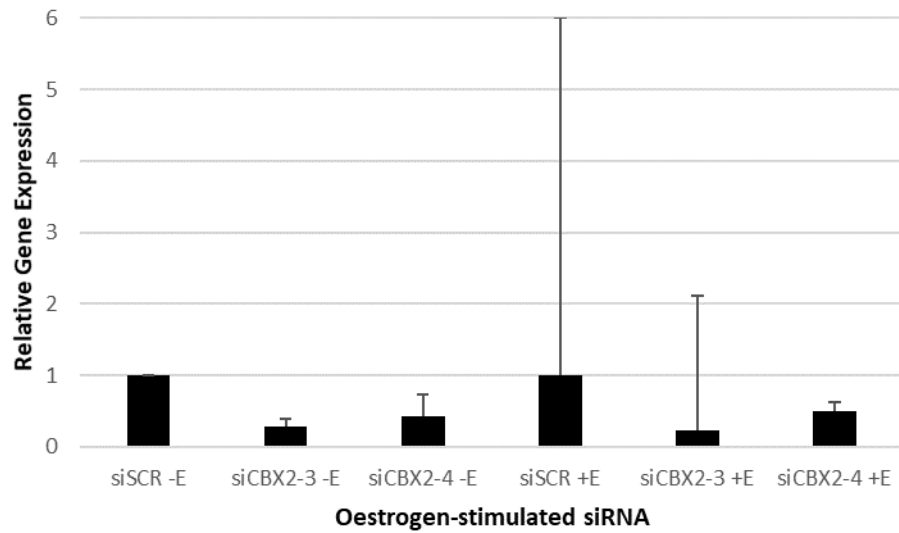
Supplementary Figure 26. Western blots showing the apoptosis marker cleaved PARP and Beta-actin loading control in T47D cells, at 48-hour incubation with siSCR and siCBX2-1/3/4. This does not seem to have worked for this cell line, possibly due to them being slow growing. A greater time point may be required for these cells.



Supplementary Figure 27. A qPCR graph showing the relative expression of CBX2 on transfected (siSCR, siCBX2-3, siCBX2-4) MCF-7 cells, stimulated with oestrogen (+E) and without (-E). This is relative to siSCR -E. This shows that CBX2 was successfully knocked down.



Supplementary Figure 28. A qPCR graph showing the relative expression of pS2 on transfected (siSCR, siCBX2-3, siCBX2-4) MCF-7 cells, stimulated with oestrogen (+E) and without (-E). This is relative to siSCR -E. Cells stimulated with oestrogen should have increased, in comparison to cells not stimulated. This experiment does not appear to have worked.



Supplementary Figure 29. A qPCR graph showing the relative expression of CCND1 on transfected (siSCR, siCBX2-3, siCBX2-4) MCF-7 cells, stimulated with oestrogen (+E) and without (-E). This is relative to siSCR -E. It was expected that cells stimulated with oestrogen should have increased CCND1 expression, in comparison to cells not stimulated. This experiment does not appear to have worked.